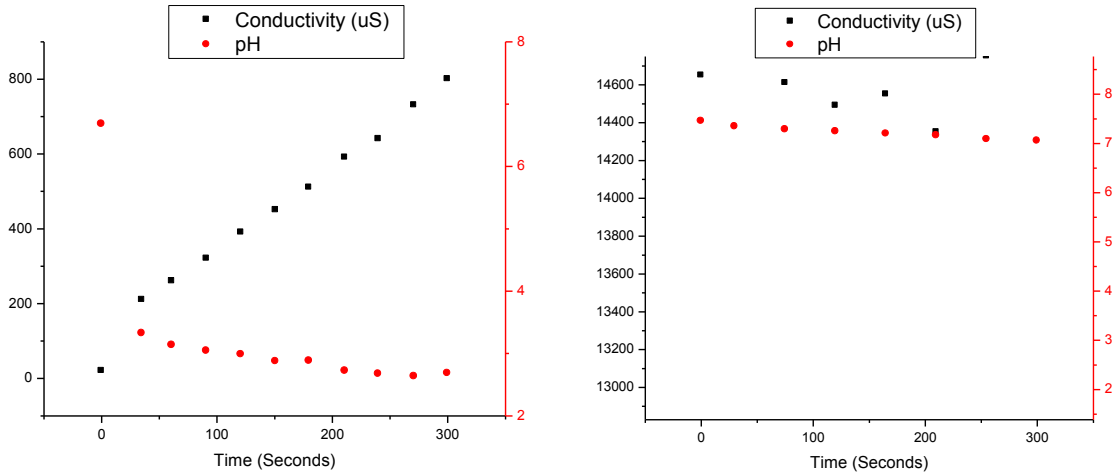

Figure 5.34: Change of conductivity and pH of MB solution without PBS (left) and with PBS (right) over plasma treatment time. (Note: the figure on the left is a copy of Figure 5.26, repeated here for convenience).

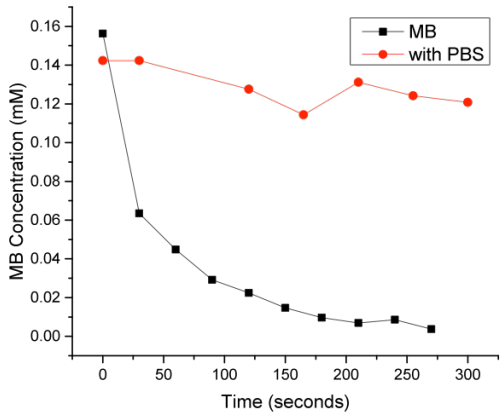

Figure 5.35: Effect of PBS on MB decomposition by air plasma jet.

Figure 5.36: MB with PBS solution before processing (left) and after 5 minutes of processing (right).

Figure 5.37: Comparison of MB solution with PBS (left vial, 5 min processing) and without (right vial, 5.5 min processing).

These results suggest that OH is one of the primary drivers of decomposition. However, it is also possible for the salts of PBS to interact with the plasma-produced active species as well. It should be noted that the name PBS does not refer to a set compound, but a host of buffer

solutions that containing various sodium-salts. For this reason, to quantitatively assess the OH^- production of the plasma, the extinction rate of OH^- by PBS must be determined first, which was not done here. A quantitative method not performed in this dissertation research, but that would be useful, is to repeat the experiment detailed above but with the amino acid, N-acetyl-L-cysteine (abbreviated NAC). Unlike PBS, which can be made by a variety of "recipes," NAC is has a set definition, and therefore, one may use the established reaction rates between NAC and OH^- to determine a OH^- generation rate by the plasma. At pH 7.0, the rate of reaction between NAC and OH^- is 1.36×10^{10} $(M\ s)^{-1}$ [**378**].

5.6.2 Halogenated Compounds

The effect of plasma treatment on halogenated organic compounds using the air plasma jet at similar powers and applied voltages. Plasma treated samples of water with and without contaminants were analyzed via gas chromatograph at the Water Research Laboratory in the Environmental and Water Resource Engineering program of the Civil and Environmental Engineering department at the University of Michigan.

The compounds that were investigated were:

1. Chloroform
2. 1,1,1-Trichloroethane
3. 1,1,2-Trichloroethane
4. Bromochloromethane

These compounds each are toxic to humans and animals and are difficult to remove from the water system. Each compound was precisely diluted via volumetric flasks to produce various concentrations (10 ppm, 1 ppm, 50 ppb, 15 ppb). These were analyzed via gas chromatograph (see description of process in Chapter 3).

Results from the decomposition of 15 ppb bromochloromethane are given as an example of plasma decomposition power of halogenated compounds. This concentration was chosen as it is comparable to the concentrations of contaminants that are currently detected in drinking water in the United States (refer to Figure 1.1 [**22**]).

5.6.2.1 Results

Figure 5.38 illustrates the decomposition of bromochloromethane as a function of plasma treatment time, and Table 5.3 outlines the change in concentration of bromochloromethane with plasma treatment time.

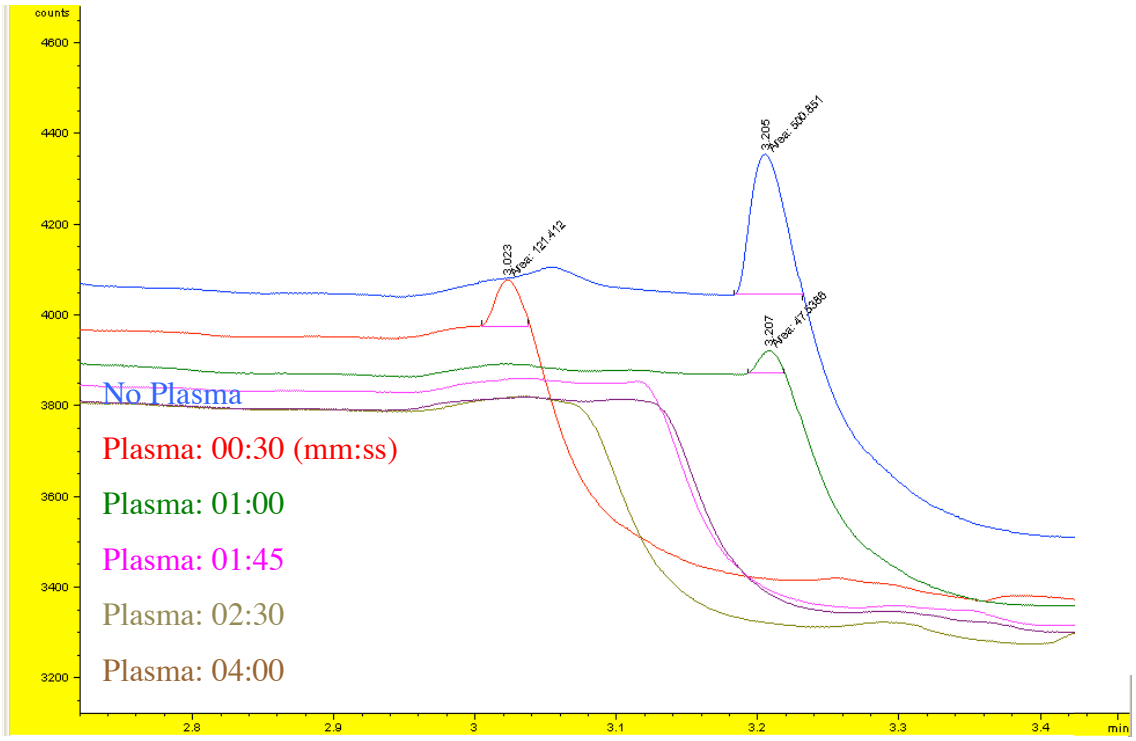

Figure 5.38: Bromochloromethane decomposition by plasma discharge. Legend insert indicates treatment time by plasma discharge (blue, no treatment; red, 30 seconds, etc.).

For bromochloromethane, the plasma reduces the below the detection level of the system (>> 1 ppb) within 60 seconds of plasma treatment time. This result is encouraging to the future development of a plasma water purification device.

Table 5.3: Concentration of bromochloromethane with plasma treatment. BDL = below detection level.

Starting Concentration	**Concentration during plasma treatment**				
	30 s	*60s*	*105 s*	*150 s*	*240 s*
15 ppb	~4 ppb	~1 ppb	BDL	BDL	BDL

5.6.2.2 Further Work/Additional Considerations

Special attention to the chemistry is absolutely essential to ensure accurate results. The following is a list of suggested considerations for those who plan to take the study further, primarily for those who do not have significant experience in chemical laboratories.

1. *Best practices.* Performing chemistry at the concentrations dealt with here (10s of ppb) demands careful analytical chemistry methods to ensure cross-contamination between samples, contamination of the solvent or the like does not occur. Appropriate storage of chemicals is important. This becomes an issue of paramount significance when the concentrations of compounds decrease (1s of ppb, 100s of ppt (parts per trillion)) and depending on the vapor pressure of the substance. It is possible to render samples unusable merely through the evaporation and subsequent sorption of a particular volatile compound.
2. *Column chemistry.* Attention to the column chemistry is necessary. For example, for the column in the experiment described above, chloromethane could not be analyzed as it coeludes with its typical GC solvent, methanol. A new column must be acquired to analyze this contaminant.
3. *Contaminant chemistry*. Additional contaminants that would be very interesting to study under plasma decomposition are persistent herbicides, especially atrazine, or organic solvents, such as toluene. However, neither of these contaminants are reasonable candidates for a gas chromatograph method due to the acidic proton of both substances, which would appear too early in the chromatogram to be useful. These and similar chemicals require a separate method for analysis, most likely an HPLC method.

5.6.3 Algae Pond Water

In addition to standards of halogenated compounds, wastewater from saltwater aquarium at NASA Glenn Research Center was treated with an air plasma jet for 30 minutes. This experiment gave a qualitative view of the processing power of the air plasma jet for in a real-world application of plasma water purifying technology. The aquarium was a closed loop aquaponics system in which plantstuffs grown for biofuel and fishes existed [**379**]. Biofouling of the water is an issue in this system as the water becomes laden with fish waste. The water needs to be treated; plasma treatment was investigated as a method of management.

The water was treated with an approximately 50 W room air plasma jet operating at 3.6 kV_{pk-pk} at 1 kHz. A typical voltage and current waveform is seen in Figure 5.39.

5.6.3.1 Results

The pH of the solution was monitored over the treatment time (see Figure 5.40). It was found the solution moved from somewhat alkaline (starting pH of 9.18) to roughly neutral (after 30 minutes of processing, the solution had a pH of 7.86).

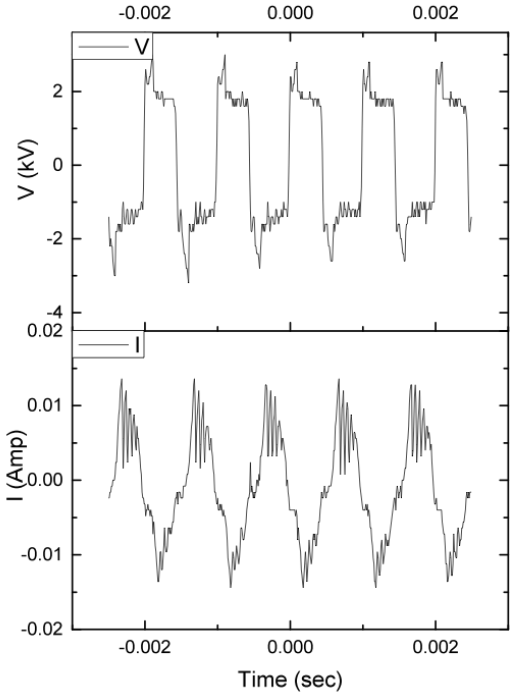

Figure 5.39: Typical voltage and current for algae pond water plasma treatment.

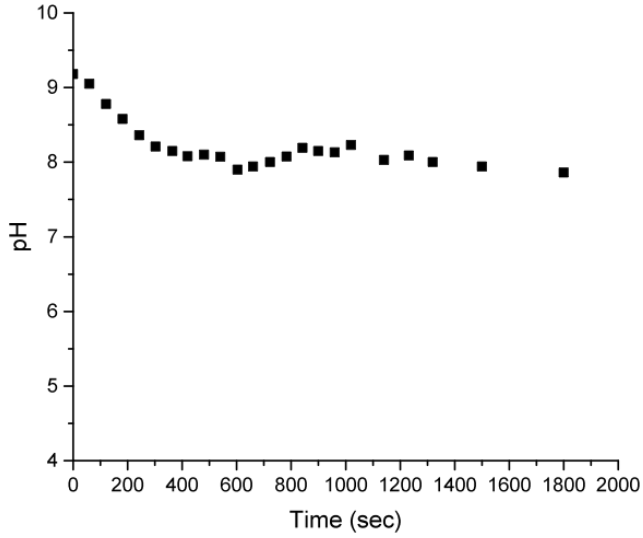

Figure 5.40: Algae processing pH curve.

The decomposition of the algae pond water may be seen in Figure 5.41; plasma processing was able to effect real change in both odor and color of the liquid. As the water is processed, the chlorophyll is broken down and the liquid loses its bright green hue. The plasma begins cause

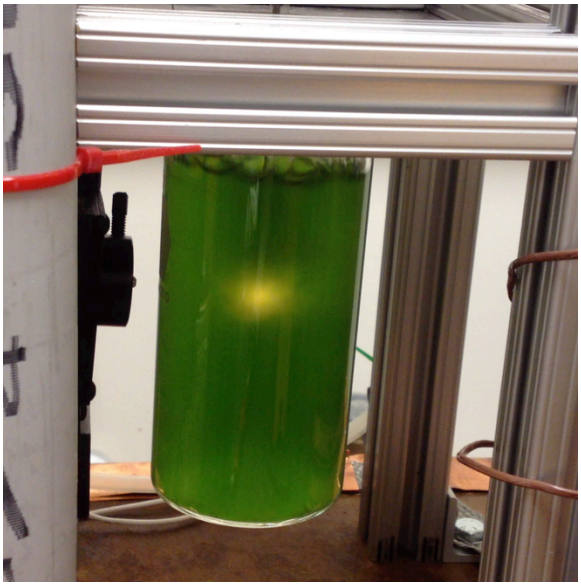

2 minutes

3 minutes

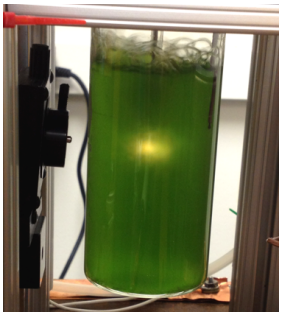

5 minutes

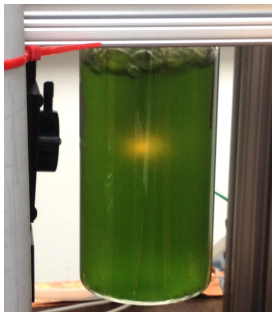

7 minutes

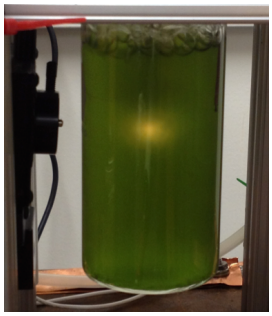

9 minutes

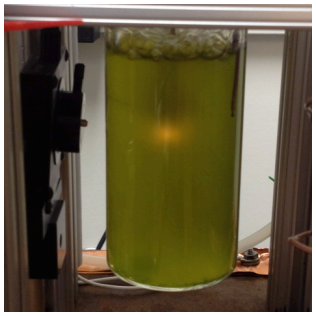

13 minutes

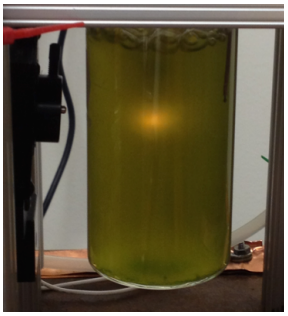

19 minutes

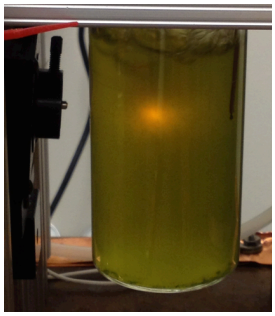

30 minutes

Figure 5.41: Plasma processing of algae water. Top, algae water with plasma at t = 10 seconds. Bottom eight images: water at various points during the treatment.

precipitation of algae and other pond water particles, which begin to visibly collect around the edge of the treatment beaker at the 7 minute mark. After 30 minutes of processing, the water has

changed to an olive-green, a sign of the daughter products of the decomposition process. After processing, when the algae is allowed to settle, a considerable amount of precipitate collects on the bottom of the beaker, which is a promising sign for future plasma water purification efforts.

This is an excellent example of plasma treatment bringing its multifaceted reactive soup to a problem system, as many toxic algal compounds that are typically responsible for wastewater treatment difficulties have slow oxidation reaction rates with ozone due to their saturated ring structures (see Figure 5.42 for sturctures of geosmin and 2-methylisoborneol, two common algal products). In general, algal products react with ozone at approximately k_{O3} ($cm^3\ s^{-1}$) < 1×10^{-20}, while the reaction rate with hydroxyl radical is several orders of magnitude greater at approximately k_{OH} ($cm^3\ s^{-1}$) ≈1×10^{-11} [**380**]. The OH production of the plasma as well as the synergistic action of the other products contributes to the fast cleaning.

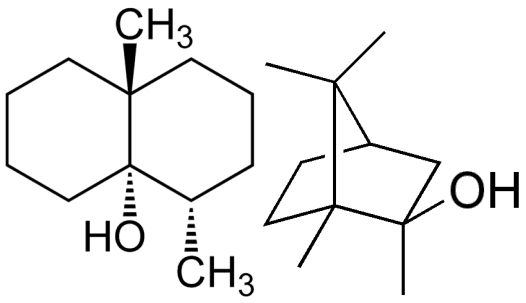

Figure 5.42: Algal products. Left, geosmin; right, 2-methylisoborneol.

5.7 Cytotoxicity

From a practical standpoint, on must access the toxicity of treated water. This is relevant for both water purification and plasma medicine applications. Cytotoxicity – toxicity to cells– is perhaps the most crucial of characteristics of plasma sterilization to understand, after basic decomposition.

As mentioned previously, disinfection by-products (DBPs, e.g., chloroform) have been linked with numerous cancers, as well as several reproductive and developmental defects, including spontaneous abortion (i.e., miscarriage) and birth defects [**23**]. Merely inactivating or destroying contaminants in drinking water is not enough; one must assess the post-treatment cytotoxicity of the treated solution.

A fundamental cytotoxicity test was completed in collaboration with the Chemistry Department at the University of Michigan. Dr. Yong-Eun Koo Lee's group of the Kopelman Laboratory applied air-processed plasma treated deionized water samples to a lab-standard line

of melanoma cells. The aim of the test was simple: as cancer cells are more robust than healthy cells, any adverse reaction of the cancer cells to the plasma treated water would be a strong indication of plasma-treated water cytotoxicity.

5.7.1 Experimental Methods

The water samples were processed at NASA Glenn Research Center. The same experimental apparatus (DBD plasma jet) previously described was used, though the power source was a nanosecond repetitively pulsed power sources as opposed to the kilohertz sinusoidal power supply that was used for all previous experiments that used the apparatus described. Although the method of plasma processing was different from that of the experiments discussed earlier in this chapter, the chemistry is very similar and is considered an appropriate analogue for this test. More details into the nanosecond pulsed power plasma source are described by Foster et al. [**96**].

As mentioned, the deionized water was treated by a nanosecond repetitively pulsed DBD atmospheric air plasma. The repetition rate was 9 kHz, and the deposited power was roughly 16 W. The solution of methylene blue treated was a 0.4 ppm concentration. The solution was treated by plasma for 30 minutes, resulting in ~90% transmission. The discharge current and applied voltage waveforms may be seen in Figure 5.43. The pH of the plasma treated water was approximately 4.

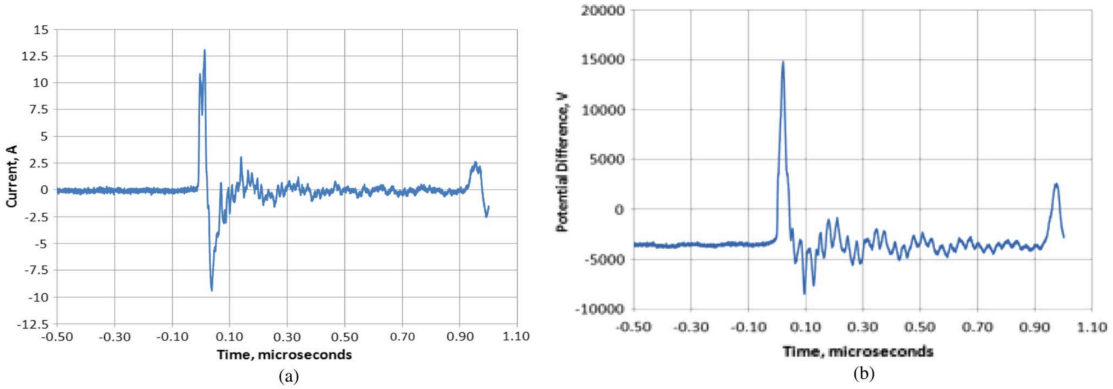

Figure 5.43: (a) Discharge current and (b) applied voltage of the nanosecond repetitively pulsed DBD plasma jet [96].

5.7.1.1 Sample Preprocessing

The pH of some of the plasma treated water samples was adjusted the range of 7-8 pH using sodium bicarbonate. This allowed for an assessment of cell sensitivity to water pH.

5.7.1.2 MTT Assay

MTT (full name 3-[4,5-dimethylthiazol-2-yl]-2,5- diphenyltetrazolium bromide) is a standard laboratory method used to determine cell proliferation. Living cells will uptake the MTT dye and during mitochondrial dehydrogenases (one of the steps in cell respiration), the soluble yellow MTT is converted to an insoluble purple formazan (a dye – refer to Figure 5.44).

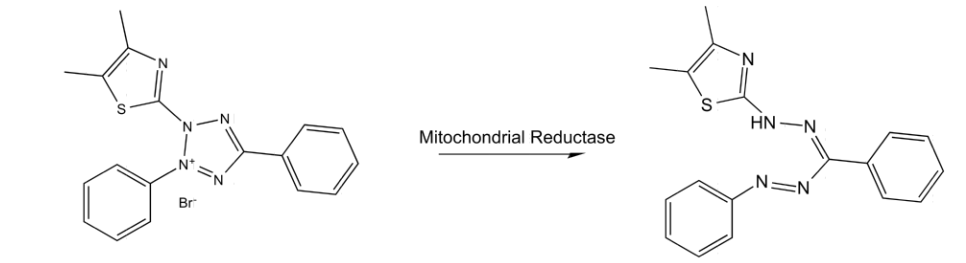

Figure 5.44: The reduction of MTT to formazan. This reaction only occurs in living cells, and is used to quantify cell growth. From [381**].**

The survivability of the cells is then assessed based on absorption of the formazan.

5.7.2 Experimental Procedure

To quantify the cell survival post-plasma treated water application, the experimental procedure given below was performed by Dr. Gwangseong Kim, research scientist in Dr. Koo Lee's group in the Department of Chemistry at the University of Michigan.

1. Sample solutions added to cells (MDA-MB-435 cell line of melanoma cells). Sample solutions were diluted to 10 fold and 100 fold.
2. Cells were incubated for 1 hour.
3. Sample solutions removed and cells washed by fresh serum-free cell media.
4. Cells were treated by 0.5 mg/mL MTT reagent for 4 hours. During this period, healthy cells generate purple colored crystal by reacting with MTT reagent while damaged cells do not.
5. After 4 hours, the cell media were removed and switched with DMSO to solubilize the purple crystal product.
6. The cells were gently rocked overnight.
7. The absorption at 550 nm was measured. Stronger absorption indicates larger percentage of cell survival and vice versa.

5.7.3 Results

The cells did not show the recognizable cytotoxicity by MTT assay, as seen in Figure 5.45. Indeed, some of the cells experienced positive growth (e.g., an extra 3% cell growth was observed with the cells given the 10x diluted water adjusted to pH 8).

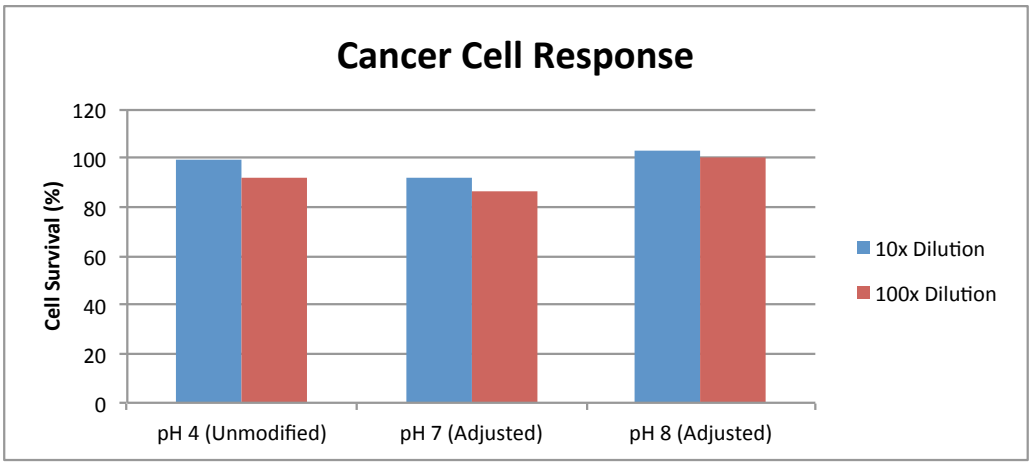

Figure 5.45: Results from cytotoxicity test. Overall, plasma treated water not cytotoxic to melanoma cells.

While the use of cancer cells to test cytotoxicity may appear uninteresting, as an industrial application of plasma wastewater treatment would be more concerned with the toxicity to healthy cells (such as human and animal populations), this experiment does provide an upper threshold of toxicity. As cancerous cells are more difficult to kill than healthy cells, if the plasma-treated wastewater (in this experiment it was a plasma-treated methylene blue solution) is unable to damage these cells, at a minimum it identifies a metric of toxicity for more robust cells. Additionally, as this study uses plasma-treated contaminated water, it gives an estimation into the environmental risk posed by using a plasma-driven treatment.

5.7.4 Final Comments

While the above test demonstrated the general non-toxic qualities of the plasma treated water to melanoma cells, careful consideration to toxicity should be given. Further work with cancerous and non-cancerous, healthy cells, should be conducted. Insight into species control and the like garnered from this chapter and the following should be taken into account while developing the optimal plasma water purification device.

Chapter 6:

The Steam Discharge[42]

6.1 Overview

In the previous chapter, an underwater dielectric barrier discharge was discussed. Various feed gases (argon, helium, nitrogen, air, and mixtures of gases) and the resulting chemistries were investigated. From an implementation perspective, the use of air as the feed gas for these discharges is especially attractive as the engineering of the system becomes far simpler and more cost effective when exotic materials, such as rare gases (e.g., helium, argon), are used to ignite the plasma.

However, the drawback of air plasmas is the acidification of the liquid water through the formation of reactive nitrogen species (RNS), such as nitrates, nitrites and peroxynitrites [**382**]. While creating acidic conditions is a desired effect in certain applications of atmospheric pressure plasma discharges (e.g., antimicrobial treatment is most efficient at pH of 3-4 and lower [**383**]), if the aim is to process contaminated water for reasonable reuse (by humans, agriculture or industry), the low pH liquid is not an acceptable end product as the treated liquid must be post-processed to raise the pH. For air-based non-thermal atmospheric plasmas, the primary acidification of the water is thought to be primarily due to the formation of nitrogen and NO_x-based species (e.g., nitric acid, among others) [**357**]. It should be possible to eliminate this acidification pathway by eliminating the nitrogen in the feedgas or using an inert gas as the feedstock (though liquid water still contains trace amounts of dissolved air, which is a potential source gas for acidification [**384**]). Regardless, if the goal is to create a commercially viable and

[42]The content presented in this chapter is based on the article published in *Plasma Sources Science and Technology*, entitled "An investigation of an underwater steam plasma discharge as alternative to air plasmas for water purification" by Sarah N. Gucker, John E. Foster, and Maria C. Garcia [**77**].

economically feasible water sterilization system, rare gases such as argon and helium should be avoided. In addition, the use of oxygen gas as the ionizing medium, while eliminating NO_x production and potentially boosting the production of other reactive species, such as ozone, presents additional challenges including safety issues.

In this chapter, a special case of this underwater DBD was developed to combat this issue. Here, instead of a feed gas pumped down the coaxial discharge tube (see Figure 3.7 and Figure 6.1), the treated water itself is the ionizing media. Water vapor becomes the discharge gas, thereby circumventing the production of NO_x. This operation mode, termed "steam discharge" or "steam mode", operates such that the treatment liquid becomes the ionized medium fueling the plasma discharge. This no-airflow discharge mode was first noticed/examined by Foster et al. [**95**] and has been spectroscopically investigated by Garcia et al. [**385**]. Numerous authors have investigated plasma formation in self-generated steam pockets in saline solutions [**386**,**69**], but this formation takes place in high conductivity solutions (e.g., roughly 1.3 S/m in [**387**]) unlike the deionized water used in this work (10s of μS/cm). Work by Shih and Locke [**112**] demonstrated the use of discharge in a steam bubble; however, their discharge was created in boiling water – the steam pocket was not self-generated. In addition, self-generation of a steam pocket within low conductivity water reduces the engineering factors of the system.

Figure 6.1: The steam discharge in operation.

This chapter examines the steam discharge, which is investigated as a means to introduce advanced oxidation species into contaminated water for the purpose of water purification. Steam discharge operation did not result in significant pH changes in the processing of water or simulated wastewater, with the actual pH remaining between pH 6 to pH 7 during processing.

Simulated wastewater was shown to continue to decompose significantly after steam treatment, suggesting the presence of long-lived plasma produced radicals. During steam discharge operation, nitrate production is limited, and nitrite production was found to be below detection limits of available instrumentation (detection threshold roughly 0.2 mg/L). This discharge may be run at a wide range of power depositions, from approximately 30 W to 300 W (the limit of the power supply). Hydrogen peroxide production scales with increasing power, and is more efficient at producing hydrogen peroxide than the rates of many plasma sources reported in the literature thus far.

6.2 Experimental Approach

6.2.1 Baseline Studies: DI Water

For comparative purposes, the air and steam discharges were run at comparable discharge voltage and input power settings (~5.5 kV_{pk-pk} and ~60 W, respectively) for 4 minutes in deionized water. pH and conductivity measurements were made at regular intervals throughout the treatment to obtain time-resolved evolution of these properties. Immediately after plasma treatment, ion chromatography of the processed liquid was performed to analyze nitrate (NO_3^-) and nitrite (NO_2^-) content. These species were chosen as they are precursors to nitric acid formation as described in (6.1 through (6.5 below [**357**].

$$3NO_2 + H_2O \rightarrow 2H^+ + 2NO_3^- + NO \quad \textbf{(6.1)}$$

$$NO_2 + OH \rightarrow HNO_3 \quad \textbf{(6.2)}$$

$$2NO_2(g) \rightarrow N_2O_4(g) + H_2O(l) \rightarrow HNO_3\ (l) + HNO_2(l) \quad \textbf{(6.3)}$$

$$NO_2(g) + NO(g) \rightarrow N_2O_3(g) + H_2O(l) \rightarrow 2HNO_2(l) \quad \textbf{(6.4)}$$

$$3HNO_2(l) \rightarrow HNO_3 + 2NO(g) + H_2O(l) \quad \textbf{(6.5)}$$

Optical emission spectroscopy of both air and steam discharges was performed to assess the species production and various plasma properties. Hydrogen peroxide formation rates of the

steam discharge were measured for various power depositions, and compared to published plasma-derived hydrogen peroxide formation rates of other plasma devices.

6.2.2 Decomposition Studies: Simulated Wastewater

To study the decomposition capability of the steam discharge relative to that air feed source, the sources were both operated in simulated wastewater. In this case, a solution of methylene blue dye was used as a surrogate for textile mill wastewater commonly used in plasma decomposition studies [**371**,**372**,**274**,**373**,**388**,**73**]. It is well established that the textile mill industry is a major contributor to wastewater production and environmental pollution in general [**96**,**389**],. A 100 mL solution of 0.1 mM methylene blue dye with deionized water was used, treated and analyzed via a spectrophotometer and mass spectroscopy. The starting pH of the solution varied between 5.71 and 6.69, and conductivity of the solution varied between 13 and 100 μS/cm.

6.3 Results: Generation of Steam Bubble

The self-generation of the steam bubble was studied from several aspects. High-speed photography provided visual confirmation of microbubble structures. Thermocouple studies revealed the steam generation driven by electrode heating was unlikely. Finally, voltage, current and photo detector and acoustic data describe the discharge from bubble formation to plasma discharge.

6.3.1 Optical Assessment via High Speed Photography

To study the origin of the steam bubble, high-speed photography was used. As mentioned in related studies [**390**], the formation of the steam bubble was studied with a Redlake Motion Pro HS-4 camera. The repetition rate used was 200,000 fps, exposure of 1 μsec. The physical area imaged by the camera was an 8 x 148 pixel area, or approximately 0.24 x 4.5 mm around and below the electrode (see Figure 6.2).

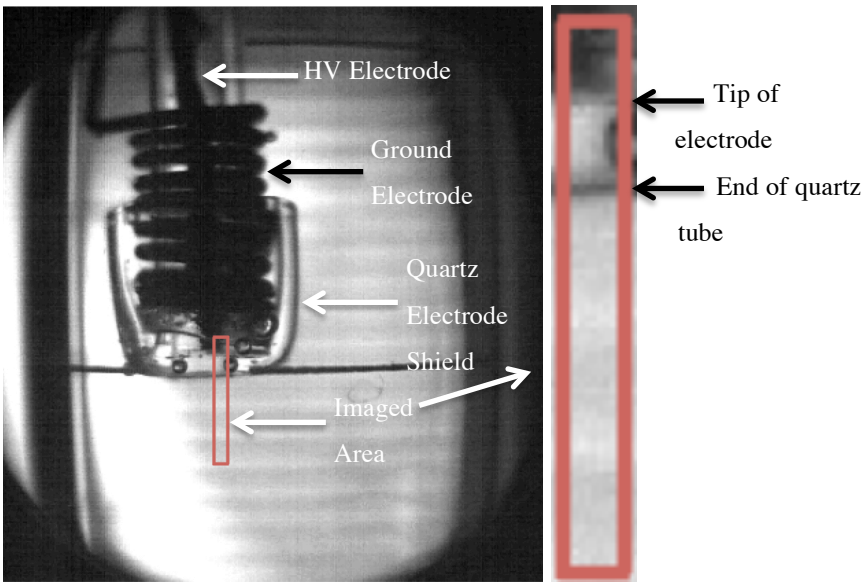

Figure 6.2: Electrode set up with imaged area highlighted (shielded electrode housing design).

Any change, other than slow bubble growth (i.e., bubbles forming on the electrode as in Frame 6 of Figure 6.4, also shown in Figure 6.5), occurs during the image taken during the rising edge of the voltage waveform, or on timescales shorter than 1 microsecond (the exposure time of the camera), eliminating the prospect of time resolution, at least at early times. It is possible that the rapidly increasing electric field at early times is sufficient to cause the localized heating responsible for the steam bubble generation. Seen in Figure 6.3 below is one such progression of images taken over the voltage cycle. The beginning of each voltage cycle of the first 19 applied voltage cycles may be seen in Figure 6.4.

As can be seen in Figure 6.4, evidence of a lower density medium is apparent in frame 6. This mass of presumably steam grows over the voltage cycle and is ejected into the liquid at the start of the next voltage cycle. The growth rate of this nascent steam bubble, which grows physically attached to the tip of the electrode, was measured to be approximately 0.33 m/s (see Figure 6.5).

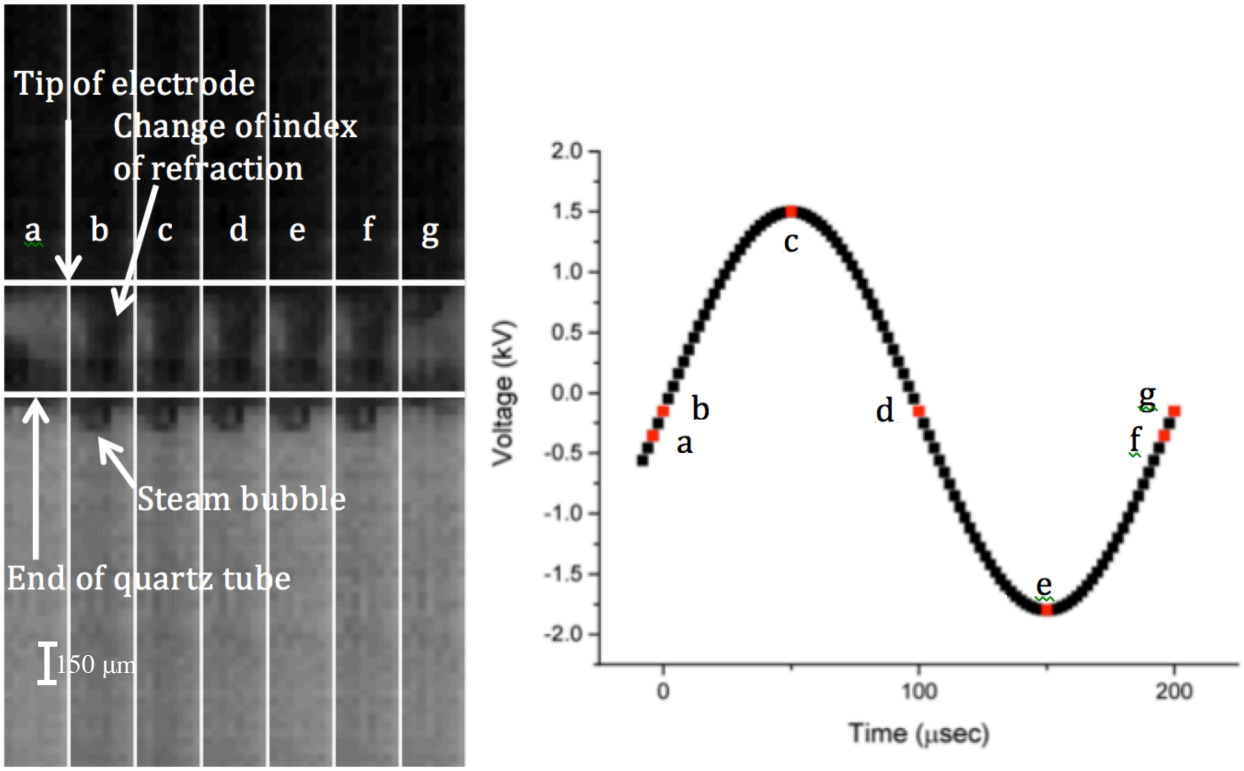

Figure 6.3: From [385]. Early stages of bubble formation. Frames taken over a voltage cycle; (a), taken at -5 µs from the start of the voltage cycle; (b), 0 µs; (c), 50 µs; (d), 100 µs; (e), 150 µs; (f) 195 µs; (g), 200 µs.

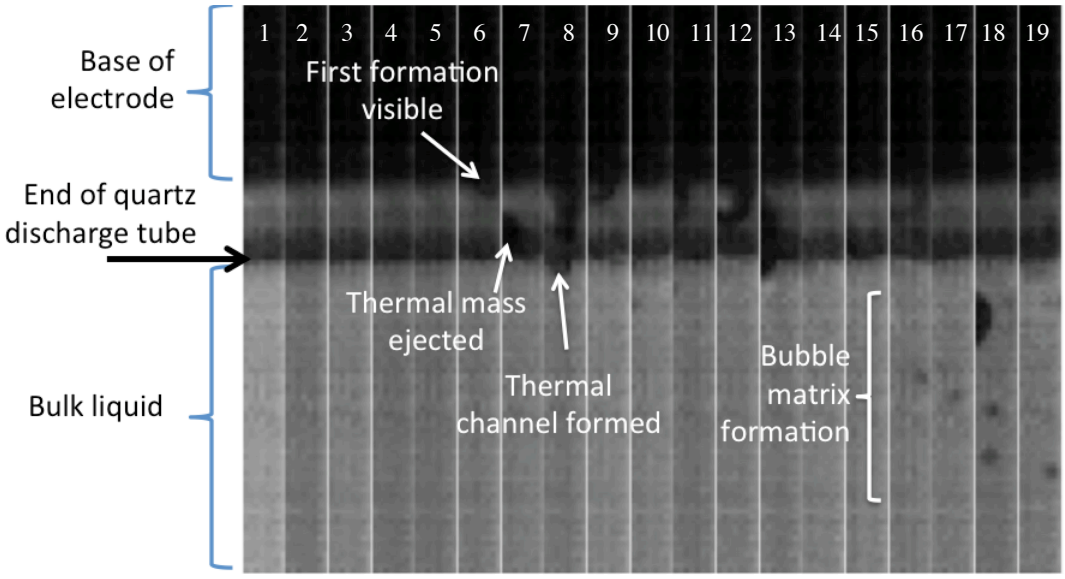

Figure 6.4: Steam bubble formation. Shown t = 0 to t = 3600 µsec. Voltage period = 200 µsec.

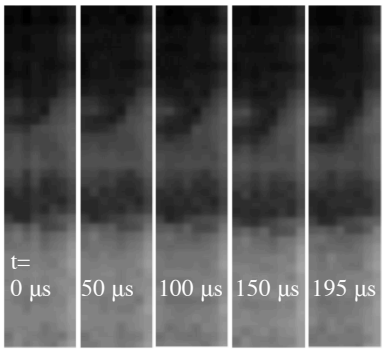

Figure 6.5: Growth of primordial steam pocket over 195 µsec.

Near the electrode, bubbles and low-density masses continue to be produced. The index of refraction changes associated with the darkened regions suggested local volume heating. At frame 16, a single steam bubble approximately 65 microns in diameter is observed 1.2 mm from the electrode tip. The following images show more bubbles appearing and moving in and out of the frame, starting to form a matrix of bubbles that eventually coalesce into the large, macroscopic bubbles that the discharge occupies.

6.3.2 Electrode Heating

To investigate the possibility of localized electrode heating of surrounding water, the temperature of the powered electrode was monitored during bubble formation. A high-temperature, ungrounded thermocouple was used to assess temperature of the electrode 10 mm away from the end of the powered electrode. During bubble formation and initial plasma formation, while subjected to high voltage for up to 3 seconds (the steam bubble had formed within the first 0.05 seconds, e.g., see Figure 6.6), the temperature of the electrode did not increase above 55 °C. Because of the high thermal conductivity of copper, it is expected that this temperature should be representative of the temperature at the actual electrode tip. In this regard, localized boiling driven by an electrode heating was ruled out as the mechanism for bubble formation.

6.4 Development of the Steam Plasma Discharge

The time evolution of the steam discharge was assessed by measuring the discharge voltage, charge transfer over a cycle using a sense capacitor, discharge current, photo diode response and resultant power deposition inferred the Lissajous method. The first 0.1 seconds after the start of application of voltage to the discharge applicator is shown in Figure 6.6. In that figure, V1 is the

applied voltage; V2, the voltage across the capacitor; I, the discharge current; and PD, the response from the photo diode. These first moments of the discharge suggest three distinct operating regimes: the Bubble Formation regime, which starts in the given figure from the onset of power application to approximately 0.03 seconds; the Transition regime which lasts from approximately 0.03 seconds to 0.045 seconds; and the Discharge region, which is the region from 0.045 seconds onward. While each region will be examined more fully in the proceeding paragraphs, an overview of all three regions shown in Figure 6.6 is useful in parsing out each operating regime.

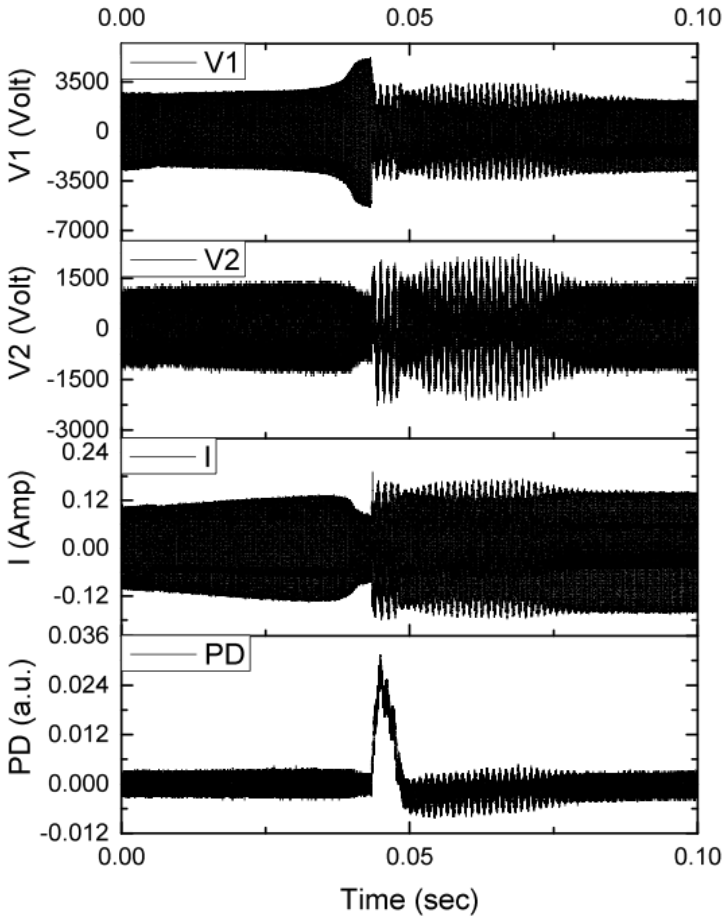

Figure 6.6: Voltage, current and photo diode response of the steam bubble plasma. Bubble formation (0 to ~0.03 seconds), transition to discharge (~0.03 to ~0.045 seconds), and plasma discharge (~0.045 seconds onward) may be observed.

As seen in Figure 6.6, the amplitude of the applied voltage stays roughly constant during the first portion of the Bubble Formation region, while the discharge current very slightly increases. This corresponds to the discharge area (i.e., the growing steam bubble surface area) increasing with current. When the bubble is fully formed, the Transition region begins (at roughly 0.035

seconds). Here, the discharge current sinks as the applied voltage begins to climb. This is expected as the system transitions into a spark. A discharge spike in the applied voltage is seen at roughly 0.044 seconds, which is followed by a response from the current, voltage across the capacitor, and photo diode. The remainder of the data (the Discharge region) gives a typical response seen by underwater DBD-type discharges [**97**]

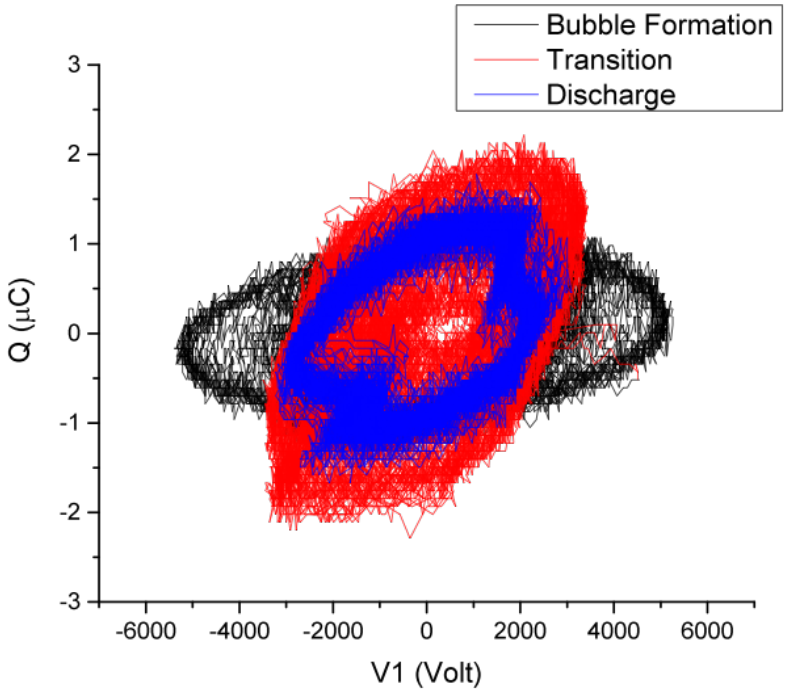

Figure 6.7: Corresponding Lissajous figures for data in Figure 6.6. The different operating regimes are illustrated with different colors.

The power dissipated throughout all three regimes is shown in Figure 6.7 and concisely demonstrates the system shifting from a primarily of liquid conduction and dissipation (the Bubble Formation region, approximately 50 W when the power supply is first turned on) to the plasma discharge regime, where the side slope of the figure are indicative of the capacitance of the dielectric (steam layer and water in this case). (The Discharge region is approximately 60 W when the discharge is fully ignited). The rotation of the parallelogram implies an increase in capacitance; indeed, the average capacitance as derived from the Lissajous figure for the Bubble Formation region is approximately 2.5×10^{-10} F, while the average capacitance from the Discharge region is approximately 6.0×10^{-10} F.

6.4.1 Bubble Formation

The first 0.03 seconds of discharge correspond to the early formation of the steam pocket. This phase may be observed in Figure 6.8, which depicts the first 0.001 seconds of discharge. The discharge current is seen to precede the applied voltage, as expected. The phase shift between the discharge current and the applied voltage is 28.3° (I leading V1), and between the applied voltage and the voltage across the capacitor is 78.2° (V1 leading V2). Here, the photo diode response, which is in phase with the applied voltage, is assumed to be pickup noise. The power deposition during the stage as determined via the Lissajous method was approximately 60 W, which is enough to vaporize approximately 26.9 mg of water per second. This vaporization is believed to fuel the microbubbles at the surface of the electrode and throughout the liquid as seen in Figure 6.4 (frame 6). The Lissajous figure characteristic of this phase may be seen in the top portion of Figure 6.12. In this phase the figure is an ellipse, signifying conduction throughout the cycle. This is observed in conventional DBD discharges operated at high frequency or low pressure. In these cases, the plasma does not decay before a new cycle begins. Charging and discharge effects are not pronounced in this case. In this present case, conductive fluid plays the role of the plasma.

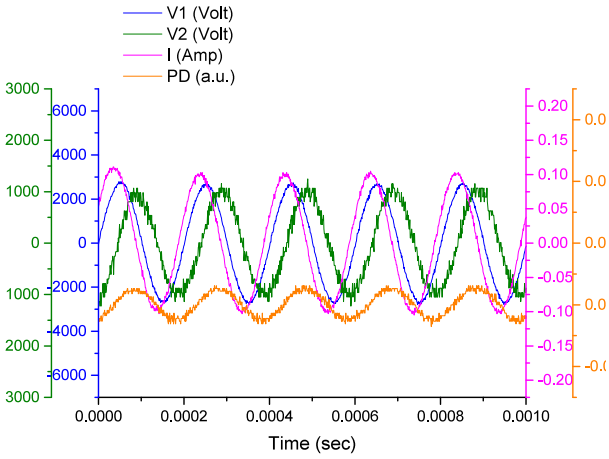

Figure 6.8: Applied voltage (V1, blue), voltage across capacitor (V2, green), discharge current (I, pink) and photo diode response (PD, arbitrary units, orange) for the first 1ms of power.

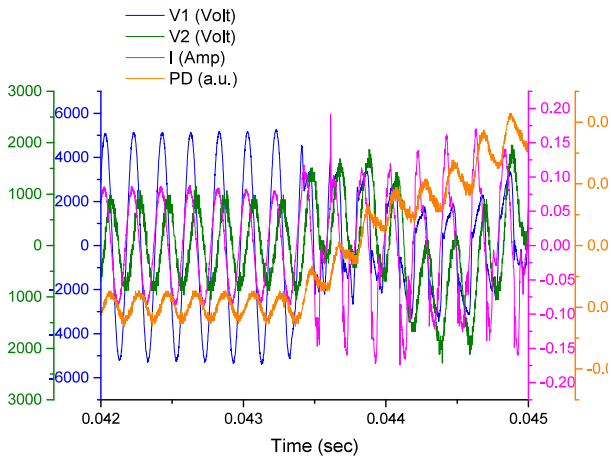

Figure 6.9: The Transition region.

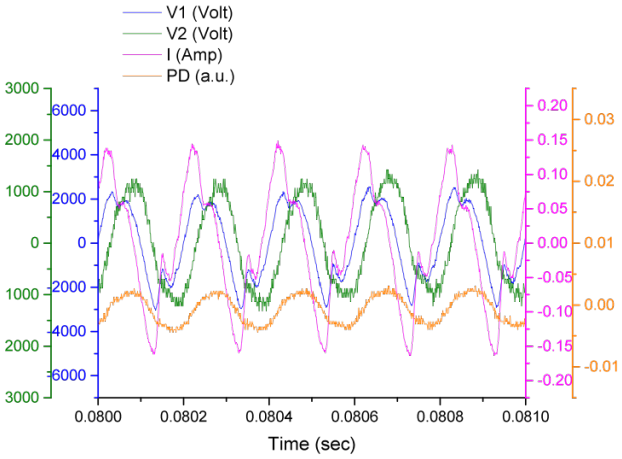

Figure 6.10: The Discharge region.

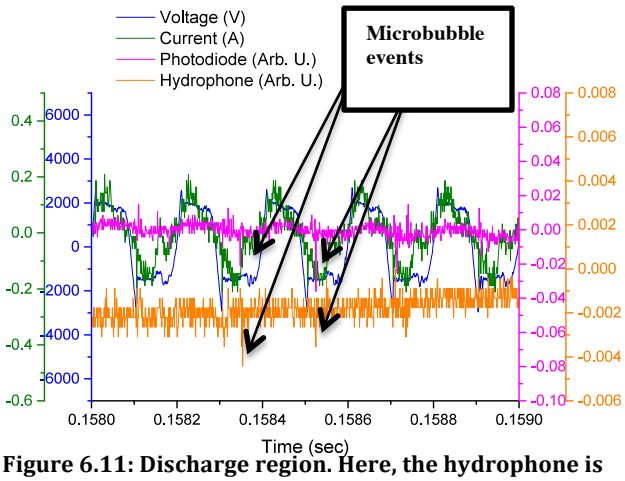

Figure 6.11: Discharge region. Here, the hydrophone is in sync with the photodiode's microspike responses to the plasma strikes.

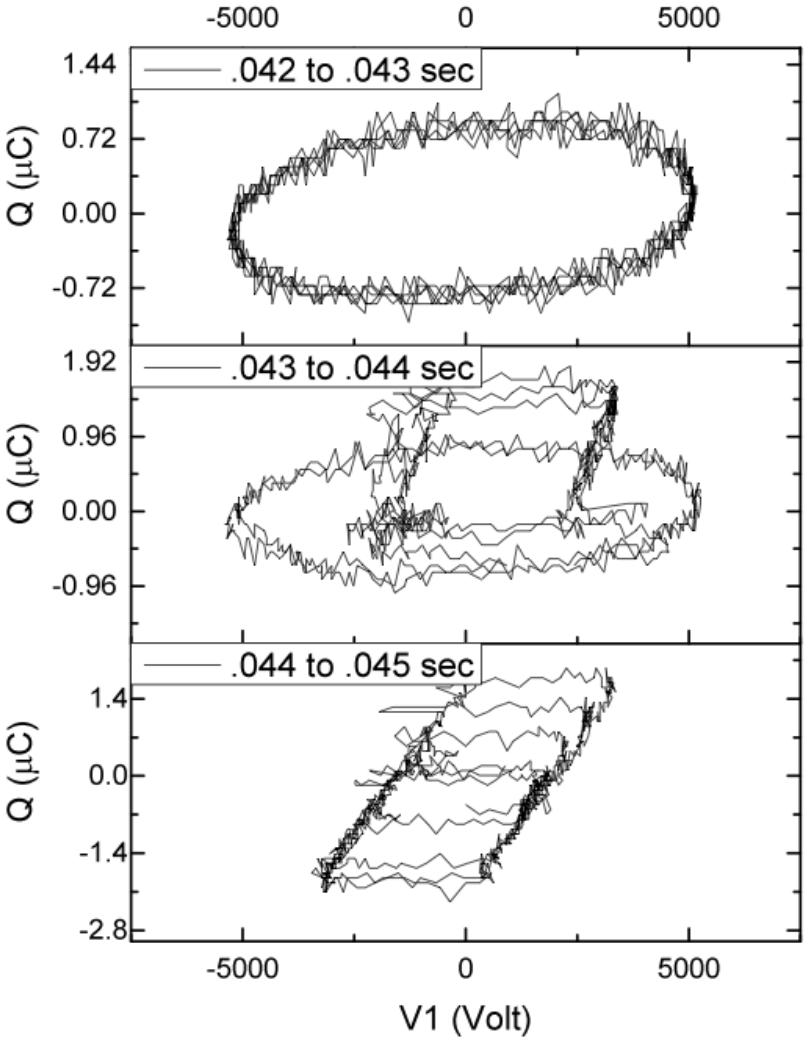

Figure 6.12: Corresponding power deposition from the Transition region. Average power for each of the three regions shown above are 71 W (top), 75 W (middle), and 84 W (bottom).

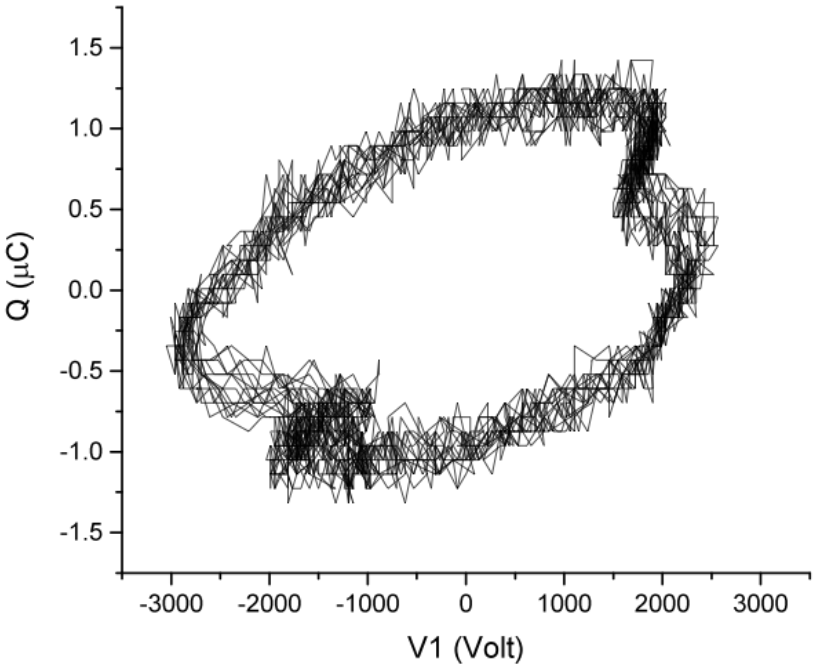

Figure 6.13: Corresponding Lissajous figure from the Discharge region, appr 60 W.

6.4.2 Transition Region – First Light

The transition between the macro-sized steam bubble and actual plasma formation can be inferred from Figure 6.9. A drop in applied voltage is observed around 0.0434 seconds. This voltage drop is immediately followed by a current spike. Only after the drop in voltage does the photo diode respond, suggesting the breakdown.

The power deposition of the Transition region may be seen in the Lissajous figures in Figure 6.12. Power dissipated increases from approximately 71 W to 84 W as the system switches from bubble formation mode to breakdown. As mentioned previously, the ellipse shaped Lissajous figures are associated with dissipation in the liquid leading to bubble formation. Formation of the vapor barrier and plasma gives rise to a parallelogram shaped. In principal, one Lissajous figure should pass from ellipse to line to parallelogram. The line would indicate full vapor coverage and thus complete isolation of the electrode from the liquid. Absence of the line Lissajous figure suggests that perhaps the electrode is not completely isolated from the liquid; that is, either certain portion of the electrode remain in contact with liquid or a rapidly developing discharge (e.g. corona) may form when coverage is sufficiently high.

6.4.3 Discharge Region

The section of data seen in Figure 6.10 and Figure 6.13 corresponds to 0.08 to 0.081 seconds after power was first applied to the electrode, well into the Discharge region of the data. These waveforms are characteristic of the steam discharge while in operation [**391**]. The power deposition of this region is roughly constant at approximately 60 W (Figure 6.13); overall, the steam discharge is fairly stable in individual regions of operation, with all changes in power associated with changes in operating mode. The fact that the Lissajous figure in Figure 6.13 is not exactly rectangular, but rather rounded, suggests that that vapor bubble coverage is not complete or steady and therefore over a cycle, the discharge current is associated with liquid conduction current as well as plasma current.

6.5 Acoustic Signal of the Steam Discharge

The premise of the discharge formation in low conductivity water is vapor formation at the electrode. Bubbles formed locally at the electrode contain super-heated vapor and thus cool rapidly and collapse.

The acoustic signature associated with bubble formation and collapse (e.g., [**392**,**393**]) gives a great deal of insight into the bubble formation process as well as subsequent bubble "tearing" and cavitation once the discharge starts. The acoustic signature for bubble and discharge formation was measured using a miniature-hydrophone. The evolution of the discharge with inclusion of the hydrophone response is shown in Figure 6.11.

Pressure pulses or spikes in the hydrophone signal occur with each spike from the photo diode, suggesting a link between plasma generation and the fluid dynamical effects driving sound generation. Possible sources of the acoustic signature include gas heating associated with steamer formation resulting in bubble formation and collapse as seen in [**392**,**393**]. Further analysis of signature is left to future work.

6.6 Summary

The measurements outlined previously suggest the generation of the steam pocket in deionized water is to be primarily due to electric field-driven processes, such as ion drag, that occur on time scales faster than 1 microsecond. This is opposed to mechanisms such as thermal-driven processes. The formation of the steam bubble is unique in that it is formed in low conductivity water (as opposed to saline solutions, e.g., [**244**]) and at low frequencies (i.e., not akin to microwave in water as in [**394**]).

6.7 Results: Baseline Tests with Deionized Water

6.7.1 pH

To access the effect of the steam plasma on water pH with that of an air driven plasma, the discharge tube was operated with air as the feed gas in deionized water for four minutes by the air mode. Deionized water was similarly processed with the steam discharge (no input air) for four minutes as well for similar applied voltages (~5.5 kV_{pk-pk}) and input powers (~60 W). During treatment, water samples were extracted periodically to access the time variation in the liquid water's pH. The time resolved variation in the pH is shown in Figure 6.14.

The pH of the water treated with air as the feed gas exhibited the expected drop-off in pH with time. After four minutes of processing, the pH of the water treated by the air discharge was approximately 3.1. This acidification behavior has been reported on extensively [**270**,**69**,**395**].

The pH of the water treated in steam mode, however, did not vary appreciably; after four minutes of processing at similar power levels, the steam discharge left the treated deionized water at a pH of 6.2. These observations support acidification theories that suggest the importance of nitrogen-based species (specifically, nitric (HNO3) and nitrous (HNO2) acids) on the acidification of liquids exposed to an air plasma (e.g., [**382**,**383**]).

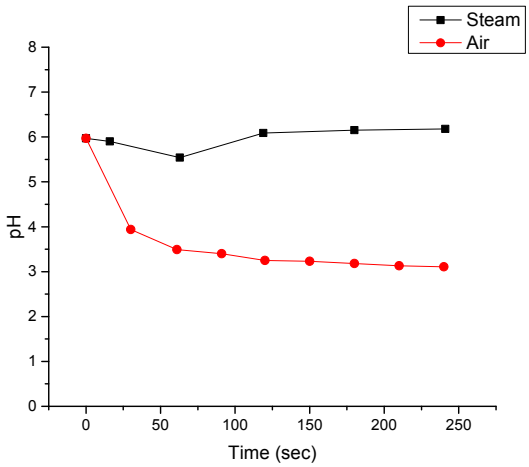

Figure 6.14: Discharges in DI water. Typical pH as a function of time for air (red) and steam (black) discharges.

Though the pH does not change appreciable with steam plasma treatment, it should be pointed out that the baseline value after treatment is weakly dependent on input power. At low input powers ~50 W, small reduction in pH (i.e., 6.2 to as low as 6.05) is typically observed in the pH while at higher powers ~250 W, the pH stays closer to neutral (pH 6.85 – 6.95). This effect is not well understood though it may be tied to dissolved nitrogen content in the water. Because the local water temperature is higher at the higher powers, then locally, the concentration of gaseous nitrogen is lower thus translating into lower acidification. In addition, the purity of the water and amount of dissolved gaseous species are also assumed to have a role in the final pH (e.g., formation of weak acids such as carbonic acid, H_2CO_3, from dissolved ambient CO_2).

In general, the self-ionization of water becomes important when the concentration of protons (H^+) is less than 3×10^{-7}, which roughly corresponds to pH values of 6.5 and greater. The dissociation of water is given as

$$H_2O\,(l) \rightleftharpoons H^+(aq) + OH^-(aq). \quad \textbf{(6.6)}$$

As free protons do not exist in water, above may also be written as

$$2H_2O\ (l) \rightleftharpoons\ H_3O^+(aq) + OH^-(aq).$$

(6.7)

At 25 °C, the water dissociation constant, K_w, is 1.01 x 10^{-14} where $K_w = [H_3O^+][OH^-]$ [**240**].

As the pH of the water treated with the steam plasma consistently falls in the range of pH 6 to 7, one should be mindful of the autoionization of water, as it can be a significant factor in the pH dynamics of the system. Analysis of possible formation of weak acids and detailed investigation into the pH chemistry is left to future work.

6.7.2 Conductivity

Conductivity is a measure of the capacity of the water sample under test to conduct electricity. The finite conductivity is in large part due to the presence of molecules that have

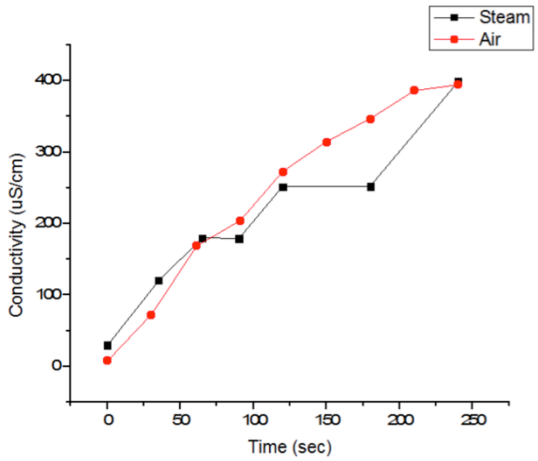

Figure 6.15: Discharges in DI water. Typical conductivity as a function of time for air (red) and steam (black) discharges.

ionized in the water, such as the disassociation of salts or acids. The conductivity of the treated water – regardless of treatment via steam or air plasma– increased with processing time.

This result is somewhat surprising at first blush, as conductivity can be significantly linked to pH due to the sensitivity of conductivity measurements on the concentration of hydrogen and are usually assumed to be a result of acidification [**357**]. The result suggests that electrolytic processes at the electrode may be to blame. For example, the dissolution of metal into the liquid would result in a measurable conductivity change. This can occur with copper electrodes [**69**]. Here the mechanism involves the formation of carbonic acid owing to the presence of residual oxygen and carbon dioxide in the water. The carbonic acid can remove the oxide layer exposing

ionic copper, which would then dissolve into the liquid, thereby increasing the conductivity. It is entirely possible that the observed changes for both discharges is due to this electrode ion dissolution effect.

Alternatively, the increased conductivity may be due to the chemistry of the steam discharge. The mobility of H^+ in water is the highest of any ion (36.25×10^{-4} cm^2 $(s\ V)^{-1}$), which gives protons the highest impact on conductivity measurements (with the hydroxide ion, OH^-, coming in second at 20.62×10^{-4} cm^2 $(s\ V)^{-1}$, or 57% proton mobility) [**265**]. This results in hydronium, H_3O^+, having a higher mobility than molecules of comparable size [**357**]. Therefore, the increase in conductivity, regardless of discharge method, may be due to the significant fraction of hydronium formed in the treated liquid. For the steam discharge, the increasing conductivity with level pH reinforces the idea that complex acid-base equilibrium chemistry is occurring (i.e., the production of some weak acid is occurring to keep the pH between 6 and 7 but the mobility of the acidic protons increases conductivity measurements).

The formation of hydronium under electron impact (may be gas or liquid phase) is due to the electron impact on water, which quickly generates hydronium [**265**].

$$H_2O + e \rightarrow H_2O^+ + 2e \quad \textbf{(6.8)}$$

$$H_2O^+ + H_2O \rightarrow H_3O^+ + OH \quad \textbf{(6.9)}$$

The formation of H_3O^+ can also form hydroxyl radicals, OH (see (6.9)). This highly reactive species (with oxidation potential of 2.80 V) is plays a key role via advanced oxidation in sterilization [**396**] and decomposition [**397**] processes.

6.7.3 Nitrate and Nitrite Concentrations

Nitrate and nitrite concentrations in both air plasma and steam plasma-treated water samples were measured. These samples were extracted after four minutes of plasma treatment. In the air plasma treated water solution, the concentration of nitrates and nitrites formed in solution was found to be around 100 ppm and 10 ppm, respectively, or ten times the EPA limit for each species for drinking water [**276**]. The water treated with discharge operating in steam mode, however, was found to have less than 0.5 ppm of nitrate and no nitrite was detected. Without injected gas, the absence of appreciable amounts of nitrogen does not give rise to the production

of NOx species. Indeed, the solubility of nitrogen in water near room temperature is half that of oxygen [**240**]. This result supports the notion that the pH drop in air discharges in liquid water is most likely due to nitrogen-based acids, especially nitric acid.

Table 6.1: Nitrate and nitrite production [73]. Copyright 2015 The Japan Society of Applied Physics.

	Average Nitrate Concentration (ppm)	**Average Nitrite Concentration (ppm)**
Untreated DI water	0.00	0.00
DI water treated via air discharge, 4 minutes	99.63	10.92
DI water treated via steam discharge, 4 minutes	0.45	0.00 (undetected)

The absence of NOx species in steam plasma treated water is desirable for peroxide production. It is well known that nitrites quickly react with H_2O_2 in acidic solutions, and can suppress H_2O_2 generation, decomposing via [**309**]

$$NO_2^- + H_2O_2 + H^+ \rightarrow NO_3^- + H_2O + H^+. \quad (6.10)$$

The very low concentrations of nitrites and nitrates produced in solution in steam plasma treatments as seen in Table 6.1 suggests that this mechanism is not expected to play a role in reducing peroxide production. It should be noted that the water was not degassed, and the limited quantities of nitrate and nitrite are due to the dissolved gases within the liquid itself.

6.7.4 Optical Emission Spectroscopy: Steam vs. Air Discharge

Optical emission spectra were acquired from both the steam and the air fed discharge. The air spectra are dominated by nitrogen emission (Figure 6.16) while the steam plasma emission spectra were found to consist primarily of OH and hydrogen peaks (Figure 6.17).

The results from the air discharge are as expected from a water-air discharge. Depending on the operating conditions, important species such as the hydrogen beta (486.1 nm), hydrogen alpha (656.3 nm), and the oxygen triplet (777 nm) may be easily observed and will vary in intensity.

Conversely, the results from the steam discharge (see Figure 6.17) confirm the speculation of a primarily water vapor-based plasma. Here, the only species visible are those of water, the

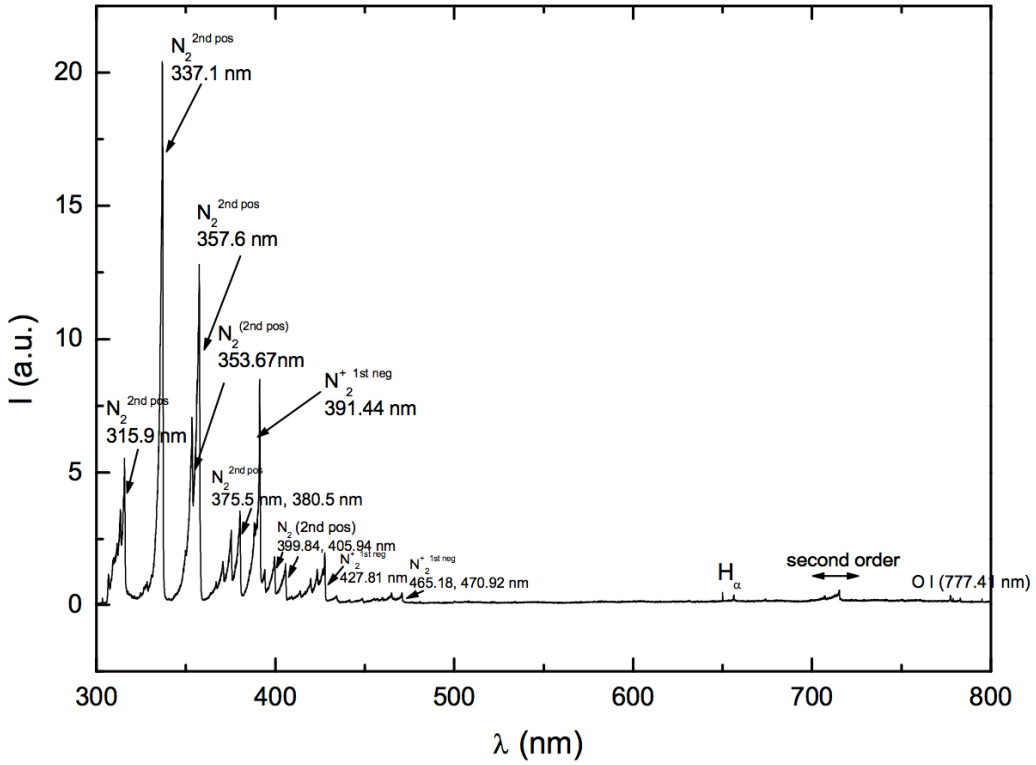

Figure 6.16: Optical emission of air discharge in deionized water. Numerous nitrogen species are visible.

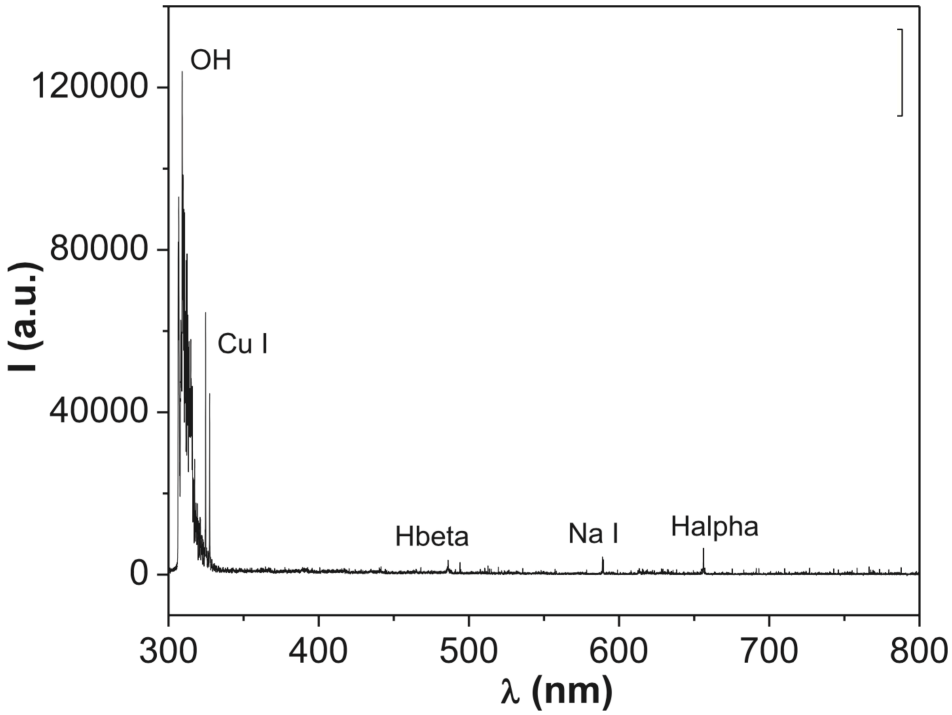

Figure 6.17: Optical emission of steam discharge in deionized water. No nitrogen emission is visible. Copper and sodium lines are emission from the electrode and quartz housing.

electrode material (copper), and the quartz electrode housing material (sodium). For water species, only the first two lines of the Balmer series (H_α and H_β) and the OH(A-X) band appear.

From these species, the electron density and gas temperature were estimated (see discussion below).

6.7.4.1 Electron Density

The electron density of the discharge (i.e., during the third phase) was determined through the Stark broadening of both the H_α and H_β lines. The relation between Stark broadening and electron density is given as [**318**]

$$\Delta\lambda_{Stark} = 4.8\ nm \times \left(\frac{n_e}{10^{23} m^{-3}}\right)^{0.68116}. \quad \textbf{(6.11)}$$

The total contributions on the broadening of the H_β line (including instrumental broadening) were assessed using the following calculations of van der Waals ((6.12) and Doppler ((6.13) broadening [**318**]:

$$\Delta\lambda_{vdW} = \frac{4.10}{T_{gas}^{7/10}} nm \quad \textbf{(6.12)}$$

$$\Delta\lambda_D = 3.48 \times 10^{-4} T_{gas}^{1/2}\ nm. \quad \textbf{(6.13)}$$

In addition to (6.11 above, the electron density may also be determined from tabulated calculated electron densities for many Stark broadening linewidths [**319**]. Using both, the electron density was calculated to be approximately $10^{21} m^{-3}$ [**385**].

6.7.4.2 Gas Temperature

Pre-2010, OH(A-X) was heavily used to determine the gas temperature of water-plasma systems, as it was assumed that rotational population of OH(A) is thermalized into an equilibrium. However, Bruggeman et al. [**398**] demonstrated the electronic quenching of OH(A) due to water can have a significant impact on the gas temperature measurement, as the distribution becomes non-Boltzmann. Other authors have demonstrated the non-equilibrium of

the excited OH molecule [**399**]. For this reason, the OH(A-X) method of determining gas temperature is best avoided and other methods are preferable [**400**].

However, determining gas temperature for the steam discharge is more difficult. Here, the spectrum clearly shows only the OH(A) band, H_β, H_α, and a few copper lines. No other species is observed, not even oxygen. The copper lines are not broadened enough to determine a gas temperature measurement.

In an attempt to gain a more accurate gas temperature measurement, nitrogen gas (<< 7.9 sccm) was leaked into the discharge to determine the gas temperature via optical emission spectroscopy of the second positive system of N_2. The gas was leaked into the discharge tube after the steam bubble and discharge were initiated. However, even at such small flow rates (no gas bubbles that could be observed by the human eye were formed), the discharge was strongly affected. The plasma quickly heated the water to boiling within a few minutes; the steam discharge on its own would take many tens of minutes to heat the water to a boil. As such a noticeable difference occurred even with a minute quantity of N_2, this method of temperature determination was abandoned.

One possible method of determining the gas temperature of the steam discharge is two-color OH-planar laser induced fluorescence (OH-PLIF) (e.g., [**400**]). Those engaging in further study of the steam discharge system should utilize this method.

Here, the gas temperature was found through simulating thermal distribution of the OH(A-X) band via LIFBASE spectroscopy software [**323**], and comparing theoretical results to experimentally observed lines. The gas temperature was found to be approximately 2800 K [**385**]. A detailed investigation into the emission spectroscopy of the steam discharge plasma into deionized water may be found elsewhere [**385**].

At the measured gas temperatures (~2800 K), thermal dissociation of water producing OH and H starts to become significant ($H_2O + H_2O \rightarrow OH + H + H_2O$; $k(T_{gas} = 2800\ \mathrm{K}) \approx 10^{-18} - 10^{-16} \mathrm{cm^3 s^{-1}}$ [**401**]). Computational models by Bruggeman and Schram [**402**] suggest production of OH by thermal dissociation becomes comparable to electron dissociation at gas temperatures of 3000 K and greater, though for electron temperatures of 1-2 eV, many authors given the reaction rate of electron dissociation of water a several orders of magnitude above

thermal dissociation (where $H_2O + e^- \rightarrow OH(X) + H + e^-$; $k(T_e = 1 - 2\ \text{eV}) \approx 10^{-12} - 10^{-10}\text{cm}^3\text{s}^{-1}$ [**402**,**403**]).

6.7.4.3 Ozone Production in Steam Discharge

Ozone is not expected to be produced in appreciable levels in the steam discharge. This is in contrast to studies such as [**404**], which use microwave excitation to form superheated bubbles in which the plasma is ignited. As optical emission spectroscopy of the system does not show any detectable oxygen lines (Figure 20), if it assumed ozone is primarily formed through [**405**]

$$O + O_2 + M \rightarrow O_3 + M,$$

(6.14)

ozone production is severely restricted. Ona and Oda [**406**] observed in a pulsed corona discharge in humid-air an increase in water vapor by 2.4% reduced ozone production by ~6. Indeed, models of DC corona discharges in 100% relative humidity air found ozone suppression by OH [**407**]:

$$O_3 + OH \rightarrow HO_2 + O_2$$

(6.15)

This leads to more OH by HO_2 recombination [**408**]:

$$HO_2 + HO_2 \rightarrow H_2O_2 + O_2$$

(6.16)

It is important to note that Foster et al. [**95**] observed weak O I lines (at 777 nm) during the initial observation of the steam discharge. While not observed in these studies, oxygen atoms will combine with ozone and water molecules, further preventing ozone production [**409**]:

$$O + O_3 \rightarrow O_2 + O_2$$

(6.17)

$$O + H_2O \rightarrow OH + OH$$

(6.18)

Because of this chemical interaction and similar observations (e.g., [**410**]), strengthened with the fact that the ionizing medium of the discharge itself is water vapor, ozone production of any significance is not expected in this discharge. Ozone generation was not measured in either discharge.

6.7.5 Hydrogen Peroxide Production

As discussed previously, optical emission spectra suggests the steam discharge generates of OH, H_α, H_β, and electrode material (see Figure 6.17). Therefore, it is assumed the steam discharge decomposes contaminants primarily through OH species and hydrogen peroxide, and any reactive daughter products. Nearly exclusive production of OH and H_2O_2 makes the steam discharge ideal for oxidation and sterilization applications.

The discharge was operated at various power levels in 50 mL of deionized water (starting pH = 6.9 ± 0.1, conductivity = 8 ± 1 μS/cm). The formation rate of hydrogen peroxide was found to increase with deposited power, as seen in Figure 6.18. These generation rates of hydrogen peroxide are comparable to rates reported in the literature and may be substantially larger to other plasma sources reported in literature. Figure 6.18 below gives an overview of several different sources and the reported hydrogen peroxide formation rates.

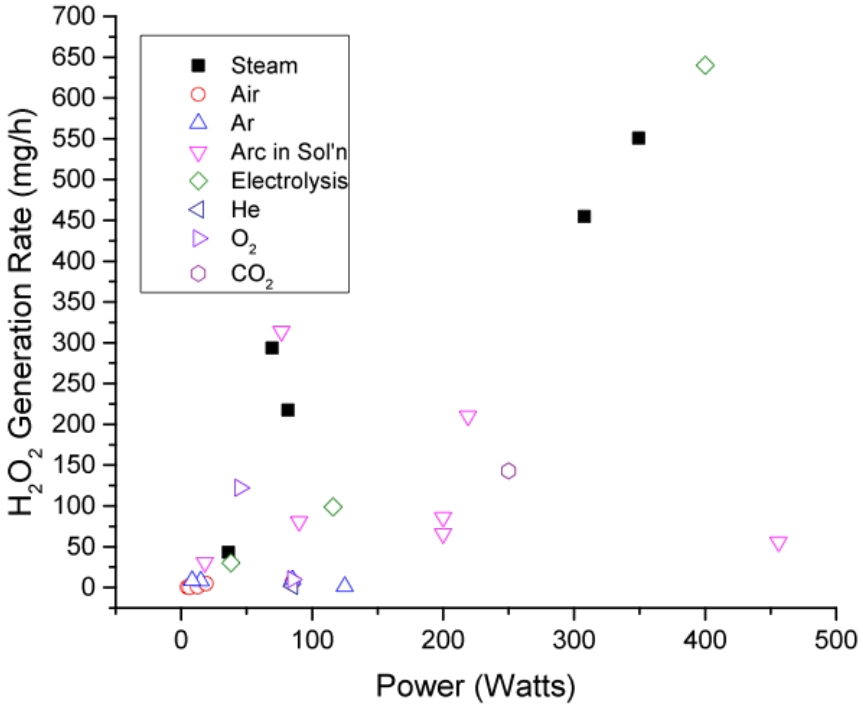

Figure 6.18: Hydrogen peroxide production in various plasma sources [177]**. Steam, this paper; Air** [411,412,413]**; Argon** [413,414]**; Arc in solution** [415,416,417,418]**; Electrolysis** [419]**; Helium** [413]**; Oxygen** [413,420]**; Carbon dioxide** [421]**.**

6.8 Computational Verification: *GlobalKIN* Model in Comparison to Experimental Findings

The production of liquid species was computationally predicted via *GlobalKIN*. Here, the steam discharge in liquid water was modeled as a 1 cm diameter water vapor pocket surrounded by a 0.5 mm layer of water. The plasma was modeled as a spherical shell that occurred within the outer most 50 μm of the sphere. Nitrogen and oxygen liquid-phase species were included to study the effect of naturally occurring dissolved air in the water. As discussed in Chapter 3, the power density was calculated from voltage and current waveforms taken from the experiments that the simulation results would be compared. The simulation was run to 0.1 seconds of processing time; an example of such results may be seen in Figure 6.19.

6.8.1 Results

Comparison of experimentally measured versus computationally predicted hydrogen peroxide generation rates for steam discharges at various power levels may be seen in Table 6.2. Comparison of experiment and computation nitrate and nitrite generation rates for air and water discharges may be seen in Table 6.3.

Table 6.2: Hydrogen peroxide generation rates; experimental observation versus computational prediction.

Steam Discharge Power (W)	**H_2O_2 Generation Rate (mg/h)**			
	Experiment		*Computation*	
	Measured	*Normalized*	*Predicted*	*Normalized*
81.6	217.3	0.395	71.7	0.376
307.8	284.2	0.516	107.4	0.563
349.3	550.7	1	190.6	1

Table 6.3: Nitrate and nitrite generation rates in air and steam discharges; experimental observation versus computational prediction.

	NO_3^- Generation Rate (mg/h)		**NO_2^- Generation Rate (mg/h)**	
	Experimentally Measured	*Computationally Predicted*	*Experimentally Measured*	*Computationally Predicted*
Air, 80 W	150	22.4	15	1.43E-03
Steam, 80 W	0.68	45	not detected	1.60E-07

Currently, the model predicts hydrogen peroxide generation rates of approximately one third the experimentally measured rate. However, as the computationally derived generation rates approximately scale with power with the experimentally derived generation rates (refer to the

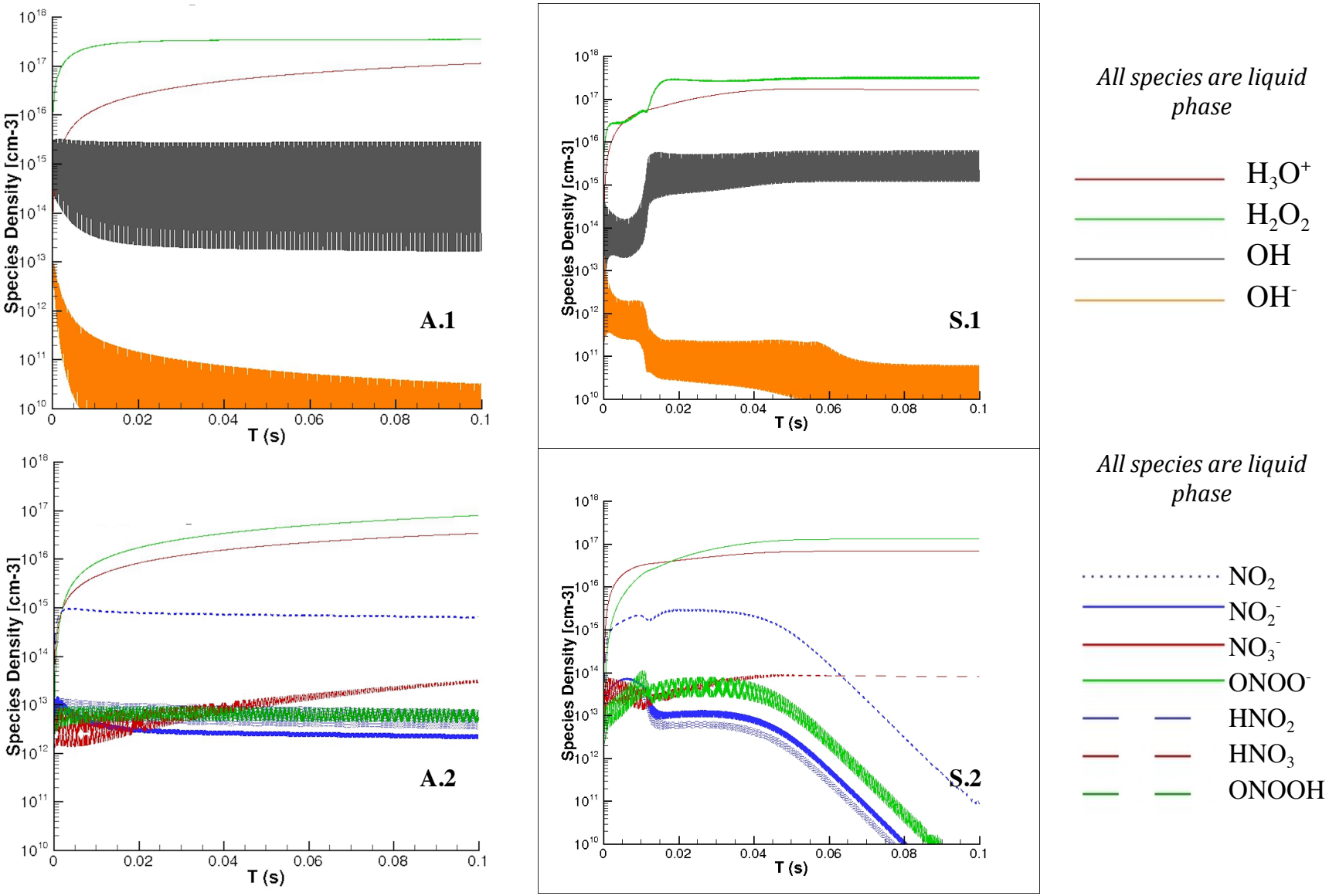

Figure 6.19: Evolution of liquid-phase species in air (A.1 and A.2) and steam discharges (S.1 and S.2). Discharge power: 80 W (both cases)

normalized values given in Table 6.2), it is assumed there are minor edits necessary to the code. As carbon-based species (e.g., COx) are not included in the liquid-phase reactions, it is assumed discrepancies are at least partially due to those missing kinetics and reactions [**324**].

When modeling nitrate and nitrite production in air and steam discharges, a stronger deviation occurs. For nitrate production, *GlobalKIN* is not a accurate predictor for the steam discharge (off by two orders of magnitude). For nitrite production, *GlobalKIN* is even worse for the air discharge, off by five orders of magnitude. Interestingly, *GlobalKIN* appears to correctly predict the steam discharge's near-zero nitrite production. It is strongly suspected that the lack of carbon and carbon-based may play a significant role in correctly predicting liquid-phase chemistry.

6.9 Results: Sterilization Efficacy of Steam Discharge to Treat Methylene Blue Dye

To study the decomposition efficiency of the steam discharge, the discharge was configured to decompose a wastewater simulant. The wastewater simulated contained 0.1 mM of methylene blue dye, an organic dye. This dye has been used in the past to study plasma decomposition efficiency of organic contaminants [**53**,**96**,**397**,**371**]).

Discharge operating conditions were varied for each source (i.e., air and steam discharges). The steam discharge was operated (a) similar and (b) greater than the operating power of the air discharge. The various discharges were operated until (a), similar levels of degradation were achieved (as inferred from spectrophotometric absorbance measurements), and (b), for various time scales.

6.9.1 Decomposition Rates and Power Levels

The percentage of methylene blue decomposed by all methods was determined spectrophotometrically, using the reduction in absorbance of a methylene blue absorbance line (609 nm) to track decomposition. Steam discharge treatment of the MB solution was performed at two different relative power levels and compared to an air discharge treatment (see Table 6.4).

Preliminary results give the maximum energy efficiency to achieve 50% dye destruction (i.e., the G_{50} value) measured by the steam plasma is around 0.16 g kWh^{-1}. This is in comparison to the air discharge, which can achieve G_{50} efficiencies of over 5 g kWh^{-1}. This difference of an order of magnitude is recognized in the decomposition parameters. For comparable operating

Table 6.4: Decomposition efficacy of air and steam discharge on MB solution.

	Deposited Power (W)	Treatment Time (mm:ss)	Initial/Final MB Concentration (μM)	% Reduction	G_{50} Value (g kWh^{-1})
Air	75	4:30	156/3.68	97.6	5.2
Steam	76	33:42	92.5/5.45	94.6	0.15
Steam	117	15:00	92.5/18.05	82.0	0.16
Steam	200	5:00	114/42.0	63.3	0.16

powers (air and steam at approximately 75 W), the steam discharge required roughly 7.5 times longer processing time to achieve similar reduction levels (~34 minutes versus ~15 minutes). Increasing the steam discharge power (to 117 W and 200 W) only increases the G_{50} value of the process slightly to 0.16. It is expected that the air discharge is a more efficient decomposition driver as it has a greater number of reactive species that contribute to the decomposition ability of the air discharge, e.g., such as RNS; this is reflected in the G_{50} value. However, the steam discharge is still attractive the pH levels are kept roughly neutral. Additionally, G_{50} values of 0.16 g kWh^{-1} are similar or an order of magnitude larger than other plasma discharges, such as glow discharge electrolysis and diaphragm discharges [**50**]. In addition, as the reduction in pollutant is an initially rapid process, using the steam discharge as a pretreatment to initiate pollutant decomposition and not as the sole driver of decomposition would decrease the energy cost while retaining specific decomposition chemistry.

Finally, it should be noted that these concentrations were determined spectrophotometrically, and are not necessarily an indication of complete destruction of the methylene blue dye molecule (see [**96**] for discussion). Molecular analysis is important, especially with the use of dyes, as merely relying on physical change (e.g., the color disappearing) is only an indication of possible decomposition thanks to the production of secondary products. Mass spectra of the methylene blue dye solutions, treated by both air and steam discharges, were analyzed using the electrospray mass spectrometer. As with similar experiments [**96**], the results of mass spectroscopy show numerous intermediaries that are formed during the violent decomposition. Many of these peaks are unidentifiable, with m/z values that most likely correspond to fragments of the dye, such as pieces of benzene rings.

6.9.2 pH

The changes of pH over time for the treatment of the methylene blue (MB) dye solution by both the steam and air discharges for both power levels mimicked the results seen with treatment of plain deionized water (see Figure 6.14). When processed with the air discharge, the MB solution pH drops off exponentially (see Figure 6.20). The solution treated with the steam discharge, on the other hand, did not experience a drop in pH, but instead stayed relatively neutral and unchanged throughout processing time (see Figure 6.20). From a plasma water purification perspective, this result suggests that the steam discharge has the ability to breakdown contaminants without creating highly acidic solutions or decomposition intermediates. It also suggests that the final pH of the processed solution is more dependent on the feed gas used in the discharge and not on the contaminant being treated.

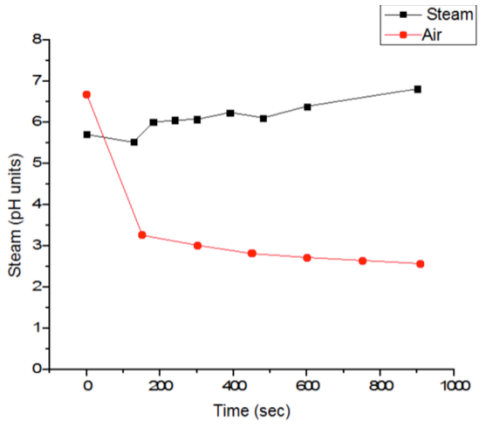

Figure 6.20: pH as a function of time for air (red) and steam (black) discharges in MB solution.

6.9.3 Conductivity

As previously seen with plain DI water, the conductively of the MB solution rose with treatment time regardless of discharge type (see Figure 6.21). Again, the rise in conductivity can be a function of the increase in hydronium in the system (see the previous section for discussion). Furthermore, with the addition of a contaminant, as the foreign molecule is destroyed and broken into secondary pieces and further mineralized, the charged fragments add to the overall conductivity. The results from the HPLC mass spectroscopy (see following section) do show a multitude of peaks corresponding with fragmentation of the mother molecule.

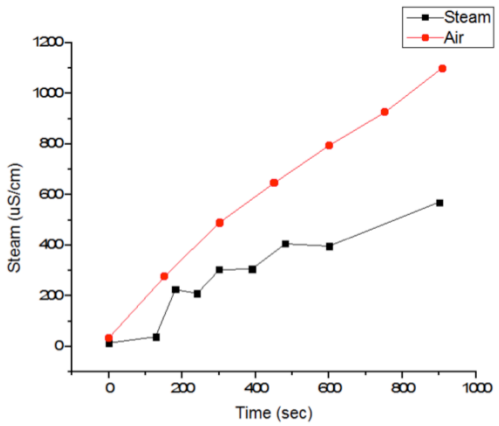

Figure 6.21: Conductivity as a function of time for air (red) and steam (black) discharges in MB solution.

6.9.4 Continued destruction post-treatment

Solutions treated with the steam discharge continue to decompose after the liquid has been subjected to the discharge. 100 mL of 0.115mM of Methylene Blue dye solution was processed for 5 minutes by the steam discharge. The decomposition curve of this treatment may be seen in Figure 6.22, where 63% reduction in dye concentration (as determined via spectrophotometer) was achieved after 300 seconds of processing via steam discharge at approximately 200 W.

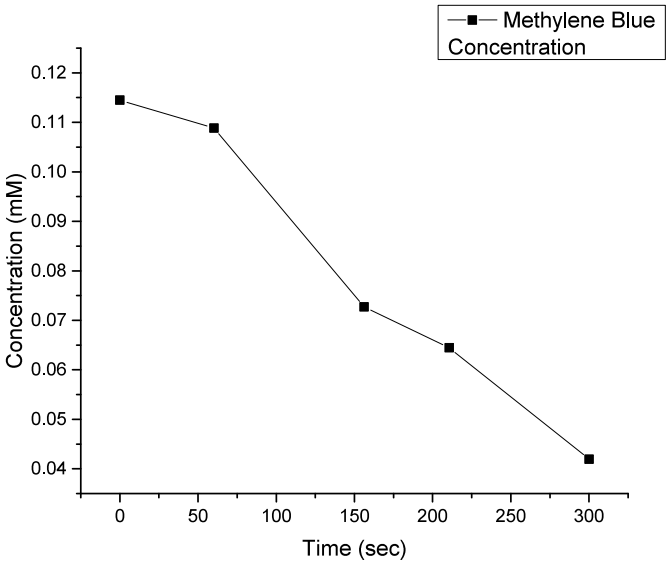

Figure 6.22: Methylene blue concentration reduction over processing time.

After steam plasma treatment, the solution was sealed from the ambient environment and left to age. After 14 days, the aged liquid was found to have a MB concentration of 6.2×10^{-3} mM. This corresponds to a further reduction in MB concentration over the 14-day period of over 85%,

and the total reduction of MB concentration by steam discharge and aging was over 94% (from 0.11 mM to 6.2×10^{-3} mM).

This continued decomposition is assumed to be due to the produced hydrogen peroxide. Immediately after the 5 minutes of steam discharge treatment, the solution contained more than 3% hydrogen peroxide. After the 14-day aging period, the solution contained no detectable hydrogen peroxide.

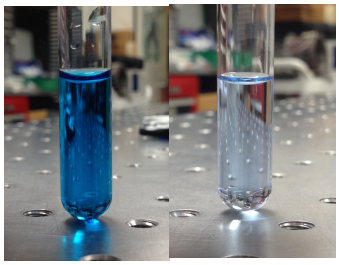

Figure 6.23: The effect of aging on steam-treated MB solutions. Left, solution after 5 minutes of steam treatment. Right, solution after 5 minutes of steam treatment and 14 days of aging.

6.9.5 Molecular Analysis

To determine the final decomposition results of the two discharges, mass spectroscopy was performed on before- and after-treatment samples. Molecular analysis is important, especially with the use of dyes, as merely relying on physical change (e.g., the color disappearing) is only an indication of possible decomposition thanks to the production of secondary products [**96**]. Mass spectra of the methylene blue dye solutions, treated by both air and steam discharges, were analyzed using the electrospray mass spectrometer. As with similar experiments [**96**], the results of mass spectroscopy show numerous intermediaries that are formed during the violent decomposition. Many of these peaks are unidentifiable, with m/z values that most likely correspond to fragments of the dye, such as pieces of benzene rings.

Figure 6.24 is the ESI-MS profile of an untreated MB solution; here, the intense peak of MB at m/z = 284 is clearly seen. Figure 6.25 and Figure 6.26 are the ESI-MS profiles of the MB solution after treatment; Figure 6.25 is after treatment with the air discharge and Figure 6.26 is after steam discharge treatment.

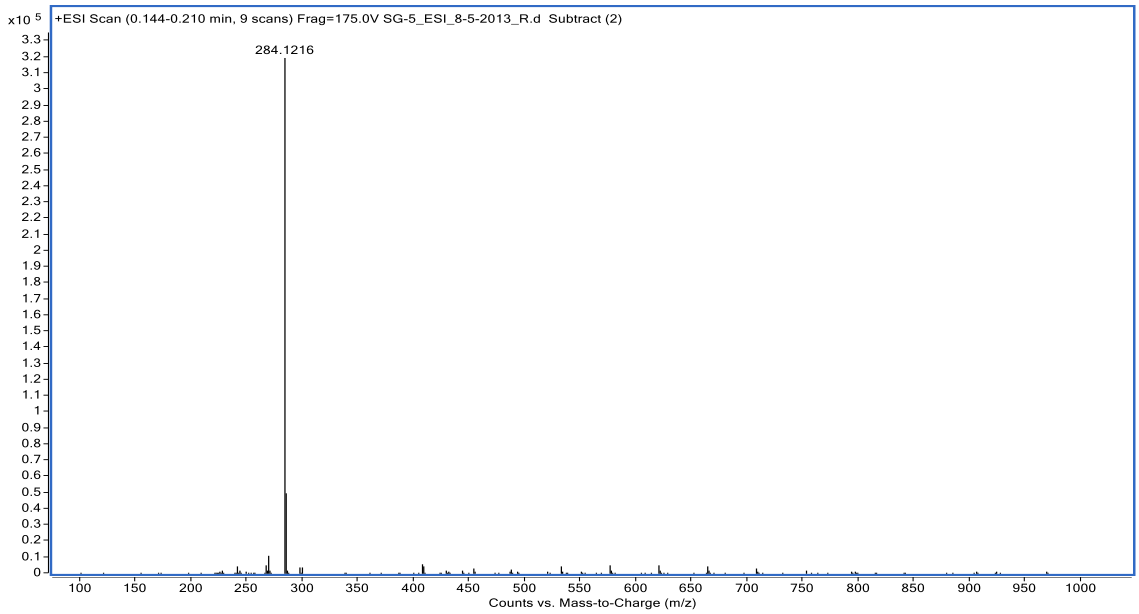

Figure 6.24: Untreated MB

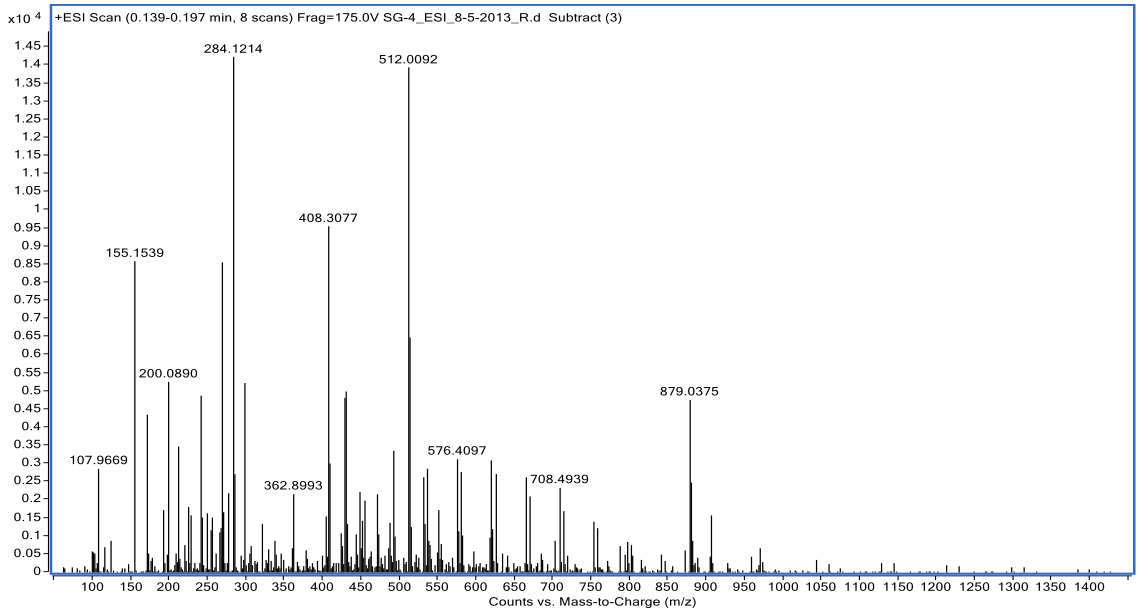

Figure 6.25: Air discharge, 17.62 minutes processing time at 80 W.

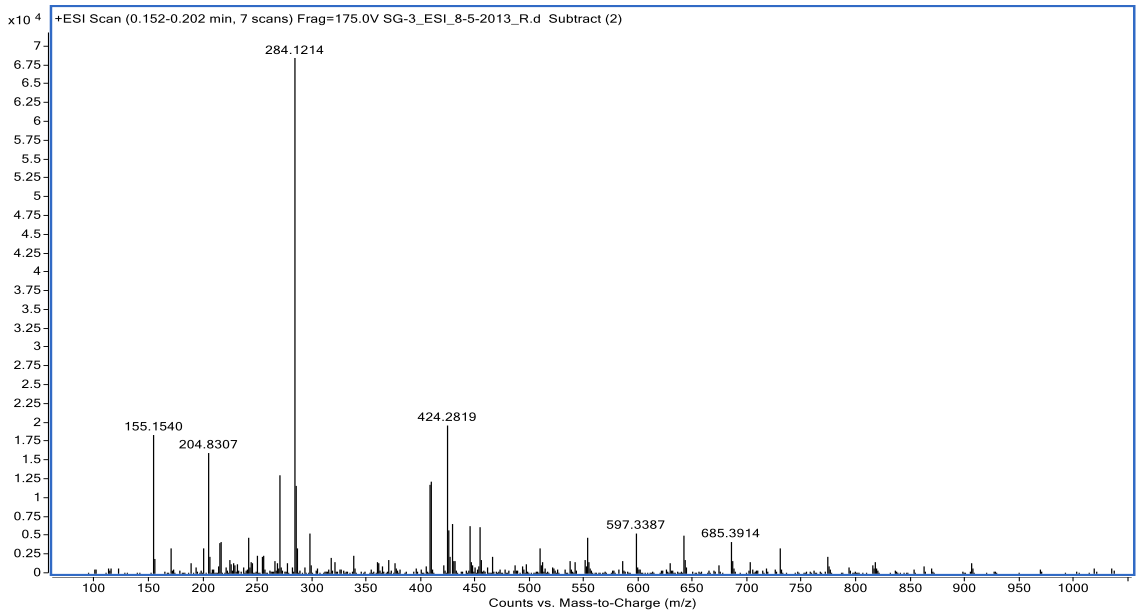

Figure 6.26: Steam discharge, 33.78 minutes processing time at 76 W.

Table 6.5: Comparison of results of methylene blue reduction by different diagnostics (HPLC and spectrophotometer).

Reduction in MB Molecule (%)		
Results from HPLC	**Results from Spectrophotometer**	**Percent Error (%)**
Air: 95.5	Air: 90.9	4.8
Steam: 78.5	Steam: 94.3	20.1

The mass spectroscopy results give a quantitative look at the treatment of the methylene blue dye by air versus steam discharge. Based on the HPLC results given above, the air treatment reduced the Methylene Blue molecule by approximately 95.5% in 17.62 minutes, whereas the steam treatment reduced the MB molecule by approximately 78.5% in 33.78 minutes. This is in contrast to the results given by the spectrophotometer, of 90.9% by air and 94.3% by steam. The spectrophotometer gives a large amount of error for the steam treatment sample (over 20% off), which is an excellent example of the need for molecular analysis of the daughter decomposition products as opposed to a simple spectrophotometer diagnostic technique.

The fragmentation of the methylene blue dye molecule differs between discharge method, which is expected as different decomposition chemistries are occurring between the two discharge modes. The exception is the peak at 155.154 m/z, present in both discharges.

6.10 Conclusion

The development of an underwater DBD plasma jet that self-generates a gas bubble of water vapor has been described and studied. This so-called steam discharge is of great interest especially to plasma-based water purification applications, as the system does not require an external feed gas to produce the discharge, which simplifies the operation. In addition, strong decomposition power is retained while the acidity of the liquid is not significantly increased as in other plasma sources (e.g., air fed discharges). This relatively non-acidic pH is also observed during the decomposition of methylene blue dye, suggesting that the pH of the liquid is more strongly dependent on the feed gas used and not the dye by-products. Energy efficiency of the steam discharge on removing methylene blue dye is measured at approximately 0.16 g kWh^{-1}. Optical emission spectroscopy and hydrogen peroxide measurements suggest the primary source of oxidative strength was derived from OH. Chemical analysis of treated samples indicated that the discharge produces copious amounts of hydrogen peroxide. These rates matched or exceeded plasma generated rates reported on in the literature to date. The lack of observed oxygen emission lines suggests ozone is not formed in substantial amounts and does not contribute to the decomposition power of the discharge. The steam plasma discharge can be used as a test bed standard for plasma in liquid studies where it is desired to minimize the variety of plasma-produced active species so that chemical pathways can be accurately elucidated. In addition, one strong potential application of the steam discharge is as a post-treatment in an industrial setting with hot wastewater; a heated wastewater would remove much of the energy requirement as well as speed the dissolution of hydrogen peroxide, increasing decomposition power.

Chapter 7:

The Two Dimensional Bubble

7.1 Introduction

Perhaps some of the most important questions pertaining to plasma chemistry dynamics that must be answered are those concerning the interface region of the system, namely, how does the reactivity from a local discharge transfer to the bulk liquid? The discharges described in Chapters 5 and 6 are essentially point sources, and yet they have the capacity to breakdown contaminants in significant volume in only a few minutes. The interface region, that is, the reaction region between the gas/plasma region and the bulk liquid (see Figure 7.1), is responsible for not only energy transport from the plasma to the liquid (may be an important heat sink for the system [**64**]), but radical species production as well. Unlocking the physics and chemistry of this region will bridge the knowledge gap for several important processes, including the relationship between gas-phase and liquid-phase plasma chemistry.

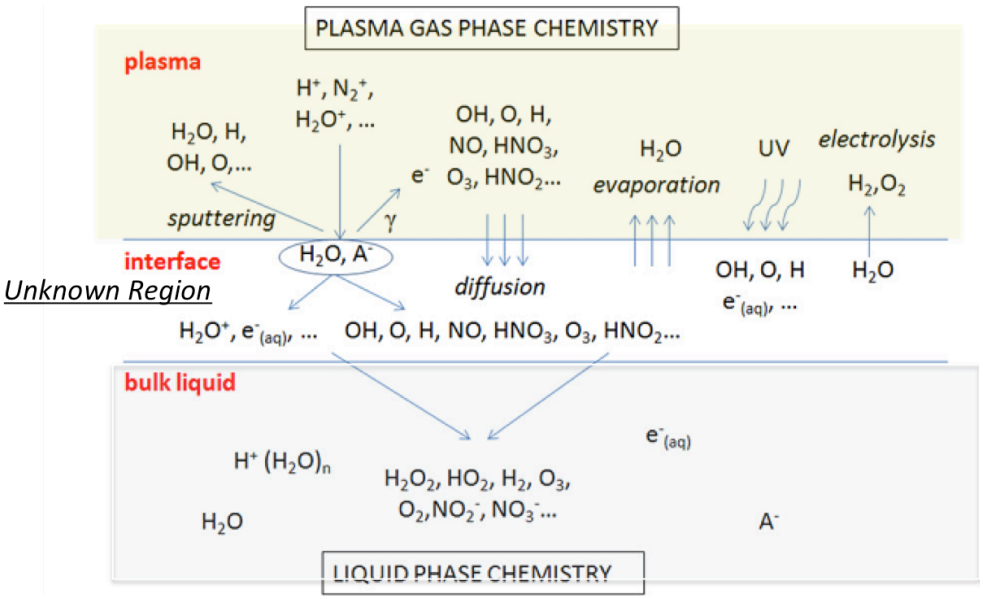

Figure 7.1: The interface region. Various species, (suggested) transport pathways depicted. Adapted from [64].

Up until very recently, this region has proved significantly difficult to study experimentally due to the inconvenience of the system properties: not only does the three-dimensionality of a bubble or gas slug present a convoluted view of the interface (i.e., the optical path length is not constant but varies depending on position), but the fact that it is surrounded by water compounds the problems. Water strongly absorbs in the UV [**355**], and many of the optical emission signatures of interest to plasma diagnostics require UV and near-UV access (e.g., the OH(A-X) system begins around 306 nm).

To compensate for the issues surrounding a three dimensional system, a two dimensional system was developed (see Figure 3.15) [**422**]. Here, the bubble is flattened between two glass plates, allowing direct optical integration of the various regions. The gas bubble is then ignited with a pulsed plasma discharge. This set up allows for experimental investigation into the boundary layer.

This chapter discusses the development and demonstration of a novel diagnostic device – the Two Dimensional Bubble – that provides unmatched access to the gas-water interface. Plasma discharge in liquid water and pH studies via chemical probes are presented.

7.2 Experimental Methods

7.2.1 Device Construction

A more detailed diagram of the 2D bubble device is given in Figure 7.2. The plates used are quartz, allowing for optical access to the UVA (400-315 nm) and UVB (315-280 nm) wavelength regions. In the preliminary design, a syringe was positioned underneath the center of the quartz plate. This syringe allowed for the creation of the air bubble through insertion of gas into the liquid pool, and acted as the powered electrode as it was biased with a high voltage pulser. In the preliminary design of the device, copper strips on either side of the powered electrode were used as the ground electrode. The liquid was sealed between the two quartz electrodes via rubber O-ring gasket.

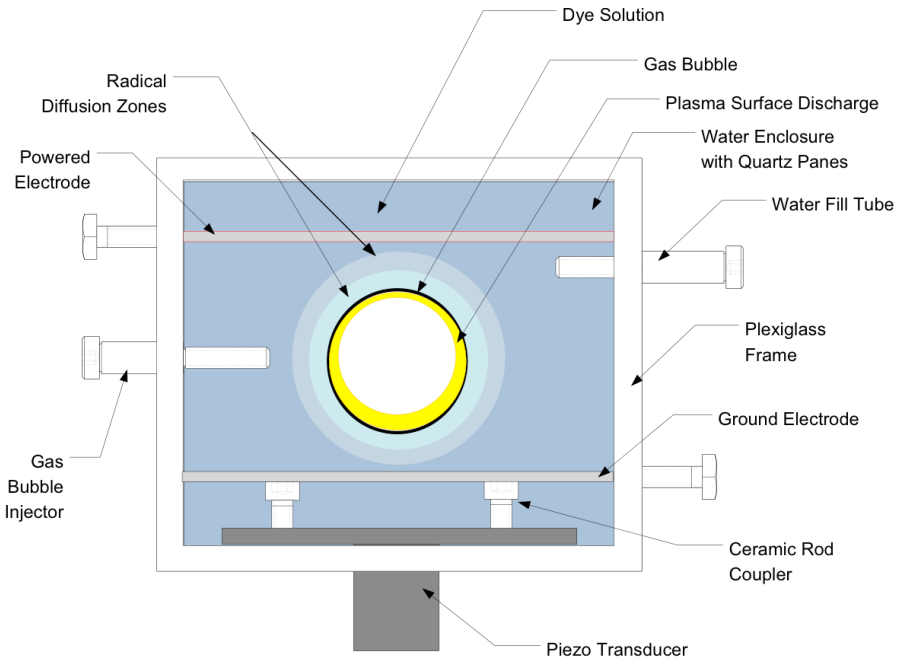

Figure 7.2: One design iteration of the of the two-dimensional bubble diagnostic.

The device may be operated with a variety of power sources, including nanosecond pulsed power and continuous wave (kHz frequencies). A typical operating voltage and current trace for CW operation may be seen in Figure 7.3. The waveforms are a typical of a dielectric barrier discharge with a negative dc offset; Figure 7.3 corresponds to an operating frequency of 26 kHz. In Figure 7.4 illustrates a typical Lissajous figure from the device in operation at 26 kHz. The calculated power consumption is approximately 2 W.

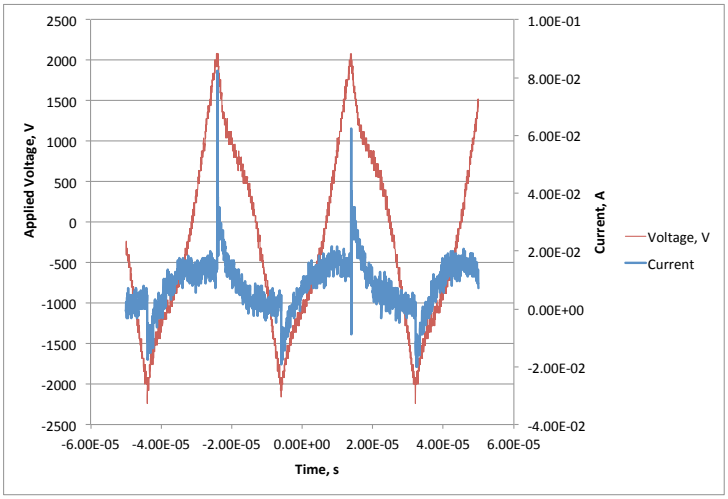

Figure 7.3: Voltage and current waveform of the two dimensional bubble in operation.

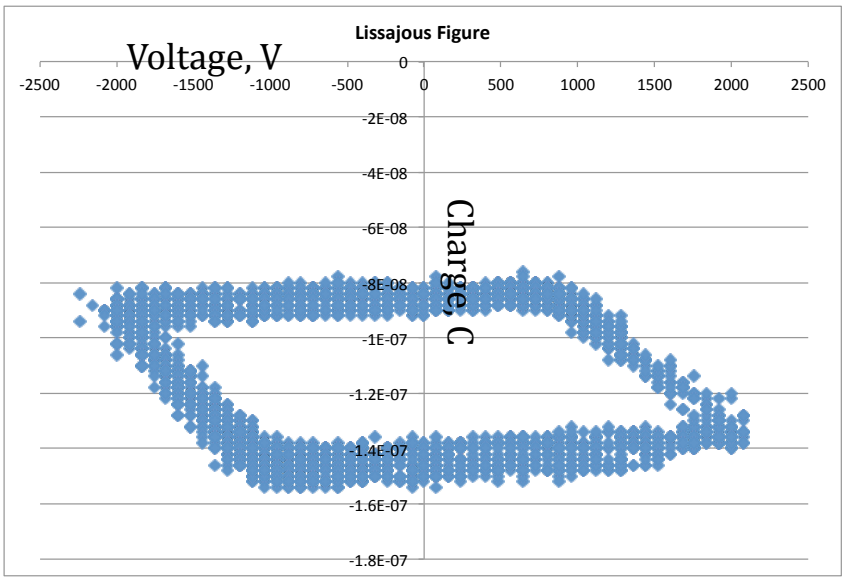

Figure 7.4: Lissajous figure of the device in operation; corresponds to approximately 2 W.

7.2.2 Chemical Probe

Methyl orange, a common colorimetric dye used in titrations, was used for preliminary tests on the cell. Here, methyl orange was used to detect pH change and to illustrate the convection of thermal processes in the treated liquid. When in solution, methyl orange changes color depending on the pH of the liquid, appearing yellow for pH of approximately 4.4 and higher, and red for pH 3.1 and lower. The crossover point for methyl orange (i.e., when it is equilibrium) is approximately pH 3.7, and the liquid will appear orange.

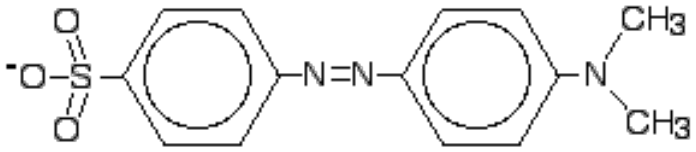

Figure 7.5: Methyl orange in its "yellow form". Image from [423].

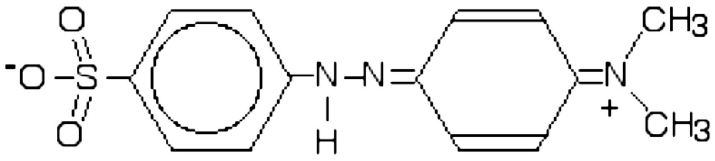

Figure 7.6: One possible arrangement of methyl orange in an acidic liquid (its "red form"). Image from [423].

Similar studies with methyl orange and atmospheric plasmas were conducted by Oehmigen et al. [**424**].

7.3 Preliminary Results

7.3.1 Methylene Blue [422]

Preliminary tests in the cell were conducted with methylene blue dye. The device was operated for approximately 10 minutes at 2W at 26 kHz. The results of the test may be observed in Figure 7.7 and Figure 7.8.

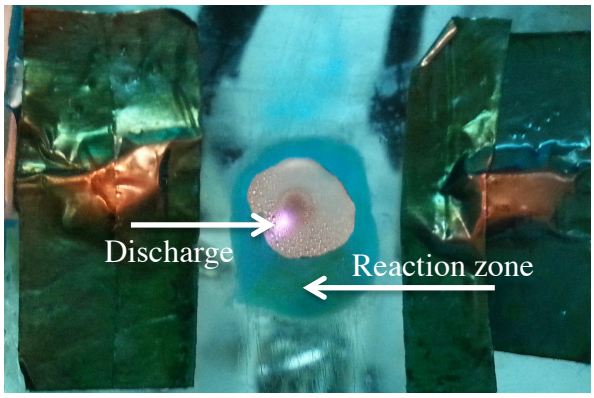

Figure 7.7: Decomposition of methylene blue [422].

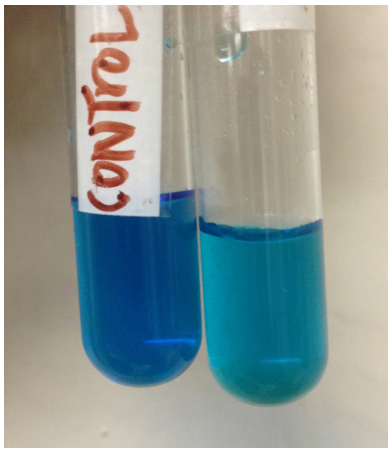

Figure 7.8: Methylene blue dye before (left) and after (right) 10 minutes of treatment in the two dimensional bubble cell [422].

7.3.2 Methyl Orange

As methyl orange detects the presence of acidic protons, the presence of red liquid is also a good analogy of how plasma-produced species most likely transport throughout the liquid. A series of time-resolved images may be seen in Figure 7.9. The power supply was increased until plasma ignited.

What is first noticed is the change of color in Figure 7.9.b (at 19 seconds), but no plasma is visible. This color change is in the region of the bubble closest to the electrode. The fact that no plasma is visible and yet noticeable chemical change is still occurring suggests the presence of a dark plasma. The change of the quantity of red liquid between Figure 7.9.b and Figure 7.9.c is not significant.

The plasma does not visually ignite until Figure 7.9.d, at 28 seconds. Now the methyl orange solution experiences color change all around the bubble perimeter, though it is most strongly present at the zones of the bubble directly interacting with the plasma, as expected.

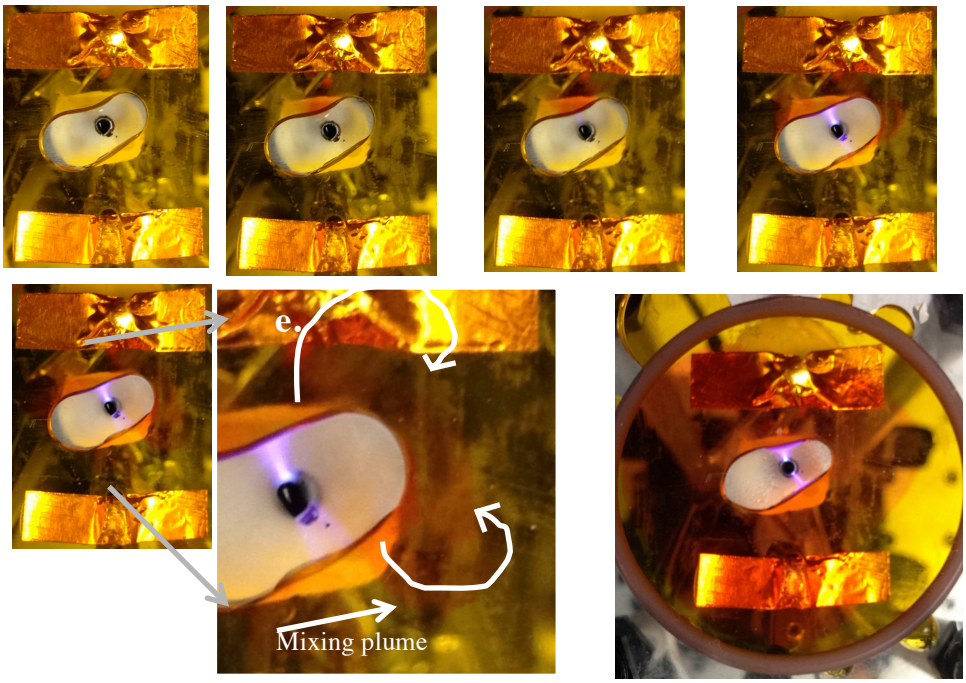

Figure 7.9: Time-resolved images of plasma interaction with methyl orange solution. (a), t = 0; (b), Δt = 19 sec; (c), Δt = 27 sec; (d), Δt = 28 sec; (e), Δt = 29 sec; (e.1.), zoomed in view of (e); (f), Δt = 56 sec.

Much of the color seen in later times, such as Figure 7.9.e, is primarily due to the diffusion of the reacted liquid from the plasma-on-boundary section of the bubble, however there is color change originating from all parts of the bubble boundary, strong evidence of the transport of gas-phase plasma-produced species from the local plasma region to other regions of the bubble. Mixing gradients may be clearly seen in Figure 7.9.d, e and f.

7.4 Summary

After development is completed, the two-dimensional bubble diagnostic will be a significant tool in understanding the interface region of bubbles. This tool will substantially reduce complexities associated with probing a three-dimensional sphere.

In addition to the optical-based diagnostics, other chemical diagnostics (i.e., titrations) similar to the performed methyl orange experiment are possible. Two examples of possible future experiments include the use of chlorophyll to detect NO_2 gas (as seen in [**425**]), or an additional colorimetric method, such as a sulfanilic acid and N-(1-naphthyl)-ethylene diamine hydrochloride reaction, in which a clear liquid turns magenta upon detection of nitrite ions (NO_2^-), as in [**424**].

Chapter 8:

Conclusion

The increasing demand on natural resources makes the requirement for adequate water security greater with each passing year. As the world becomes more industrial, the demand for freshwater increases, which has real effects on human ecology and the general environment. Plasma processing of contaminated liquids enables decomposition of pollutants of varying compositions and chemistries. This work has demonstrated the decomposition of many pollutants from a variety of chemical compositions, with the time-resolved analysis of the decomposition process. A new, steam discharge method has been developed, which address many of the unwanted effects of the air discharge method. The steam discharge has the potential to be a strong contributor to the field of plasma-based water purification; one strong potential application of the steam discharge is as a post-treatment in an industrial setting with hot wastewater. A heated wastewater would remove much of the energy requirement as well as speed the dissolution of hydrogen peroxide, increasing decomposition power.

One may trace the use of plasmas in liquids for water purification to the end of the 19th century, though careful and controlled investigation did not begin until 1987. Still today, the field remains fairly undeveloped. This dissertation research has contributed to the understanding on several fronts namely understanding breakdown characteristics and chemical species production. Breakdown scaling for single air bubbles in liquid water has been measured, however this relation should be assessed in the light of the potential bubble charging phenomenon evidence. Bubble breakdown scaling and the effect of bubble charging on the breakdown voltage have significant impact on the implementation of this technology on a real-world device; the evidence of such phenomena have been first recorded in this work.

8.1 Summary of Dissertation Research

This dissertation research has presented a multifaceted investigation into the physics and chemistry of gas bubbles in liquids subjected to electrical discharges and the resulting phenomenon, all through the lens of developing advanced water purification technology. Through this work, the production of plasma in bubbles unattached and attached to the powered electrode has been analyzed with the goal of identifying knobs at which to control plasma production, and by extension, controlling plasma-driven chemistry.

Plasma production in isolated bubbles was studied and various characteristics and dependencies of the discharges were observed and detailed. Gas bubbles close to the electrode could be ignited with plasma remotely (i.e., no visible discharge connecting electrode and bubble), whereas bubbles far from the electrode typically ignited via liquid streamer that reached the bubble and subsequently ignited a glow-like discharge within the bubble. Isolated bubbles were also investigated to determine if a breakdown voltage scaling law exists. Current data suggests a Paschen-like relation between breakdown voltage and the product of bubble pressure and diameter (the effective *pd*).

Plasma production in bubbles attached to the electrode took two forms. The first form was similar to the isolated bubbles in that small, ~mm diameter bubbles touching the electrode were ignited with plasma. These bubbles, along with the isolated bubbles, were investigated to determine any existing breakdown voltage scaling. With the isolated bubbles, a Paschen-like curve is created.

The second form of bubbles attached to the electrode were bulk gas bubbles, gas slugs produced through bubbling gas into the treatment liquid or through self-generation of steam pockets. Spectroscopic techniques were used to study the properties of discharges in these bubbles in detail, investigating aspects such as the asymmetric quality of emission with changing voltage polarity and the effect of system properties, such as feed gas and electrode material. Electrical properties of the system were investigated. The resulting chemistry, including time-resolved breakdown by-products, contaminant decomposition, and cytotoxicity studies were all performed.

8.2 Future Work and Design Suggestions for a Functioning Plasma Reactor

8.2.1 Breakdown Mechanisms

The experiments discussed in Chapter 4 should be continued, with efforts focused on 1, continued investigation into the proposed bubble charging mechanism; 2, probing the breakdown curve as low as possible; and 3, further study on inducing streamer hopping in bubble ensembles. Keeping the experimental conditions (e.g., water qualities) consistent, especially dissolved oxygen and conductivity, should be a priority during these efforts. Bubble charging and the effect on breakdown should be further explored experimentally but also through computational models. Assessment of breakdown mechanisms with planar electrodes should be continued. Various power sources (especially pulsed with higher max voltage, lower voltages with longer pulse widths) should be investigated.

8.2.2 Computer Simulation Work

Much of this work would benefit from computational investigation. A few suggested areas that would contribute to a clearer understanding include modeling the formation of the steam bubble, a more complete model of the chemical output of the air and steam discharges, and the bubble charging mechanism. Experimentally, this work has outlined *how* the steam bubble forms, but the *why* still needs to be addressed. Modeling the steam bubble formation would give great insight into the formation mechanisms and the underlying physics. This work has also begun the modeling of the chemical output of the steam and air plasmas, however with the exclusion of carbon-based species (e.g., CO_2) dissolved in the liquid.

8.2.3 Plasma Reactor Development

The experiments discussed in Chapters 5 and 6 examine different qualities and factors of various discharges with the end goal of developing a functional plasma-based water treatment device. The following are a few comments pertaining to the development of a functioning plasma reactor.

8.2.3.1 Gas Type

The steam discharge appears to be the most promising as far as the chemistry and equipment requirements are concerned. However, more work is required to determine if desired plasma properties are superior through the use of a non-steam or non-air gas.

8.2.3.2 Electrode Design

Electrode design should be investigated thoroughly, especially multiple applicators. Cross-talk that appears in multi-jet plasma arrays needs to be understood [**181**].

8.2.3.3 Electrode Material

Investigations into electrode material would be useful, due to the synergistic characteristics of various materials with processing.

8.2.3.4 Chemical Analysis

Continued chemical analysis and cytotoxicity studies are paramount. Investigations into controlling daughter products should be carried out. Cytotoxicity studies using non-cancerous, healthy cells should be conducted. Human consumption of the water is strongly discouraged until adequate study has been conducted.

8.3 Final Comments

The success of plasma-based water purification relies on not just smart physics but also on a thorough understanding of the chemistry driven by plasma discharges. This is most strongly apparent in the need for toxicology studies. Many investigators are quick to point to dye degradation experiments and discuss contaminant removal simply because the liquid is clear, or the mass peak of the contaminant is gone, or the like (e.g., [**426**,**427**]). While complete mineralization is possible, steps must be taken to ensure the daughter products are not toxic.

Additionally, establishing universal metrics for the plasma in liquids community with application foci is strongly suggested. The field of plasmas in liquids (n.b., plasma medicine included in this category) can tend toward the Edisonian in methodology; while empirical observations and data are obviously important, determining what standards and metrics for experiments and devices will elevate the field from exploratory investigations to established science.

Plasma discharges for water purification is most certainly a viable technology that should – must – be explored and implemented. It is possible that inadequate attention to the chemical side (of processing and post-processing) will result in the premature and unnecessary death of plasma water purification, either from the physicists abandoning the endeavor due to lack of chemical knowledge (e.g., insufficient knowledge of what questions to ask) or the chemists who can't make headway due to serious deficiencies in the electromagnetic (and related) sciences.

Success can only come from a serious multidisciplinary effort from both the chemical and physics communities. Depending on the application, biochemical expertise is also essential to ensure environmental health.

Appendix

Reactions used in *GlobalKIN* simulations. Rate coefficients may be found elsewhere [**184**,**185**,**186**].

1. E + N2 > N2V + E
2. E + N2 > N2V + E
3. E + N2 > N2V + E
4. E + N2 > N2V + E
5. E + N2 > N2V + E
6. E + N2 > N2V + E
7. E + N2 > N2V + E
8. E + N2 > N2V + E
9. E + N2 > N2* + E
10. E + N2 > N2* + E
11. E + N2 > N2* + E
12. E + N2 > N2*** + E
13. E + N2*** > N2 + E
14. E + N2 > N2** + E
15. E + N2** > N2 + E
16. E + N2 > N + N + E
17. E + N2 > N2+ + E + E
18. E + N2V > N2 + E
19. E + N2V > N2* + E
20. E + N2V > N2+ + E + E
21. E + N2* > N2V + E
22. E + N2* > N2 + E
23. E + N2* > N2+ + E + E
24. E + N2+ > N* + N
25. E + N > N* + E
26. E + N > N* + E
27. E + N > N+ + E + E
28. E + N* > N + E
29. E + N* > N+ + E + E
30. E + O2 > O2 + E
31. E + O2 > O- + O
32. E + O2 > O2V + E
33. E + O2 > O2V + E
34. E + O2 > O2V + E
35. E + O2 > O2V + E
36. E + O2 > O2* + E
37. E + O2 > O2* + E
38. E + O2 > O + O + E
39. E + O2 > O + O + E
40. E + O2 > O2* + E
41. E + O2 > O2* + E
42. E + O2 > O2+ + E + E
43. E + O2 > O + O+ + E + E
44. E + O2 + O2 > O2- + O2
45. E + O2 + N2 > O2- + N2
46. E + O2V > O + O-
47. E + O2V > O2 + E
48. E + O2V > O2* + E
49. E + O2V > O2* + E
50. E + O2V > O + O + E
51. E + O2V > O + O* + E
52. E + O2V > O2+ + E + E
53. E + O2V > O* + O* + E
54. E + O2V > O+ + O + E + E
55. E + O2* > O2* + E
56. E + O2* > O- + O
57. E + O2* > O2 + E
58. E + O2* > O + O + E
59. E + O2* > O + O + E
60. E + O2* > O2+ + E + E
61. E + O2* > O + O+ + E + E
62. E + O2* + O2 > O2- + O2
63. E + O2* + N2 > O2- + N2
64. E + O3 > O- + O2
65. E + O3 > O2- + O
66. E + O > O + E

67. E + O > O* + E
68. E + O > O* + E
69. E + O > O+ + E + E
70. E + O+ > O*
71. E + E + O+ > O* + E
72. E + O* > O* + E
73. E + O* > O + E
74. E + O* > O+ + E + E
75. E + O2+ > O + O
76. E + O2+ > O* + O
77. E + H2 > H2+ + E + E
78. E + H2 > H + H + E
79. E + H2+ > H + H
80. E + H2O > H- + OH
81. E + H2O > H2O+ + E + E
82. E + H2O > H + OH + E
83. E + H2O > H + OH + E
84. E + H2O+ > OH + H
85. E + H2O+ > O + H + H
86. E + H2O+ > O + H2
87. E + CO2 > CO2V + E
88. E + CO2 > CO2V + E
89. E + CO2 > CO2V + E
90. E + CO2 > CO2V + E
91. E + CO2 > CO2V + E
92. E + CO2 > CO2V + E
93. E + CO2 > CO2V + E
94. E + CO2 > CO2V + E
95. E + CO2 > CO + O-
96. E + CO2 > CO + O + E
97. E + CO2 > CO + O + E
98. E + CO2 > CO2+ + E + E
99. E + CO2V > CO2 + E
100. E + CO2+ > CO + O
101. E + CO > COV + E
102. E + CO > C + O + E
103. E + CO > CO+ + E + E
104. E + CO > CO+ + E + E
105. E + CO > CO+ + E + E
106. E + CO > CO+ + E + E
107. E + CO > CO+ + E + E
108. E + COV > CO + E
109. E + CO+ > C + O
110. E + N3+ > N + N2
111. E + NO2+ > NO + O
112. E + NO2+ > NO + O*
113. E + H2NO+ > H2O + N
114. E + NO+ > N* + O
115. E + C+ > C
116. E + NH3+ > NH2 + H
117. E + NH4+ > NH3 + H
118. E + H3O+ > H2O + H
119. E + H3O+*H2O > H + H2O + H2O
120. E + H2O+ > OH + H
121. E + H2O+ > O + H + H
122. E + H2O+ > O + H2
123. E + NO+ > N + O*
124. E + N4+ > N2 + N2
125. E + NO2 > NO2-
126. N2* + N2* > N2* + N2
127. N2* + N2 > N2 + N2
128. N2*** + N2 > N2* + N2
129. N2*** + N2* > N4+ + E
130. N2*** + N2** > N4+ + E
131. N2*** + N2*** > N4+ + E
132. N2** > N2
133. N2** > N2*
134. N2*** > N2*
135. N2* + NO > NO + N2
136. N2* + O2 > O + O + N2
137. N2* + O2 > O2 + N2
138. N2* + N2O > N2 + N2 + O
139. N2* + N2O > N2 + N2O
140. N2* + NO2 > NO + O + N2
141. N2* + CO2 > N2 + CO2
142. N2* + CO > N2 + CO
143. N2* + H2 > N2 + H2
144. + O2 + M > O3 + M
145. H + OH + M > H2O + M
146. N2O5 > NO2 + NO3
147. NO + O2 + NO > NO2 + NO2
148. NO + HO2 > NO2 + OH
149. N* + N2 > N + N2
150. NO + O + O2 > NO2 + O2
151. N* + O2 > NO + O
152. NO + OH + M > HNO2 + M

153. N* + NO > N2 + O
154. NO + H + M > HNO + M
155. N* + N2O > NO + N2
156. NO + NO3 > NO2 + NO2
157. HO2 + NO + M > HNO3 + M
158. HO2 + NO > O2 + HNO
159. N* + NO2 > N2O + O
160. NO + O3 > NO2 + O2
161. N* + NO2 > NO + NO
162. NO + N > N2 + O
163. H + O2 + M > HO2 + M
164. H + H + M > H2 + M
165. H + NO2 > OH + NO
166. H + HO2 > OH + OH
167. H + O3 > OH + O2
168. H + HNO > H2 + NO
169. H + HNO > OH + NH
170. H + HNO > O + NH2
171. N + NO2 > N2O + O
172. N + NO2 > NO + NO
173. N + N + M > N2 + M
174. N + OH > NO + H
175. N + OH > O + NH
176. O* + N2 > O + N2
177. N + O + M > NO + M
178. O* + O2 > O + O2
179. N + O2 > NO + O
180. N + O3 > NO + O2
181. N + H2O > NH + OH
182. N + H2 > NH + H
183. O* + H2O > O + H2O
184. O* + H2O > OH + OH
185. + HO2 > OH + O2
186. + O3 > O2 + O2
187. + NO2 + M > NO3 + M
188. OH + CO > CO2 + H
189. NO3 + NO3 > NO2 + NO2 + O2
190. OH + OH > O + H2O
191. N2O5 + H2O > HNO3 + HNO3
192. NH + NO > N2O + H
193. OH + NO2 + N2 > HNO3 + N2
194. NH + O2 > HNO + O
195. OH + HNO3 > NO3 + H2O
196. OH + HNO > H2O + NO
197. OH + HO2 > H2O + O2
198. H2O+ + H2O > H3O+ + OH
199. OH + HNO2 > NO2 + H2O
200. H2O+ + O2 > O2+ + H2O
201. OH + O3 > HO2 + O2
202. N3+ + O2 > NO+ + N2O
203. OH + N2O > HNO + NO
204. N3+ + O2 > NO2+ + N2
205. HO2 + NO2 + N2 > HO2NO2 + N2
206. N3+ + NO > NO+ + N + N2
207. HO2 + O3 > OH + O2 + O2
208. N3+ + NO2 > NO+ + NO + N2
209. NO2 + O3 > NO3 + O2
210. N3+ + NO2 > NO2+ + N + N2
211. N3+ + N2O > NO+ + N2 + N2
212. + NO2 > NO + O2
213. + NO3 > O2 + NO2
214. N3+ + NO2- > N + N2 + NO2
215. + OH > H + O2
216. O+ + N2 > NO+ + N
217. O+ + CO2 > CO2+ + O
218. OH + OH + O2 > H2O2 + O2
219. O+ + NO > NO+ + O
220. OH + H2O2 > H2O + HO2
221. O+ + O2 > O2+ + O
222. H + HO2 > H2 + O2
223. O+ + NO2 > NO2+ + O
224. HO2NO2 + O2 > HO2 + NO2 + O2
225. O+ + NO2- > O + NO2
226. O2+ + NO > NO+ + O2
227. O2+ + NO2 > NO2+ + O2
228. O2+ + NO2- > O2 + NO2
229. H3O+ + H2O > H3O+*H2O
230. H3O+*H2O +M > H3O+ + H2O+M
231. NO2+ + NO > NO+ + NO2
232. NO2+ + NO2- > NO2 + NO2
233. CO2+ + NO > NO+ + CO2
234. NO2+ + NO3- > NO2 + NO3
235. CO2+ + O2 > O2+ + CO2
236. CO2+ + O > O+ + CO2
237. CO2+ + O > O2+ + CO
238. CO2+ + CO > CO2 + CO+

239. CO+ + CO2 > CO2+ + CO
240. CO+ + O2 > O2+ + CO
241. CO+ + O > O+ + CO
242. N2+ + NO > NO+ + N2
243. N3+ + H2O > H2NO+ + N2
244. N2+ + NO2 > NO2+ + N2
245. N2+ + NO2 > NO+ + N2O
246. H2NO+ + NO2- > H2O + N + NO2
247. H2NO+ + NO3- > H2O + N + NO3
248. NO2- + HNO3 > NO3- + HNO2
249. N2+ + NO2- > N2 + NO2
250. NO2- + NO2 > NO3- + NO
251. N2+ + NO3- > N2 + NO3
252. NO2- + N2O > NO3- + N2
253. NO2- + N2O5 > NO3- + NO2 + NO2
254. NO2- + O3 > NO3- + O2
255. NO3- + NO > NO2- + NO2
256. NO+ + NO2- > NO + NO2
257. NO+ + NO3- > NO + NO3
258. O2- + NO2 > NO2- + O2
259. O- + O2 > O2- + O
260. O- + O > O2 + E
261. O- + CO > CO2 + E
262. O2- + O > E + O3
263. O2- + O > O- + O2
264. O2- + O2* > E + O2 + O2
265. O2- + N2+ > N2 + O2
266. N* + NH3 > NH + NH2
267. OH + NH3 > NH2 + H2O
268. O* + NH3 > NH2 + OH
269. NH2 + NO > N2 + H2O
270. NH2 + NO2 > N2O + H2O
271. NH3 + O > OH + NH2
272. NH2 + H + M > NH3 + M
273. NH2 + H > NH + H2
274. N+ + O2 > NO+ + O
275. O2+ + NH3 > NH3+ + O2
276. N+ + O2 > O2+ + N
277. NH3+ + NH3 > NH4+ + NH2
278. N+ + O2 > O+ + NO
279. H3O+ + NH3 > NH4+ + H2O
280. N+ + NO > NO+ + N
281. N+ + NH3 > NH3+ + N
282. N3+ + NH3 > NH3+ + N + N2
283. N2+ + O2 > O2+ + N2
284. N2+ + NH3 > NH3+ + N2
285. N4+ + NO > NO+ + N2 + N2
286. N4+ + NO2 > NO2+ + N2 + N2
287. NH3+ + NO3- > NH3 + NO3
288. N4+ + NO2 > NO+ + N2O + N2
289. N4+ + O2 > O2+ + N2 + N2
290. NH2 + O > NH + OH
291. NH2 + O > HNO + H
292. HO2NO2 + N2 > HO2 + NO2 + N2
293. OH + NO2 + O2 > HNO3 + O2
294. OH + H2 > H2O + H
295. O* + H2O > H2 + O2
296. O* + H2 > OH + H
297. + H2O2 > OH + HO2
298. + H2 > OH + H
299. H + HO2 > H2O + O
300. + O2 + N2 > O2 + O + N2
301. HO2 + HO2 + M > H2O2 + O2 + M
302. + NO + N2 > NO2 + N2
303. NO2 + NO3 + M > N2O5 + M
304. N+ + H2O > H2O+ + N
305. N4+ + NO2- > NO2 + N2 + N2
306. N4+ + NO3- > NO3 + N2 + N2
307. N4+ + O2- > N2 + N2 + O2
308. H2O+ + NO2- > H2O + NO2
309. H2O+ + NO3- > H2O + NO3
310. H2O+ + O2- > H2O + O2
311. H3O+ + NO2- > H2O + H + NO2
312. H3O+ + NO3- > H2O + H + NO3
313. H3O+ + O2- > H2O + H + O2
314. O2+ + NO3- > O2 + NO3
315. O2+ + O2- > O2 + O2
316. N3+ + NO3- > N2 + N + NO3
317. N3+ + O2- > N2 + N + O2
318. NO+ + O2- > NO + O2
319. NO2+ + O2- > NO2 + O2
320. O+ + NO3- > O + NO3
321. O+ + O2- > O + O2
322. N+ + O2- > N + O2
323. N+ + NO2- > N + NO2
324. N+ + NO3- > N + NO3

325. H3O+*H2O + NO2- > H + H2O + H2O + NO2
326. H3O+*H2O + NO3- > H + H2O + H2O + NO3
327. H3O+*H2O + O2- > H + H2O + H2O + O2
328. CO2+ + NO2- > CO2 + NO2
329. CO2+ + NO3- > CO2 + NO3
330. CO2+ + O2- > CO2 + O2
331. CO+ + O2- > CO + O2
332. H2NO+ + O2- > H2O + N + O2
333. NH3+ + NO2- > NH3 + NO2
334. NH3+ + O2- > NH3 + O2
335. NH4+ + NO2- > NH3 + H + NO2
336. NH4+ + NO3- > NH3 + H + NO3
337. NH4+ + O2- > NH3 + H + O2
338. + H + M > OH + M
339. H + H2O2 > H2O + OH
340. OH + CO > H + CO2
341. NO2 + NO2 + M > N2O4 + M
342. N2O4 + M > NO2 + NO2 + M
343. NH2 + H2 > NH3 + H
344. NH3 + H > NH2 + H2
345. OH + NO3 > HO2 + NO2
346. HO2 + NO3 > OH + NO2 + O2
347. HO2 + NO3 > HNO3 + O2
348. H + H2O2 > HO2 + H2
349. HNO3 + NO > HNO2 + NO2
350. H2 + O2 > H + HO2
351. H + O2 > OH + O
352. OH + M > O + H + M
353. OH + O2 > O + HO2
354. OH + H > O + H2
355. HO2 + M > H + O2 + M
356. HO2 + H2 > H2O2 + H
357. H2O2 + O2 > HO2 + HO2
358. H2O + H > H2 + OH
359. H2O + O > OH + OH
360. CO2 + H > CO + OH
361. CO2 + O > CO + O2
362. CO + O2 > CO2 + O
363. CO + O + M > CO2 + M
364. CO + HO2 > OH + CO2
365. H- + N2+ > H + N2
366. O- + N2+ > O + N2
367. O- + H2+ > O + H2
368. O2- + H2+ > O2 + H2
369. H- + H2+ > H + H2
370. H- + H2O+ > H + H2O
371. O- + H2O+ > O + H2O
372. H- + H3O+ > H2 + H2O
373. O- + H3O+ > OH + H2O
374. H- + O2+ + M > HO2 + M
375. O- + O2+ > O + O2
376. H- + N3+ > NH + N2
377. O- + N3+ > NO + N2
378. H- + NO+ + M > HNO + M
379. O- + NO+ > NO + O
380. H- + NO2+ + M > HNO2 + M
381. O- + NO2+ > NO2 + O
382. H- + O+ + M > OH + M
383. O- + O+ + M > O2 + M
384. H- + N+ + M > NH + M
385. O- + N+ + M > NO + M
386. H- + N4+ > H + N2 + N2
387. O- + N4+ > O + N2 + N2
388. H- + H3O+*H2O > H2 + H2O + H2O
389. O- + H3O+*H2O > OH + H2O + H2O
390. H- + CO2+ > H + CO2
391. O- + CO2+ > O + CO2
392. O- + CO+ > O + CO
393. H- + H2NO+ > H2 + HNO
394. O- + H2NO+ > OH + HNO
395. H- + NH3+ > H + NH3
396. O- + NH3+ > O + NH3
397. H- + NH4+ > H2 + NH3
398. O- + NH4+ > OH + NH3
399. OH + NO2 + H2O > HNO3 + H2O
400. C+ + H- > C + H
401. C+ + NO2- > C + NO2
402. C+ + O- > C + O
403. C+ + NO3- > C + NO3
404. C+ + O2- > C + O2
405. N2+ + H2O > H2O+ + N2

406. + OH + M > HO2 + M
407. O* + O3 > O2 + O + O
408. O* + NO > O2 + N
409. NH + NO > N2 + OH
410. N3 + NO > N2O + N2
411. NH2 + O > H2 + NO
412. OH + NO2 > HO2 + NO
413. NO3 + NO2 > NO + NO2 + O2
414. O* + NO2 > O2 + NO
415. O* + N2O > NO + NO
416. NO2 + O3 > O2 + O2 + NO
417. + N3 > NO + N2
418. + HNO > OH + NO
419. HNO + O2 > NO + HO2
420. HNO + H2 > NH + H2O
421. + O + M > O2 + M
422. CN + O > CO + N
423. CN + N > N2 + C
424. CN + NO > N2 + CO
425. CN + O2 > NCO + O
426. CN + CO2 > NCO + CO
427. NCO + O > NO + CO
428. NCO + O2 > NO + CO2
429. NCO + NO > CO + N2 + O
430. NCO + NO > CO2 + N2
431. NCO + NO > N2O + CO
432. CO + NO2 > CO2 + NO
433. CO + O3 > O2 + CO2
434. C + CO + M > C2O + M
435. C2O + O > CO + CO
436. C2O + O2 > CO2 + CO
437. C2O + N > CO + CN
438. C + N + M > CN + M
439. C + NO > CN + O
440. C + N3 > CN + N2
441. C + O2 > CO + O
442. NO + M > N + O + M
443. N2 + M > N + N + M
444. O2 + M > O + O + M
445. CO2 + M > CO + O + M
446. NO2 + M > NO + O + M
447. NO3 + M > NO + O2 + M
448. N2O + M > NO + N + M
449. O3 + M > O2 + O + M
450. NO2 + NO2 > NO + NO + O2
451. NO2 + NO2 > NO + NO3
452. N2+ + N2 + M > N4+ + M
453. N2+ + N2 > N3+ + N
454. N4+ + M > N2+ + N2 + M
455. N+ + N2 + M > N3+ + M
456. O* + CO > CO2
457. O* + CO > CO + O
458. O* + O3 > O2 + O2
459. O* + CO2 > O2 + CO
460. O* + CO2 > O + CO2
461. O* + O2* > O + O2
462. O* + O > O + O
463. O2* + O2 > O2 + O2
464. O2* + O2 > O + O3
465. O2* + CO2 > O2 + CO2
466. O2* + O3 > O2 + O2 + O
467. CO2V + M > CO2 + M
468. CO2 + M > CO2V + M
469. COV + M > CO + M
470. CO + M > COV + M
471. O2V + M > O2 + M
472. O2 + M > O2V + M
473. N2V + N2 > N2 + N2
474. N2 + M > N2V + M
475. N2V + N > N + N2
476. N2V + O2 > O2 + N2
477. N2V + O > O + N2
478. N2V + H2O > H2O + N2
479. CO2 + N > CO + NO
480. HO2 + NO2 > HNO2 + O2
481. + HNO2 > NO2 + OH
482. O2* + N2 > O2 + N2
483. O2* + M > O2 + M
484. H2O_L > H2O+_L + E_L
485. H2O_L > OH_L + H_L
486. E_L + H2O_L > H2OEL_L
487. N2+_L + H2O_L > H2O+_L + N2_L
488. N4+_L + H2O_L > H2O+_L + N2_L + N2_L
489. O2+_L + H2O_L > H2O+_L + O2_L
490. NO+_L + H2O_L > H2O+_L +

NO_L

491. H+_L + H2O_L > H3O+_L

492. H3O+*H2O_L + H2O_L > H3O+_L + H2O_L + H2O_L

493. N2**_L + H2O_L > OH_L + H_L + N2_L

494. H2OEL_L + H2O_L > H_L + OHL-_L + H2O_L

495. H2OEL_L + H2O+_L > H_L + OH_L + H2O_L

496. H2OEL_L + H_L > H2_L + OHL-_L

497. H2OEL_L + O_L > O-_L + H2O_L

498. H2OEL_L + O2_L > O2-_L + H2O_L

499. H2OEL_L + OH_L > OHL-_L + H2O_L

500. H2OEL_L + H2O2_L > OH_L + OHL-_L + H2O_L

501. H2OEL_L + O-_L > OHL-_L + OHL-_L

502. H2OEL_L + HO2L-_L > OHL-_L + OHL-_L + OH_L

503. H2OEL_L + H2OEL_L > H2_L + OHL-_L + OHL-_L

504. H2O+_L + H2O_L > H3O+_L + OH_L

505. H3O+_L + OHL-_L > H_L + OH_L + H2O_L

506. H3O+_L + O-_L > OH_L + H2O_L

507. H3O+_L + O2-_L > HO2_L + H2O_L

508. OH_L + OH_L > H2O2_L

509. OH_L + H_L > H2O_L

510. OH_L + H2_L > H_L + H2O_L

511. OH_L + HO2_L > O2_L + H2O_L

512. OH_L + H2O2_L > HO2_L + H2O_L

513. OH_L + OHL-_L > O-_L + H2O_L

514. OH_L + O-_L > HO2L-_L

515. OH_L + O2-_L > O2_L + OHL-_L

516. OH_L + HO2L-_L > HO2_L + OHL-_L

517. H_L + H2O_L > H2_L + OH_L

518. H_L + H_L > H2_L

519. H_L + OHL-_L > H2OEL_L

520. H_L + HO2_L > H2O2_L

521. H_L + H2O2_L > OH_L + H2O_L

522. H2_L + H2O2_L > H_L + OH_L + H2O_L

523. O_L + H2O_L > OH_L + OH_L

524. O_L + O2_L > O3_L

525. O2_L + H_L > HO2_L

526. O-_L + H2O_L > OHL-_L + OH_L

527. O-_L + H2_L > H_L + OHL-_L

528. O-_L + O2_L > O3L-_L

529. O-_L + H2O2_L > O2-_L + H2O_L

530. O-_L + HO2L-_L > O2-_L + OHL-_L

531. HO2_L + H2O_L > H3O+_L + O2-_L

532. OH_L + NO2-_L > OHL-_L + NO2_L

533. H_L + NO2-_L > NO_L + OHL-_L

534. O-_L + NO2-_L+H2O_L > NO2_L + OHL-_L + OHL-_L

535. O2-_L + NO_L > NO3-_L

536. HNO2_L + H2O_L > H3O+_L + NO2-_L

537. HNO3_L + H2O_L > H3O+_L + NO3-_L

538. NO2_L + NO2_L + H2O_L + H2O_L > H3O+_L + NO3-_L + HNO2_L

539. NO2_L+NO2_L+H2O_L+H2O_L+H2O_L>H3O+_L+NO3-_L+H3O+_L+NO2-_L

540. H3O+_L + NO2-_L > H_L + NO2_L + H2O_L

541. H3O+_L + NO3-_L > HNO3_L + H2O_L

542. NO_L + NO_L + O2_L > NO2_L + NO2_L

543. NO_L + NO2_L + H2O_L > HNO2_L + HNO2_L

544. NO3_L + H2O_L > HNO3_L + OH_L

545. NO_L + HO2_L > HNO3_L

546. NO2_L + H_L > HNO2_L
547. OH_L + NO_L > HNO2_L
548. OH_L + NO2_L > HNO3_L
549. OH_L + HNO3_L > NO3_L + H2O_L
550. H_L + HNO2_L > NO_L + H2O_L
551. O2_L + NO_L + NO_L > NO2_L + NO2_L
552. N2O3_L + H2O_L > HNO2_L + HNO2_L
553. N2O4_L + H2O_L > HNO2_L + HNO3_L
554. N2O5_L + H2O_L > HNO3_L + HNO3_L
555. N2O5_L + H2O_L > ONOOH_L + ONOOH_L
556. NO_L + HO2_L > ONOOH_L
557. NO2_L + OH_L > ONOOH_L
558. ONOOH_L + H2O_L > H3O+_L + ONOOL-_L
559. ONOOH_L + H2O_L > H3O+_L + NO3-_L
560. H2O2_L + NO2-_L > ONOOL-_L + H2O_L
561. NO_L + O2-_L > ONOOL-_L
562. O2*_L + H2O_L > O2_L + H2O_L
563. N2*_L + H2O_L > N2_L + H2O_L
564. H2O_L + N2*_L > OH_L + N2_L + H_L
565. O3_L > O2_L + O_L
566. HO2NO2_L > HNO2_L + O2_L
567. HO2NO2_L > HO2_L + NO2_L

Bibliography

[1] Roberto Rosal et al., "Occurrence of emerging pollutants in urban wastewater and their removal through biological treatment followed by ozonation," *Water Research*, vol. 44, no. 2, p. 578, 2010.

[2] F. Ferrari, *Journal of Toxicology*, 2011.

[3] P. Stackelberg, *Science of the Total Environment*, vol. 329, 2004.

[4] J. E. Foster and et al., "A comparative study of the time-resolved decomposition of methylene blue dye under the action of a nanosecond repetitively pulsed dbd plasma jet using liquid chromatography and spectrophotometry," *IEEE Transactions on Plasma Science*, vol. 41, no. 3, pp. 503-512, 2013.

[5] E. Klimiuk, K. Kabardo, Z. Gusiatin, and U. Filipkowaska, "The absorption of reactive dyes from mixtures containing surfactants onto Chitin," *Polish J. Environ. Studies*, vol. 14, no. 6, pp. 771-780, 2005.

[6] J. Lintelmann, A. Katayama, N. Kurihara, L. Shore, and A. Wenzel, "Endocrine disruptors in the environment," *Pure Appl. Chem.*, vol. 75, no. 5, pp. 631-681, 2003.

[7] Tim Robinson, Geoff McMullan, Roger Marchant, and Poonam Nigam, "Remediation of dyes in textile effluent: a critical review on current treatment technologies with a proposed alternative," *Bioresource Technology*, vol. 77, no. 3, pp. 247-255, 2001.

[8] Tyrone Hayes et al., "Atrazine-induced hermaphroditism at 0.1 ppb in American leopard frogs (Rana pipiens): laboratory and field evidence," *Environ. Health Perspect.*, vol. 111, no. 4, pp. 568-575, 2003.

[9] T. Colborn, "Environmental Health Perspective," vol. 101, 1993.

[10] F. Diamanti-Kandarakis and et al., *Endocrine Reviews*, vol. 30, 2009.

[11] J.S. Zogorski and et al., US Geological Survey, Circular 1292 2006.

[12] KE Arnold et al., "Assessing the exposure risk and impacts of pharmaceuticals in the environment on individuals and ecosystems," *Biol Lett*, vol. 9, p. 20130492, 2013.

[13] M. Klavarioti and et al., *Environmental International*, vol. 35, 2009.

[14] A. E. et al. Mather, "Distinguishable Epidemics of Multidrug-Resistant Salmonella Typhimurium DT104 in Different Hosts," *Science*, vol. 341, no. 6153, pp. 1514-1517, 2013.

[15] Center for Disease Control, "Anitbiotic resistance threats in the United States," 2013.

[16] UN General Assembly, Resolution No. GA/10967.

[17] National Academy of Engineering, "Grand Challenges for Engineering," 2008.

[18] K. Watkins and et al., "Human Development Report 2006," United Nations Development Programme, 2006.

[19] William A, Wurts, "Understanding Water Hardness," *Journal of the World Aquaculture Society*, vol. 24, no. 1, p. 18, 1993.

[20] John C. Crittenden, R. Rhodes Trussell, David W. Hand, Kerry J. Howe, and George Tchobanoglous, *Water treatment principles and design*, 2nd ed. Hoboken, NJ, USA: John Wiley and Sons, Inc., 2005.

[21] "Drugs in the water," *Harvard Health Letter*, vol. 36, June 2011.

[22] U.S. Geological Survey, "Fact Sheet 2011-3062," June 2011.

[23] R. L. Calderon, *Food and Chemical Toxicology*, vol. 38, 2000.

[24] O et al. Marincas, "The improvement of removal effects on organic pollutants in Wastewater Treatment Plants (WWTP)," *J. Phys.: Conf. Ser. 182*, p. 012040 , 2009.

[25] C. Binnie, M. Kimber, and G. Smethurst, *Basic Water Treatment*, 3rd ed. London: Thomas Telford, 2002.

[26] MWH, *Water Treatment: Principles and Design*, 2nd ed., John C. Crittenden et al., Eds. Hoboken, NJ: John Wiley & Sons, Inc., 2005.

[27] R. Andreozzi, *Catalysis Today*, vol. 53, 1999.

[28] C. Comninellis and et al., *Journal of Chemical Technology & Biotechnology*, vol. 83, 2008.

[29] A. S. Stasinakis, "Use of Selected Advanced Oxidation Processes (AOPs) for Wastewater Treatment - A Mini Review," *Global NEST Journal*, vol. 10, no. 3, pp. 376-385, 2008.

[30] Marc Pera-Titus, Verónica Garcia-Molina, Miguel A. Baños, Jaime Giménez, and Santiago Esplugas, "Degradation of chlorophenols by means of advanced oxidation processes: a general review ," *Applied Catalysis B: Environmental*, vol. 47, pp. 219-256, 2004.

[31] Roberto Andreozzi, Vincenzo Caprio, Amedeo Insola, and Raffaele Marotta, "Advanced oxidation processes (AOP) for water purification and recovery," *Catalysis Today*, vol. 53, pp. 51-59, 1999.

[32] Mark R. Servos, *Nanotechnology for Water Treatment and Purification*. New York: Springer, 2014.

[33] W. Choi, A. Termin, and M. R. Hoffmann, "The Role of Metal Ion Dopants in Quantum-Sized TiO2: Correlation between Photoreactivity and Charge Carrier Recombination Dynamics," *J. Phys. Chem.*, vol. 98, pp. 13669-13679, 1994.

[34] K. Rajeshwar, "Photoelectrochemistry and the environment," *Journal of Applied Electrochemistry*, vol. 25, no. 12, pp. 1067-1082, 1995.

[35] Isik Kabdasli and Idil Arslan-Alaton, *Chemical Oxidation Applications for Industrial Wastewaters*. London: IWA Publishing, 2010.

[36] R. G. Rice and A. Netzer, *Handbook of Ozone Technology and Applications*. Butterworths, UK: Ann Arbor Science Publishers, 1982, vol. 1.

[37] Computational and Theoretical Chemistry Group, Southern Methodist University. CATCO Research: Ozone. [Online]. https://sites.smu.edu/dedman/catco/

[38] J. H. Baxendale and J. A. Wilson, "The photolysis of hydrogen peroxide at high light intensities," *Trans. Faraday Soc.*, vol. 53, p. 344, 1957.

[39] R. R. Giri, H. Ozaki, Y. Takayanagi, S. Taniguchi, and R. Takanami, "Efficacy of ultraviolet radiation and hydrogen peroxide oxidation to eliminate large number of pharmaceutical compounds in mixed solution," *Int. J. Environ. Sci. Tech.*, vol. 8, no. 1, pp. 19-30, 2011.

[40] S. Bhattacharjee and Y. T. Shah, "Mechanisms for advanced photooxidation of aqueous organic waste compounds," *Rev. Chem. Eng.*, vol. 14, no. 1, p. 1, 1998.

[41] G. R. Peyton and W. H. Glaze, "Destruction of pollutants in water with ozone in combination with ultraviolet radiation. Part 3. Photolysis of aqueous ozone. Mechanism of photolytic ozonation," *Environ. Sci. Technol.*, vol. 22, p. 761, 1988.

[42] D. F. Ollis, "Chapter 2: Comparative Aspects of Advanced Oxidation Processes," in

Emerging Technologies in Hazardous Waste Management III, D. W. Tedder and F.G. Pohland, Eds. Washington, D. C.: ACS Symposium Series 518, 1993.

[43] William H. Glaze, Joon-Wun Kang, and Douglas H. Chapin, "The Chemistry of Water Treatment Processes Involving Ozone, Hydrogen Peroxide and Ultraviolet Radiation," *Ozone: Science and Engineering*, vol. 9, no. 4, p. 335, 1987.

[44] Rein Munter, "Advanced Oxidation Processes: Current Status and Prospects," *Proceedings of the Estonian Academy of Sciences. Chemistry*, vol. 50, no. 2, pp. 59-80, 2001.

[45] Callie Sue Rogers, "Economic costs of conventional surface-water treatment: A case study of the McAllen Northwest facility," Agricultural Economics, Texas A&M University, Master Thesis 2008.

[46] Jay H. Lehr, *Wiley's Remediation Technologies Handbook: Major Contaminant Chemicals and Chemical Groups*. New York: John Wiley & Sons, 2004.

[47] M. A. Malik and et al., *Plasma Sources Sci Technol.*, vol. 10, pp. 82-91, 2001.

[48] Michel Moisan et al., "Plasma sterilization. Methods and mechanisms," *Pure and Applied Chemistry*, vol. 74, no. 3, pp. 349-358, 2002.

[49] B. Locke, M. Sato, P. Sunka, M. R. Hoffmann, and J.-S. Chang, "Electrohydraulic Discharge and Nonthermal Plasma for Water Treatment," *Industrial & Engineering Chemistry Research*, vol. 45, pp. 882-905, 2006.

[50] M. Malik, "Water Purification by Plasmas: Which Reactors are Most Energy Efficient?," *Plasma Chemistry and Plasma Processing*, vol. 30, no. 1, pp. 21-31, 2010.

[51] Yong Yang, Young I. Cho, and Alexander Fridman, *Plasma Discharge in Liquid: Water Treatment and Applications*. Boca Raton, FL, USA: CRC Press, 2012.

[52] M. J. Pavlovich, H.-W. Chang, Y. Sakiyama, D. S. Clark, and D. B. Graves, "Ozone correlates with antibacterial effects from indirect air dielectric barrier discharge treatment of water," *J. Phys. D: Appl. Phys.*, vol. 46, p. 145202, 2013.

[53] John E. Foster, Bradley S. Sommers, Sarah N. Gucker, Isaiah M. Blankson, and Grigory Adamovsky, "Perspectives on the Interaction of Plasmas With Liquid Water for Water Purification," *IEEE Transactions on Plasma Science*, vol. 40, no. 5, pp. 1311-1323, May 2012.

[54] J. E. Foster and et al., *Plasma Sources Science and Technology*, vol. 19, 2010.

[55] M. et al. Margureanu, *Plasma Chemistry and Plasma Processing*, vol. 28, 2008.

[56] S. N. Gucker and J. E. Foster, "Power studies of an underwater DBD plasma jet," in *38th IEEE International Conference on Plasma Science*, Chicago, 2011.

[57] Kil-Seong Kim, Churl-Shin Yang, and Y. S. Mok, "Degradation of veterinary antibiotics by dielectric barrier discharge plasma," *Chemical Engineering Journal*, vol. 219, pp. 19-27, 2013.

[58] A. Gotvajn and et al., *Journal of Environmental Engineering*, vol. 133, 2007.

[59] Matthew J. Traylor et al., "Long-term antibacterial efficacy of plasma-activated water," *J. Phys. D: Appl. Phys.*, vol. 44, p. 472001, 2011.

[60] M Laroussi and F Leipold, "Evaluation of the roles of reactive species, heat, and UV radiation in the inactivation of bacterial cells by air plasmas at atmospheric pressure," ," *International Journal of Mass Spectrometry*, vol. 233, pp. 81-86, 2004.

[61] Bing Sun, Masayuki Sato, and J. Sid Clements, "Optical study of active species produced by a pulsed streamer corona discharge in water," *Journal of Electrostatics*, vol. 39, pp. 189-202, 1997.

[62] J. F. Kolb, R. P. Joshi, S. Xiao, and K. H. Schoenbach, "Streamers in water and other dielectric liquids," *J. Phys. D: Appl. Phys.*, vol. 41, p. 234007, 2008.

[63] S. N. Gucker, B. S. Sommers, and J. E. Foster, "Plasma production in isolated bubbles," *IEEE Transactions on Plasma Science*, 2014.

[64] Seiji Samukawa et al., "The 2012 Plasma Roadmap," *Journal of Physics D*, vol. 45, no. 25, p. 253001, 2012.

[65] R. P. Joshi, J. F. Kolb, S. Xiao, and K. H. Schoenbach, "Aspects of Plasma in Water: Streamer Physics and Applications," *Plasma Processes Polym.*, vol. 6, p. 763, 2009.

[66] Anto Tri Sugiarto, Takayuki Ohshima, and Masayuki Sato, "Advanced oxidation processes using pulsed streamer corona discharge in water," *Thin Solid Films*, vol. 407, pp. 174-178, 2002.

[67] Gregory Fridman et al., "Comparison of Direct and Indirect Effects of Non-Thermal Atmospheric-Pressure Plasma on Bacteria," *Plasma Processes and Polymers*, vol. 4, no. 4, p. 370, 2007.

[68] D. Wetz, J. Mankowski, D. McCauley, J. Dickens, and M. Kristiansen, "The impact of water conductivity, electrode material, and electrode surface roughness on the pulsed

breakdown strength of water," in *Conf. Rec. 27th Int. Power Modulator Symp.*, 2006, p. 104.

[69] P. Bruggeman and C. Leys, "Non-thermal plasmas in and in contact with liquids," *Journal of Physics D: Applied Physics*, vol. 42, no. 5, p. 053001, 2009.

[70] Andrey Starikovskiy, Yong Yang, Young I Cho, and Alexander Fridman, "Non-equilibrium plasma in liquid water: dynamics of generation and quenching," *Plasma Sources Science and Technology*, vol. 20, no. 2, p. 024003, 2011.

[71] Alexander Fridman, Young Cho, George Greene, Avram Bar-Cohen, and James Hartnett, "Non-thermal Atmospheric Pressure Plasma," *Advances in Heat Transfer*, vol. 40, 2007.

[72] Bradley S. Sommers, "Plasma Ignition in Underwater Gas Bubbles," Nuclear Engineering and Radiological Sciences, University of Michigan, Ann Arbor, MI, Ph.D. Dissertation 2013.

[73] John E Foster, Bradley Sommers, and Sarah Gucker, "Towards understanding plasma formation in liquid water via single bubble studies," *Japanese Journal of Applied Physics*, vol. 54, no. 1S, p. 01AF05, 2015.

[74] A. Fridman, *Plasma Chemistry*. New York: Cambridge University Press, 2008.

[75] M. Goldman, A. Goldman, and R. S. Sigmond, "The corona discharge, its properites and specific uses," *Pure and Applied Chemistry*, vol. 57, pp. 1353-1362, 1985.

[76] Ming-wei Li, Gen-hui Xu, Yi-ling Tian, Li Chen, and Hau-feng Fu, "Carbon Dioxide Reforming of Methane Using DC Corona Discharge Plasma Reaction," *The Journal of Physical Chemistry*, vol. 108, no. 10, pp. 1687-1693, 2004.

[77] S. N. Gucker, J. E. Foster, and M. C. Garcia, "An investigation of an underwater steam plasma discharge as alternative to air plasmas for water purification," *Plasma Sources Science and Technology*, vol. 24, p. 055005, August 2015.

[78] Francois Baudin et al., *Plasma Chemistry and Catalysis in Gases and Liquids*, Vasile I. Parvulescu, Monica Magureanu, and Petr Lukes, Eds. Weinheim, Germany: Wiley-VCH, 2012.

[79] Gao Jin-zhang, Wang Xiao-yan, Hu Zhong-ai, Hou Jing-guo, and Lu Quan-fang, "A Review on Chemical Effects in Aqueous Solution induced by Plasma with Glow Discharge ," *Plasma Science and Technology*, vol. 3, no. 3, p. 765, 2001.

[80] N. Sano et al., "Decomposition of Organic Compounds in Water by Direct Contact of Gas

Corona Discharge: Influence of Discharge Conditions," *Ind. Eng. Chem. Res.*, vol. 41, p. 5906, 2002.

[81] J. Velikonja, M. A. Bergougnou, G. S. P. Castle, W. L. Cairns, and I. I. Inculet, "Co-generation of Ozone and Hydrogen Peroxide by Dielectric Barrier AC Discharge in Humid Oxygen," *Ozone Sci. Eng.*, vol. 23, p. 467, 2001.

[82] S. Katsuki, H. Abou-Ghazala, A. Akiyama, and K. H. Schoenbach, "Parallel Streamer Discharges Between Wire and Plate Electrodes in Water," *IEEE Trans. Dielectr. Electr. Insul.*, vol. 9, p. 498, 2002.

[83] I. Suarasan, L. Ghizdavu, I. Ghizdavu, S. Budu, and L. Dascalescu, "Experimental Characterization of Multi-Point Corona Discharge Devices for Direct Ozonation of Liquids," *J. Electrostat.*, vol. 54, p. 207, 2002.

[84] M. Laroussi, X. Lu, and C. M. Malott, "A Non-equilibrium Diffuse Discharge in Atmospheric Pressure Air," *Plasma Sources Sci. Technol.*, vol. 12, p. 53, 2003.

[85] N. A. Aristova and I. M. Piskarev, "Characteristic Features of Reactions Initiated by a Flash Corona Discharge.," *Technol. Phys.*, vol. 47, p. 1246, 2002.

[86] Alexander Fridman, Sergei Nester, Lawrence A. Kennedy, Alexei Saveliev, and Ozlem Mutaf-Yardimci, "Gliding arc gas discharge," *Progress in Energy and Combustion Science*, vol. 25, no. 2, pp. 211-231, 1999.

[87] A. J. Wu et al., "Determination of Spectroscopic Temperatures and Electron Density in Rotating Gliding Arc Discharge," *IEEE Transactions on Plasma Science*, vol. 43, no. 3, p. 836, 2015.

[88] C. S. Kalra, A. Gutsol, and A. Fridman, "Gliding Arc Discharges as a Source of Intermediate Plasma for Methane Partial Oxidation ," *IEEE Transactions on Plasma Science*, vol. 33, no. 1, p. 32, 2005.

[89] H. Ohneda, A. Harano, M. Sadakata, and T. Takarada, "Improvement of NOx removal efficiency using atomization of fine droplets into corona discharge," *J. Electrostat.*, vol. 55, p. 321, 2002.

[90] R. Burlica and B. R. Locke, *IEEE Trans. Ind. Appl.*, vol. 44, p. 482, 2008.

[91] Ulrich Kogelschatz, "Dielectric-barrier Discharges: Their History, Discharge Physics, and Industrial Applications," *Plasma Chemistry and Plasma Processing*, vol. 23, no. 1, pp. 1-46, 2003.

[92] Michael Meisser, *Resonant Behaviour of Pulse Generators for the Efficient Drive of Optical Radiation Sources Based on Dielectric Barrier Discharges*.: KIT Scientific Publishing, 2013.

[93] K. Buss, *Arch. Elektrotech.*, vol. 26, p. 261, 1932.

[94] J Reece Roth, Jozef Rahel, and Daniel M Sherman, "The physics and phenomenology of One Atmosphere Uniform Glow Discharge Plasma (OAUGDP™) reactors for surface treatment applications ," *Journal of Physics D: Applied Physics*, vol. 38, p. 555, 2005.

[95] John E. Foster, Brandon Weatherford, Eric Gillman, and Benjamin Yee, "Underwater operation of a DBD plasma jet," *Plasma Sources Sci. Technol.*, vol. 19, p. 025001, 2010.

[96] John E. Foster, Grigory Adamovsky, Sarah N. Gucker, and Isaiah M. Blankson, "A Comparative Study of the Time-Resolved Decomposition of Methylene Blue Dye Under the Action of a Nanosecond Repetitively Pulsed DBD Plasma Jet Using Liquid Chromatography and Spectrophotometry," *IEEE Transactions on Plasma Science*, vol. 41, no. 3, pp. 503-512, March 2013.

[97] Sarah Gucker, Maria García, Benjamin Yee, and John Foster, "Time Resolved Spectroscopy: Dynamic Study of a Dielectric Barrier Discharge Plasma," in *65th Annual Gaseous Electronics Conference*, Austin, TX, 2012.

[98] G. Fridman and et al., "Blood coagulation and living tissue sterilization by floating-electrode dielectric barrier discharge in air," *Plasma Chemistry and Plasma Processing*, vol. 26, pp. 425-442, 2006.

[99] H. Ayan and et al., "Nanosecond-pulsed uniform dielectric-barrier discharge," *IEEE Transactions on Plasma Science*, vol. 36, no. 2, 2008.

[100] G. Fridman and et al., "Floating electrode dielectric barrier discharge plasma in air promoting apoptotic behavior in melanoma skin cancer cell lines," *Plasma Chemistry and Plasma Processing*, vol. 27, pp. 163-176, 2007.

[101] M. Vandamme and et al., "Antitumor effect of plasma treatment on U87 Glioma Xenografts: preliminary results," *Plasma Processes and Polymers*, vol. 7, pp. 264-273, 2010.

[102] K. Sato and K. Yasuoka, "PulsedDischarge Development in Oxygen, Argon, and Helium Bubbles in Water ," *IEEE Transactions on Plasma Science*, vol. 36, no. 4, p. 1144, 2008.

[103] Wei Tian, Kunhide Tachibana, and Mark J Kushner, "Plasmas sustained in bubbles in water: optical emission and excitation mechanisms," *Journal of Physics D: Applied*

Physics, vol. 47, p. 055202, 2014.

[104] K. Tachibana and Y. Takekata, *Plasma Sources Sci. Technol.* , vol. 20, p. 034005, 2011.

[105] C. Yamabe, F. Takeshita, T. Miichi, N. Hayashi, and S. Ihara, "Water treatment using discharge on the surface of a bubble in water," *Plasma Processes and Polymers*, vol. 2, pp. 246-251, 2005.

[106] Bradley S. Sommers, John E. Foster, Natalia Yu Babaeva, and Mark J Kushner, "Observations of electric discharge streamer propagation and capillary oscillations on the surface of air bubbles in water," *Journal of Physics D: Applied Physics*, vol. 44, no. 8, p. 082001, 2011.

[107] B. S. Sommers and J. E. Foster, "Plasma formation in underwater gas bubbles," *Plasma Sources Sci. Technol.*, vol. 23, no. 1, p. 015020, 2014.

[108] P. Vanraes, A. Nikiforov, and C. Leys, *J. Phys. D: Appl. Phys.*, vol. 45, p. 245206, 2012.

[109] T. Miichi, S. Ihara, S. Satoh, and C. Yamabe, *Vacuum*, vol. 59, pp. 236-43, 2000.

[110] J. E. Foster, S. N. Gucker, B. S. Sommers, and M. C. Garcia, "A review of plasma ignition in liquid water," *J. Phys. D: Appl. Phys.*, p. Manuscript under review, 2015.

[111] S. Gershman, O. Mozgina, A. Belkind, K. Becker, and E. Kunhardt, "Pulsed Electrical Discharge in Bubbled Water," *Contrib. Plasma Phys.*, vol. 47, pp. 19-25, 2007.

[112] Kai-Yuan Shih and Bruce R. Locke, "Effects of Electrode Protrusion Length, Pre-Existing Bubbles, Solution Conductivity and Temperature, on Liquid Phase Pulsed Electrical Discharge," *Plasma Processes and Polymers*, vol. 6, pp. 729-740, 2009.

[113] M. Sato, D. Konno, T. Oshima, and A. Sugiarto, *J. Adv. Oxid. Technol.*, vol. 8, p. 198, 2005.

[114] N. Y. Babaeva and M. J. Kushner, "Effect of inhomogeneities on streamer propagation: II. Streamer dynamics in high pressure humid air with bubble ," *Plasma Sources Sci. Technol.*, vol. 18, p. 035010, 2009.

[115] S. N. Gucker, B. S. Sommers, and J. E. Foster, "Breakdown Voltage Scaling in Gas Bubbles Immersed in Liquid Water," in *66th Annual Gaseous Electronics Conference*, Sept. 30 - Oct. 4, 2013.

[116] S N Gucker, B S Sommers, and J E Foster, "Plasma Production in Isolated Bubbles," *IEEE Transactions on Plasma Science*, vol. 42, pp. Accepted for publication, to be published late 2014, 2014.

[117] M B Chang and S J Wu, "Experimental Study on Ozone Synthesis via Dielectric Barrier Discharges," *Ozone: Science and Engineering*, vol. 19, no. 3, pp. 241-254, 1997.

[118] Eric Keightley Rideal, *Ozone: Treatise of electro-chemistry*, Bertram Blount, Ed. New York, USA: D. Van Nostrand Co., 1920.

[119] Roger Curry. (2012, July) Lateral Science. [Online]. http://lateralscience.blogspot.com/2012/07/martinus-van-marum-1750-1837-discovers.html

[120] Werner von Siemens, "Ueber die elektrostatische Induction und die Verzögerung des Stroms in Flaschendrähten," *Annalen der Physik*, vol. 178, no. 9, pp. 66-122, 1857.

[121] W J Masschelein, *Unit Processes in Drinking Water Treatment*. New York: Marcel Dekker, Inc., 1992.

[122] United States Environmental Protection Agency (US EPA), "Alternative Disinfectants and Oxidants Guidance Manual," Office of Water, EPA 815-R-99-014, 1999.

[123] Jean Marie Auguste Lacomme and Walter Lauder, "Device for the Purification of Water," 672,231, April 16, 1901.

[124] Jean Marie Auguste Lacomme and Walter Lauder, "Device for purifying water," 696,647, April 1, 1902.

[125] George Warren Fuller, *Report on the Investigations Into the Purification of the Ohio River Water*. Louisville, KY: D. Van Nostrand Company, 1898.

[126] James F. Lester, "Apparatus for Electrically Purifying Water," 799,605, September 12, 1905.

[127] Harry B. Hartman, "Apparatus for the electrical purification of water," 1,101,278, June 23, 1914.

[128] Y. Kim, B. Lee, and J. Yi, "Preparation of functionalized mesostructed silica containing magnetitie (MSM) for the removal of copper ions in aqueous solutions and its magnetic separation," *Sep. Sci. Technol.*, vol. 38, no. 11, pp. 2533-2548, 2003.

[129] R. Gehr, Z. A. Zhai, J. A. Finch, and R. S. Ram, "Reduction of soluble mineral concentrations in CaSO4 saturated water using a magnetic field," *Water Research*, vol. 29, no. 3, pp. 933-940, 1995.

[130] A. Fathia, T. Mohamed, G. Claude, G. Maurin, and B. A. Mohamed, "Effect of a magnetic water treatment on homogeneous and heterogeneous percipitation of calcium

carbonate," *Water Research*, vol. 40, no. 10, pp. 1941-1950, 2006.

[131] Ritu D. Ambashta and Mika Sillanpää, "Water purification using magnetic assistance: a review.," *Journal of Hazardous Materials*, vol. 180, pp. 38-49, 2010.

[132] A. A. Frost and O. Oldengerg, "Kinetics of OH Radicals as Determined by Their Absorption Spectrum," *Journal of Chemical Physics*, vol. 4, p. 642, 1936.

[133] R. W. Wood, "Plasmoidal High-Frequency Oscillatory Discharges in "Non-Conducting" Vacua," *Phys. Rev.*, vol. 35, p. 673, 1930.

[134] D. A. Saville, "Electrohydrodynamics: The Taylor-Melcher Leaky Dielectric Model," *Annual Review of Fluid Mechanics*, vol. 29, pp. 27-64, 1997.

[135] R. S. Allan and S. G. Mason, "Particle Behaviour in Shear and Electric Fields. I. Deformation and Burst of Fluid Drops," *Proceedings of the Royal Society of London A*, vol. 267, p. 45, 1962.

[136] A. I. Ioffe and K. A. Naugol'nykh, "Formation of shock waves by an electric discharge in water," *Journal of Applied Mechanics and Technical Physics*, vol. 9, pp. 96-100, 1968.

[137] W. J. Vaughan, "Underwater shock waves formed by exploding wires," Naval Research Laboratory, NRL Report 5901, 1963.

[138] V. V. Arsent'ev, "On the theory of pulse discharge in a liquid," *Journal of Applied Mechanics and Technical Physics*, vol. 6, no. 5, pp. 34-37, 1965.

[139] B. Brandt et al., "The effect of submerged electrical discharges on bacteria," *TVF*, vol. 33, p. 222, 1962.

[140] Matthew J Traylor et al., "Long-term antibacterial efficacy of air plasma-activated water," *Journal of Physics D: Applied Physics*, vol. 44, no. 47, p. 472001, 2011.

[141] L. Edebo, T. Holme, and I. Selin, "Microbicidal action of compounds generated by transient electric arcs in aqueous systems," *Microbiology*, vol. 53, pp. 1-7, 1968.

[142] L. Edebo and I. Selin, "The Effect of the Pressure Shock Wave and Some Electrical Quantities in the Microbicidal Effect of Transient Electric Arcs in Aqueous Systems," *Microbiology*, vol. 50, no. 2, pp. 253-259, 1968.

[143] L. Edebo, "The Effect of the Photon Radiation in the Microbicidal Effect of Transient Electric Arcs in Aqueous Systems," *Microbiology*, vol. 50, no. 2, pp. 261-270, 1968.

[144] H. E. Radford, *Phys. Rev.*, vol. 122, p. 114, 1961.

[145] A. Carrington and D. Levy, "Electron resonance of free radicals in the gas phase," *J. Phys. Chem.*, vol. 71, no. 1, p. 2, 1967.

[146] R. F. Gould, Ed., *Advances in Chemistry Series, Chemical Reactions in Electrical Discharges*. Washington, DC: American Chemical Society Publications, 1969.

[147] G. Buxton and et al., "Critical review of rate constants for reactions of hydrated electrons, hydrogen atoms and hydroxyl radicals (-OH/-O-) in aqueous solution," *Journal of Physical and Chemical Reference Data*, vol. 17, no. 2, pp. 513-886, 1988.

[148] Knud Sehested, Ole L. Rasmussen, and Hugo Fricke, "Rate constants of OH with HO2,O2-, and H2O2+ from hydrogen peroxide formation in pulse-irradiated oxygenated water," *J. Phys. Chem*, vol. 72, pp. 626-631, 1968.

[149] S. Hashimoto, T. Miyata, N. Suzuki, and W. Kawakami, *Radiation Physics and Chemistry*, vol. 13, p. 107, 1979.

[150] A. Sakumoto and T. Miyata, "Treatment of Waste Water by a Combined Technique of Radiation and Conventional Method," *Radiation Physics and Chemistry*, vol. 24, no. 1, p. 99, 1984.

[151] M. G. Nickelsen, W. J. Cooper, C. N. Kurucz, and T. D. Waite, *Environmental Science and Technology*, vol. 26, p. 144, 1991.

[152] A. K. Sharma, B. R. Locke, P. Arce, and W. C. Finney, "A preliminary study of pulsed streamer corona discharge for the degradation of phenol in aqueous solutions," *Hazardous Waste & Hazardous Materials*, vol. 10, no. 2, p. 209, 1993.

[153] J. Sidney Clements, Masayuki Sato, and H. Robert Davis, "Preliminary Investigation of Prebreakdown Phenomena and Chemical Reactions Using a Pulsed High-Voltage Discharge in Water," *IEEE Transactions on Industry Applications*, vol. IA-23, no. 2, p. 224, 1987.

[154] B. Sun, M. Sato, A. Harano, and J. S. Clements, "Non-uniform pulse discharge-induced radical production in distilled water," *Journal of Electrostatics*, vol. 43, pp. 115-126, 1998.

[155] Bing Sun, Masayuki Sato, and J. Sid Clements, "Optical study of active species produced by a pulsed streamer corona discharge in water," *Journal of Electrostatics*, vol. 39, pp. 189-202, 1997.

[156] D. M. Willberg, P. S. Lang, R. H. Hochemer, A. Kratel, and M. R. Hoffmann, *Environmental Science and Technology*, vol. 30, p. 2526, 1996.

[157] M. Sato, T. Ohgiyama, and J. S. Clements, "Formation of chemical species and their effects on microorganisms using pusled high-voltage discharge in water," *IEEE Trans. Ind. Appl.*, vol. 32, no. 1, p. 106, 1996.

[158] A. A. Joshi, B. R. Locke, P. Arce, and W. C. Finney, "Formation of hydroxyl radicals, hydrogen peroxide and aqueous electrons by pulsed streamer corona discharge in aqueous solution," *Journal of Hazardous Materials*, vol. 41, no. 1, pp. 3-30, 1995.

[159] Igor V. Lisitsyn, Hiroaki Nomiyama, Sunao Katsuki, and Hidenori Akiyama, "Streamer discharge reactor for water treatment by pulsed power," *Review of Scientific Instruments*, vol. 70, no. 8, p. 3457, 1999.

[160] H. Akiyama, "Streamer Discharges in Liquids and their Applications," *IEEE Transactions on Dielectrics and Electrical Insulation*, vol. 7, no. 5, p. 646, 2000.

[161] Baldur Eliasson and Ulrich Kogelschatz, "Nonequilibrium volume plasma chemical processing," *IEEE Transactions on Plasma Science*, vol. 19, no. 6, p. 1063, 1991.

[162] M. Goldman and R. S. Sigmond, "Corona and Insulation," *IEEE Transactions on Electrical Insulation*, vol. EI-17, p. 90, 1982.

[163] P. Šunka et al., "Generation of chemically active species by electrical discharges in water," *Plasma Sources Science and Technology*, vol. 8, no. 2, p. 258, 1999.

[164] Petr Lukeš, "Water Treatment by Pulsed Streamer Corona Discharge," Institute of Chemical Technology and Institute of Plasma Physics, Prague, PhD Thesis 2001.

[165] W F L M Hoeben, E M van Veldhuizen, W R Rutgers, and G M W Kroese, "Gas phase corona discharges for oxidation of phenol in an aqueous solution ," *J. Phys. D: Appl. Phys.*, vol. 32, p. L133, 1999.

[166] B. Sun, M. Sato, and J. S. Clements, "Use of a pulsed high-voltage discharge for removal of organic compounds in aqueous solution," *Journal of Physics D*, vol. 32, p. 1908, 1999.

[167] M. Tezuka and M. Iwasaki, "Liquid-phase reactions induced by gaseous plasma. Decomposition of benzoic acids in aqueous solution," *Plasmas & Ions*, vol. 1, pp. 23-26, 1999.

[168] M. Laroussi, "Sterilization of contaminated matter with an atmospheric pressure plasma," *IEEE Transactions on Plasma Science*, vol. 24, pp. 1188-1191, 1996.

[169] H. W. Herrmann, I. Henins, J. Park, and G. S. Selwyn, "Decontamination of chemical and biological warfare (CBW) agents using an atmospheric pressure plasma jet (APPJ)," *Phyics of Plasmas*, vol. 6, no. 5, p. 2284, 1999.

[170] L. A. Rosocha, "Processing of hazardous chemicals using silent-discharge plasmas," in *Plasma Science and the Environment*, W. Manheimer, L. E. Sugiyama, and T. H. Stix, Eds. New York, NY: Woodbury, 1997, pp. 261-298.

[171] R. E. Sladek and et al., "Plasma treatment of dental cavities: A feasibility study," *IEEE Transactions on Plasma Science*, vol. 32, no. 4, 2004.

[172] J. Heinlin and et al., "Plasma applications in medicine with a special focus on dermatology," *Journal of the European Academy of Dermatology and Venereology*, vol. 25, no. 1, pp. 1-11, 2011.

[173] J. D. Holcomb and et al., "Nitrogen plasma skin regeneration and aesthetic facial surgery: multicenter evaluation of concurrent treatment," *Archives of Facial Plastic Surgery*, vol. 11, no. 3, pp. 184-193, 2009.

[174] S. U. Kalghatgi and et al., "Mechanism of blood coagulation by nonthermal atmospheric pressure dielectric barrier discharge plasma," *IEEE Transactions on Plasma Science*, vol. 35, no. 5, 2007.

[175] J.L. Glover and et al., "The plasma scalpel: A new thermal knife," *Lasers in Surgery and Medicine*, vol. 2, no. 1, pp. 101-106, 1982.

[176] Gunnar R. Stratton, Christopher L. Bellona, Fei Dai, Thomas M. Holsen, and Selma Mededovic Thagard, "Plasma-based water treatment: Conception and application of a new general principle for reactor design," *Chemical Engineering Journal*, vol. 273, pp. 543-550, 2015.

[177] Bruce R Locke and Kai-Yuan Shih, "Review of the methods to form hydrogen peroxide in electrical discharge plasma with liquid water," *Plasma Sources Science and Technology*, vol. 20, no. 3, p. 034006, 2011.

[178] J. K. Olthoff and K. E. Greenberg, "The Gaseous Electronics Conference RF Reference Cell - An Introduction," *Journal of Research of the National Institute of Standards and Technology*, vol. 100, no. 4, p. 327, 1995.

[179] J. E. Foster, G. Adamovsky, S. N. Gucker, and I. M. Blankson, "A Comparative Study of the Time-Resolved Decomposition of Methylene Blue Dye Under the Action of a Nanosecond Repetitively Pulsed DBD Plasma Jet Using Liquid Chromatography and Spectrophotometry," *IEEE Transactions on Plasma Science*, vol. 41, no. 3, pp. 503-512,

2013.

[180] Huijuan Wang, Jie Li, and Xie Quan, "Decoloration of azo dye by a multi-needle-to-plate high-voltage pulsed corona discharge system in water," *Journal of Electrostatics*, vol. 64, pp. 416-421, 2006.

[181] Z. Cao et al., "Spatially extended atmospheric plasma arrays," *Plasma Sources Science and Technology*, vol. 19, p. 025003, 2010.

[182] Xu Tao Deng and Michael G Kong, "Frequency Range of Stable Dielectric-Barrier Discharges in Atmospheric He and N2," *IEEE Transactions on Plasma Science*, vol. 32, no. 4, pp. 1709-1715, 2004.

[183] Natalia Yu Babaeva and Mark J Kushner, "Interaction of multiple atmospheric-pressure micro-plasma jets in small arrays: He/O 2 into humid air," *Plasma Sources Science and Technology*, vol. 23, no. 1, p. 015007, 2014.

[184] R. Dorai, K. Hassouni, and M. J. Kushner, *J. Appl. Phys.*, vol. 88, no. 10, 2000.

[185] Rajesh Dorai, "Modeling of atmospheric pressure plasma processing of gases and surfaces," University of Illinois at Urbana-Champaign, PhD Thesis 2002.

[186] Amanda M. Lietz and Mark J. Kushner, "Addressing Plasma-Liquid Interactions in a Global Model: Capabilities and Limitations," in *Proceedings from the 22nd International Symposium on Plasma Chemistry*, Antwerp, 2015.

[187] Glenn F. Knoll, *Radiation Detection and Measurement*, 4th ed. Hoboken, NJ: John Wiley & Sons, Inc., 2010.

[188] A. V. Phelps and Z. Lj. Petrovic, "Cold-cathode discharges and breakdown in argon: surface and gas phase production of secondary electrons," *Plasma Sources Science and Technology*, vol. 8, no. 3, p. R21, 1999.

[189] A. I. Korotkov, N. A. Nikonov, and N. I. Petrov, "Energy distribution of secondary electrons during relaxation of metastable atoms of inert gases at the surface of tantalum," *Soviet Physics Journal*, vol. 20, no. 7, pp. 847-851, 1977.

[190] Ulrich Kogelschatz, Baldur Eliasson, and W. Egli, "Dielectric-Barrier Discharges. Principle and Applications," *Journal de Physique IV*, vol. 7, pp. C4-47, 1997.

[191] R. R. Stout and G. A. Dawson, "Primary ionization coefficients for dry and moist air; secondary ionization coefficients for a water surface," *Pure and Applied Geophysics*, vol. 116, no. 1, pp. 159-166, 1978.

[192] J. Dutton, "A survey of electron swarm data," *Journal of Physical and Chemical Reference Data*, vol. 4, no. 3, p. 577, 1975.

[193] A. N. Prasad and J. D. Craggs, "Measurement of Ionization and Attachment Coefficients in Humid Air in Uniform Fields and the Mechanism of Breakdown," *Proceedings of the Physical Society*, vol. 76, no. 2, pp. 223-232, 1960.

[194] M. Naidu and A. Prasad, "Mobility, diffusion and attachment of electrons in oxygen," *Journal of Physics D: Applied Physics*, vol. 3, p. 957, 1970.

[195] A. Fridman, A. Chirokov, and A. Gutsol, "Non-thermal atmospheric pressure discharges for surface modification," *Journal of Physics D: Applied Physics*, vol. 38, pp. R1-R24, 2005.

[196] C. Raja Rao and G. R. Govinda Raju, "Growth of Ionization Currents in Dry Air at High Values of E/N," *J. Phys. D: Appl. Phys.*, vol. 4, pp. 494-503, 1971.

[197] F. H. Sanders, "Measurement of the Townsend Coefficients for Ionization by Collision," *Phys. Rev.*, vol. 44, pp. 1020-1024, 1933.

[198] K. Masch, "Uber Elektronenionisierung von Stickstoff Sauerstoff und Luft bei Geringen und Hohen Drucken," *Arch. Elektrotech.*, vol. 26, p. 587, 1932.

[199] G. R. Govinda Raju and R. Hackam, "Sparking potentials of dry air, humid air, and water vapor between concentric sphere-hemisphere electrodes," *Proc. IEE*, vol. 120, no. 8, pp. 927-933, 1973.

[200] G. G. Raju, *Gaseous electronics: theory and practice*. Boca Raton, FL: CRC Press, 2006.

[201] E. Kuffel, *Proc. Phys. Soc. (London)*, vol. 74, p. 297, 1959.

[202] J. S. Townsend, *Electrons in Gases*. London, UK: Hutchinson, 1947.

[203] K. T. A. L. Burm, "Calculation of the Townsend Discharge Coefficients and the Paschen Curve Coefficients," *Contrib. Plasma Phys.*, vol. 47, no. 3, pp. 177-182, 2007.

[204] D. Marić et al., "On the possibility of long path breakdown affecting the Paschen curves for microdischarges," *Plasma Sources Science and Technology*, vol. 21, p. 035016, 2012.

[205] A. Tilles, *Phys. Rev.*, vol. 46, p. 1015, 1934.

[206] J. M. A. Meek, "Theory of Spark Discharge," *Phys. Rev.*, vol. 57, p. 722, 1940.

[207] L. B. Loeb, *Fundamental Processes of Electrical Discharges in Gases*. New York: John

Wiley, 1939.

[208] F. G. Dunnington, *Phys. Rev.*, vol. 38, p. 1535, 1931.

[209] E. Flegler and H. Raether, *Zeitschrift für Physik*, vol. 99, p. 635, 1936.

[210] L. Loeb and J. Meek, "The mechanism of spark discharge in air at atmospheric pressure. I," *Journal of Applied Physics*, vol. 11, no. 6, pp. 438-447, 1940.

[211] H. Raether, "Zur Entwicklung von Kanalentladungen," *Archiv für Electrotechnik*, vol. 34, pp. 49-56, 1940.

[212] Jordan E. Chaparro, "Investigation of Sub-Nanosecond Breakdown through Experimental and Computational Methods," Texas Tech University, PhD Thesis 2008.

[213] S. Nakamura and et al, *IEEE Trans. Dielectric. Electrical. Insul.*, vol. 16, no. 4, p. 117, 2009.

[214] J. M. Meek and J. D. Craggs, *Electrical Breakdown of Gases*. Oxford, UK: Clarendon Press, 1953.

[215] E. M. van Veldhuizen and W. R. Rutgers, "Pulsed positive corona streamer propagation and branching," *J. Phys. D: Appl. Phys.*, vol. 35, pp. 2169-2179, 2002.

[216] Won J. Yi and P. F. Williams, "Experimental study of streamers in pure N2 and N2/O2 mixtures and a ≈13 cm gap," *J. Phys. D: Appl. Phys.*, vol. 35, pp. 205-218, 2002.

[217] S Nijdam, F M J H van de Wetering, R Blanc, E M van Veldhuizen, and U Ebert, "Probing photo-ionization: experiments on positive streamers in pure gases and mixtures," *Journal of Physics D: Applied Physics*, vol. 43, no. 14, p. 145204, 2010.

[218] Paul Ceccato, "Filamentary plasma discharge inside water: initiation and propagation of a plasma in a dense medium," Ecole Polytechnique Palaiseau, Paris, PhD Thesis 2009.

[219] A. Luque, V. Ratushnaya, and U. Ebert, "Positive and negative streamers in ambient air: modeling evolution and velocities," *J. Phys. D: Appl. Phys.*, vol. 41, p. 234005, 2008.

[220] A. Fridman and L. A. Kennedy, *Plasma Physics and Engineering*. Boca Raton, FL: CRC Press, 2004.

[221] C. D. Bradley and L. B. Snoddy, "Ion distribution during the initial stages of spark discharge in nonuniform fields," *Phys. Rev.*, vol. 47, p. 541, 1935.

[222] S. Pancheshnyi, "Role of electronegative gas admixtures in streamer start, propagation and branching phenomena," *Plasma Sources Science and Technology*, vol. 14, p. 645,

2005.

[223] M. Szklarczyk and et al., *J. Electrochem. Soc.*, vol. 136, p. 2512, 1989.

[224] J. Qian and et al., *J. Applied Physics*, vol. 97, p. 113304, 2005.

[225] T. J. Lewis, *IEEE Trans. Dielectrics and Electrical Insul.*, vol. 10, p. 949, 2003.

[226] P.H. Ceccato and et al., *J. Phys. D: Appl. Phys.*, vol. 43, p. 175202, 2010.

[227] M. F. Toney et al., "Voltage-dependent ordering of water molecules at an electrode-electrolyte interface," *Nature*, vol. 368, p. 444, 1996.

[228] R.P. Joshi, J. Qian, and K.H. Schoenbach, *J. Appl. Phys.*, pp. 96:5129, 2004.

[229] E. V. Yanshin, I. T. Ovchinnikov, and Y. N. Vershinin, *Sov. Phys. Tech. Phys.*, vol. 18, p. 1303, 1974.

[230] M. Zahn and et al., "Dielectric properties of water and water/ethylene glycol mixtures for use in pulse power system design," *Proceedings of the IEEE*, vol. 74, no. 9, p. 1182, 1986.

[231] B. Cabane and R. Vuilleumier, "The physics of liquid water," *C.R. Geoscience*, vol. 337, p. 150, 2005.

[232] E.S. Yakub, *Journal of Structural Chemistry*, vol. 24, p. 204, 1983.

[233] W.A. Stygar and et al., *Phys. Rev. ST Accel. Beams*, vol. 10, p. 030401, 2007.

[234] D. Tommasini, "Dielectric insulation and high-voltage issues," *arXiv preprint*, pp. arXiv:1104.0802, 2011.

[235] K. C. Kao, *British Journal of Applied Physics*, vol. 12, p. 632, 1961.

[236] Charles E. Swenberg, Gerda Horneck, and E.G. Stassinopoulous, *Biological Effects and Physics of Solar and Galactic Cosmic Radiation, Part 2*. New York: Springer Science & Business Media, 2012.

[237] A. Mozumder, *Fundamentals of Radiation Chemistry*. San Diego, CA: Academic Press, 1999.

[238] Katrin R. Siefermann et al., "Binding energies, lifetimes and implications of bulk and interface solvated electrons in water," *Nature Chemistry*, vol. 2, pp. 274-279, 2010.

[239] C. Montijn and U. Ebert, "Diffusion correction to the Raether–Meek criterion for the avalanche-to-streamer transition," *Phys. D: Appl. Phys.*, vol. 39, p. 2979, 2006.

[240] *CRC Handbook of Chemistry and Physics*, 94th ed. Boca Raton, FL, USA: CRC Press, 2013-2014.

[241] Philip L. Geissler, "Autoionization in Liquid Water," *Science*, vol. 291, p. 2121, 2001.

[242] A. M. Saitta, F. Saija, and P. V. Giaquinta, "Ab initio molecular dynamics study of dissociation of water under an electric field," *arXiv:1204.1120v1 [cond-mat.soft]*, 2012.

[243] A. Metaxas, *Foundations of Electroheat: A Unified Approach*. New York: John Wiley and Sons, 1996.

[244] L. Schaper, W. G. Graham, and K. R. Stalder, "Vapour layer formation by electrical discharges through electrically conducting liquids—modelling and experiment," *Plasma Sources Science and Technology*, vol. 20, no. 3, p. 034003, 2011.

[245] J. M. Spurgeon and N. S. Lewis, "Proton exchange membrane electrolysis sustained by water vapor," *Energy and Environmental Science*, vol. 4, pp. 2993-2998, 2011.

[246] A. Hickling and M. D. Ingram, "Contact glow-discharge electrolysis," *Transactions of the Faraday Society*, vol. 60, pp. 783-793, 1964.

[247] T. J. Lewis, "A new model for the primary process of electrical breakdown in liquids," *IEEE Transactions on Dielectrics and Electrical Insulation*, vol. 5, no. 3, pp. 306-315, 1998.

[248] R.P. Joshi and et al, "Model Analysis of Brekdown in High voltage, water based switches," in *Proceedings of the 14th IEEE Pulsed Power Conference*, Dallas, TX, 2003.

[249] N.F. Bunkin and F. V. Bunkin, *Sov. Phys.*, vol. 74, p. 271, 1992.

[250] S. M. Korobeinikov, A. V. Melekhov, and A. S. Besov, "Breakdown Initiation in Water with the Aid of Bubbles," *High Temperature*, vol. 40, no. 5, pp. 652-659, 2002, Translated from Russian from Teplofizika Vysokikh Temperatur, Vol. 40, No. 5, 2002, pp. 706-713.

[251] R. P. Joshi and et al, *J. Appl. Phys.*, vol. 96, no. 9, p. 5129, 2004.

[252] M. N. Shneider, M. Pekker, and A. Fridman, "Theoretical Study of the Initial Stage of Sub-nanosecond Pulsed Breakdown in Liquid Dielectrics," *IEEE Transactions on Dielectrics and Electrical Insulation*, vol. 19, no. 5, p. 1579, 2012.

[253] A. Starikovskiy, Y. Yang, Y. I. Cho, and A. Fridman, "Non-equilibrium plasma in liquid water: dynamics of generation and quenching," *Plasma Sources Science and Technology*, vol. 20, p. 024003, 2011.

[254] Danil Dobrynin et al., "Non-equilibrium nanosecond-pulsed plasma generation in the liquid phase (water, PDMS) without bubbles: fast imaging, spectroscopy and leader-type model," *Journal of Physics D: Applied Physics*, vol. 46, p. 105201, 2013.

[255] L. W. Anderson et al., *Fundamentals of Plasma Chemistry*, B. Bederson, H. Walther, and M. Inokuti, Eds. San Diego: Academic Press, 2000.

[256] B. Eliasson and U. Kogelschatz, "N2O formation in ozonizers," *J. Chimie Phys.*, vol. 83, no. 4, pp. 279-282, 1986.

[257] Muhammad Arif Malik, Abdul Ghaffar, and Salman Akbar Malik, "Water purification by electrical discharges," *Plasma Sources Science and Technology*, vol. 10, pp. 82-91, 2001.

[258] N. P. Dubinin, *Modern Problems of Radiation Genetics*. Moscow: Atomizdat, 1969.

[259] Gregory Fridman et al., "Comparison of Direct and Indirect Effects of Non-Thermal Atmospheric-Pressure Plasma on Bacteria," *Plasma Processes and Polymers*, vol. 4, no. 4, pp. 370-375, 2007.

[260] Peter Bruggeman and Ronny Brandenburg, "Atmospheric pressure discharge filaments and microplasmas: physics, chemistry and diagnostics," *Journal of Physics D: Applied Physics*, vol. 46, p. 464001, 2013.

[261] D. X. Liu, F. Iza, X. H. Wang, M. G. Kong, and M. Z. Rong, "He+O2+H2O plasmas as a source of reactive oxygen species," *Applied Physics Letters*, vol. 98, p. 221501, 2011.

[262] B. Winter et al., "Full Valence Band Photoemission from Liquid Water Using EUV Synchrotron Radiation," *Journal of Physical Chemistry A*, vol. 108, no. 14, pp. 2625-2632, 2004.

[263] Ondřej Svoboda, Daniel Hollas, Milan Ončák, and Petr Slavíček, "Reaction selectivity in an ionized water dimer: nonadiabatic ab initio dynamics simulations.," *Physical Chemistry Chemical Physics*, vol. 15, no. 27, pp. 11531-11542, 2013.

[264] S. S. Iyengar et al., "The properties of ion-water clusters. I. The protonated 21-water cluster," *Journal of Chemical Physics*, vol. 123, no. 8, p. 084309, 2005.

[265] Noam Agmon, "Mechanism of hydroxide mobility," *Chemical Physics Letters*, vol. 319, no. 3-4, pp. 247-252, 2000.

[266] V. L. Talrose, *Sov. Phys. Doklady.*, vol. 86, p. 909, 1952.

[267] A. N. Prasad and J. D. Craggs, "Measurement of Ionization and Attachment Coefficients in Humid Air in Uniform Fields and the Mechanism of Breakdown," *Proceedings of the Physical Society*, vol. 76, no. 2, pp. 223-232, 1960.

[268] T. Ishijima, H. Hotta, and H. Sugai, "Multibubble plasma production and solvent decomposition in water by slot-excited microwave discharge," *Applied Physics Letters*, vol. 91, p. 121501, 2007.

[269] J E Foster, G Adamovsky, S N Gucker, and I M Blankson, "A comparative study of the time-resolved decomposition of methylene blue dye under the action of a nanosecond repetitively pulsed DBD plasma jet using liquid chromatography and spectrophotometry," *IEEE Transactions on Plasma Science*, vol. 41, pp. 503-512, 2013.

[270] Radu Burlica, Michael J. Kirkpatrick, Wright C. Finney, Ronald J. Clark, and Bruce R. Locke, "Organic dye removal from aqueous solution by glidarc discharges," *Journal of Electrostatics*, vol. 62, no. 4, pp. 309-321, 2004.

[271] Bing Sun, Masayuki Sato, and J. Sid Clements, "Optical study of active species produced by a pulsed streamer corona discharge in water," *Journal of Electrostatics*, vol. 39, pp. 189-202, 1997.

[272] Yoshiro Nakagawa, Susumu Mitamura, Yasuhiro Fujiwara, and Takashi Nishitani, "Decolorization of Rhodamine B in Water by Pulsed High-Voltage Gas Discharge ," *Japanese Journal of Applied Physics*, vol. 42, p. 1422, 2003.

[273] Bing Sun, Masayuki Sato, and J. S. Clements, "Use of a pulsed high-voltage discharge for removal of organic compounds in aqueous solution," *Journal of Physics D*, vol. 32, no. 15, p. 1908, 1999.

[274] B. R. Locke, M. Sato, P. Sunka, and M. R., Chang, J.-S. Hoffmann, "Electrohydraulic discharge and nonthermal plasma for water treatment," *Ind. Eng. Chem. Res.*, vol. 45, pp. 882-905, 2006.

[275] W. Bian, M. Zhou, and L. Lei, "Formations of Active Species and By-Products in Water by Pulsed High-Voltage Discharge," *Plasma Chem Plasma Process*, vol. 27, p. 337, 2007.

[276] US Environmental Protection Agency, "National Primary Drinking Water Regulations," EPA, EPA 816-F-09-004, 2009.

[277] J. Chang, P. Lawless, and T. Yamamoto, "Corona discharge processes," *IEEE Transactions in Plasma Science*, vol. 19, no. 6, pp. 1152-1166, 1991.

[278] R. Ono and T. Oda, "Ozone production process in pulsed positive dielectric barrier discharge," *Journal of Physics D: Applied Physics*, vol. 40, no. 1, p. 176, 2007.

[279] Matthew J Pavlovich, Hung-Wen Chang, Yukinori Sakiyama, Douglas S Clark, and David B Graves, "Ozone correlates with antibacterial effects from indirect air dielectric barrier discharge treatment of water," *Journal of Physics D: Applied Physics*, vol. 46, no. 14, p. 145202, 2013.

[280] Diane Gumuchian et al., "Study of organic pollutants oxidation by atmospheric plasma discharge," in *Bulletin of the American Physical Society 66th Annual Gaseous Electronics Conference*, vol. 58, Princeton, NJ, 2013, p. ET3.3.

[281] J. Hoigne and H. Bader, "Rate constants of reaction of ozone with organic and inorganic compounds in water. Part II. Dissociating organic componds.," *Water Research*, vol. 17, p. 185, 1983.

[282] A. Farhataziz and B. Ross, "Selectrive specific rates of reactions of transients in water and aqueous solutions. Part III. Hydroxyl radical and perhydroxyl radical and their radical ions," *Natl. Stand. Ref. Data Ser. (USA Natl. Bur. Stand.)*, vol. 59, 1977.

[283] George V. Buxton, Clive L. Greenstock, W. Phillips Helman, and Alberta B. Ross, "Critical Review of rate constants for reactions of hydrated electrons, hydrogen atoms and hydroxyl radicals in Aqueous Solution," *Journal of Physical and Chemical Reference Data*, vol. 17, no. 2, p. 513, 1988.

[284] A. Fridman and G. Friedman, *Plasma Medicine*. Hoboken, NJ: John Wiley & Sons, 2012.

[285] P. Sunka et al., "Generation of chemically active species by electrical discharges in water," *Plasma Sources Science and Technology*, vol. 8, p. 258, 1999.

[286] WTW. WTW.de. [Online]. http://www.wtw.de/fileadmin/upload/Kataloge/Online/US/Onl_028_033_Conductivity_220-KB_US-pdf.pdf

[287] James W. Robinson, Mooyoung Ham, and Ammon N. Balaster, "Ultraviolet radiation from electrical discharges in water," *Journal of Applied Physics*, vol. 44, p. 72, 1973.

[288] D. M. Willberg, P. S. Lang, R. H. Hochemer, A. Kratel, and M. R. Hoffmann, "Degradation of 4-Chlorophenol, 3,4-Dichloroaniline, and 2,4,6-Trinitrotoluene in an Electrohydraulic Discharge Reactor," *Environmental Science and Technology*, vol. 30, pp. 2526-2534, 1996.

[289] T. A. Conner-Kerr and et al., "The effects of ultraviolet radiation on antibiotic-resistant

bacteria in vitro," *Ostomy Wound Management*, vol. 44, no. 10, pp. 50-56, 1998.

[290] A. A. Bogomaz, V. L. Goryachev, A. S. Remennyi, and F. G. Rutberg, "The Effectiveness of a Pulsed Electrical Discharge in Decontaminating Water," *Sov. Technol. Phys. Lett.*, vol. 17, p. 448, 1991.

[291] J. Guillemin, *Anthrax: The Investigation of a Deadly Outbreak.*. Oakland, CA: University of California Press, 1999.

[292] H. Halfmann and et al., "Identification of the most efficient VUV/UV radiation for plasma based inactivation of Bacillus atrophaeus spores," *J. Phys. D: Appl. Phys.*, vol. 40, no. 19, 2007.

[293] C. O. Laux, T. G. Spence, C. H. Kruger, and R. N. Zare, "Optical diagnostics of atmospheric pressure air plasmas," *Plasma Sources Sci. Technol.*, vol. 12, pp. 125-138, 2003.

[294] O. Kylian and F. Rossi, "Sterilization and decontamination of medical instruments by low-pressure plasma discharges: application of Ar/O2/N2 ternary mixture," *Journal of Physics D: Applied Physics*, vol. 42, 2009.

[295] M. K. Boudam and et al., "Bacterial spore inactivation by atmospheric-pressure plasmas in the presence or absence of UV photons as obtained with the same gas mixture," *J. Phys. D*, vol. 39, pp. 3494-3507., 2006.

[296] X. Deng and et al., "Physical mechanisms of inactivation of Bacillus subtilis spores using cold atmospheric plasmas," *IEEE Transactions on Plasma Science*, vol. 34, pp. 1310-1316., 2006.

[297] E. Stoffels and et al., "Cold atmospheric plasma: Charged species and their interactions with cells and tissues," *IEEE Transactions on Plasma Science*, vol. 36, pp. 1441-1457, 2008.

[298] Jérôme Thiebaud, Alina Aluculesei, and Christa Fittschen, "Formation of HO2 radicals from the photodissociation of H2O2 at 248 nm ," *The Journal of Chemical Physics*, vol. 126, p. 186101, 2007.

[299] J E Foster, B S Sommers, S N Gucker, I M Blankson, and G Adamovsky, "Perspectives on the interaction of plasmas with liquid water for water purification," *IEEE Transactions on Plasma Science*, vol. 40, pp. 1311-1323, 2012.

[300] J. Pelletier, *Agressologie*, vol. 33, pp. 105-110, 1993.

[301] M. Laroussi, "Low Temperature Plasma-Based Sterilization: Overview and State-of-the-

Art," *Plasma Processes and Polymers*, vol. 2, no. 5, pp. 391-400, 2005.

[302] M G Kong et al., "Plasma medicine: an introductory review," *New Journal of Physics*, vol. 11, no. 11, p. 115012, 2009.

[303] Murielle Naïtali, Georges Kamgang-Youbi, Jean-Marie Herry, Marie-Noelle Bellon-Fontaine, and Jean-Louis Brisset, "Combined Effects of Long-Living Chemical Species during Microbial Inactivation Using Atmospheric Plasma-Treated Water ," *Applied and Environmental Microbiology*, vol. 76, no. 22, pp. 7662-7664, 2010.

[304] Muhammad Arif Malik, "Synergistic effect of plasmacatalyst and ozone in a pulsed corona discharge reactor on the decomposition of organic pollutants in water," *Plasma Sources Science and Technology*, vol. 12, pp. S26-S32, 2003.

[305] J. Hoigne, "Chemistry of Aqueous Ozone and Transformation of Pollutants by Ozonation and Advanced Oxidation Processes," in *The Handbook of Environmental Chemistry*, J. Hrubec, Ed. Berline: Springver-Verlag, 1998, vol. 5.

[306] P. Chris Wilson, "Water Quality Notes: Alkalinity and Hardness," Soil and Water Science Department, Florida Cooperative Extension Service, Institute of Food and Agricultural Sciences, , University of Florida, Gainesville, FL, SL 332 2013.

[307] Guus Ijpelaar, Danny Harmsen, Charles M. Sharpless, Karl G. Linden, and Joop C. Kruithof, *Fluence Monitoring in UV Disinfection Systems: Development of a Fluence Meter*. Denver, CO: American Water Works Research Foundation, 2006.

[308] Gina Melin (Ed.), National Water Research Institute, "Treatment Technologies for Removal of Methyl Tertiary Butyl Ether (MTBE) from Drinking Water," National Water Research Institute, 2000.

[309] Michael Anbar and Henry Taube, "Interaction of nitrous acid with hydrogen peroixde and with water," *J. Am. Chem. Soc.*, vol. 76, no. 24, pp. 6243-6247, 1954.

[310] T. G. Leighton, A. J. Walton, and M. J. W. Pickworth, "Primary Bjerknes forces," *European Journal of Physics*, vol. 11, pp. 47-50, 1990.

[311] Leon Poltawski and Tim Watson, "Relative transmissivity of ultrasound coupling agents commonly used by therapists in the UK," *Ultrasound in Medicine & Biology*, vol. 33, no. 1, pp. 120–128, 2007.

[312] Monica Z. Bruckner. Microbial Life - Carleton College. [Online]. http://serc.carleton.edu/microbelife/research_methods/environ_sampling/oxygen.html

[313] Sarah Nowak and John Foster, "Power studies of an underwater DBD plasma jet," in *2011 Abstracts IEEE International Conference on Plasma Science (ICOPS)*, Chicago, 2011.

[314] M C Garcia, S N Gucker, and J E Foster, "Characterization of self-generated steam bubble discharge: plasma properties and decomposition efficiency," *Journal of Physics D: Applied Physics*, Under review, Submitted for publication Nov 2014.

[315] Wilfried Neumann, *Fundamentals of dispersive optical spectroscopy systems*. Bellingham, WA, USA: SPIE, The International Society for Optical Engineering, 2014.

[316] H. R. Griem, *Spectral Line Broadening by Plasmas*. New York: Academic Press, 1974.

[317] C. Yubero, M. D. Calzada, and M. C. Garcia, *J. Phys. Soc. Japan*, vol. 74, p. 2249, 2005.

[318] P. Bruggeman et al., "Characterization of a direct dc-excited discharge in water by optical emission spectroscopy," *Plasma Sources Science and Technology*, vol. 18, p. 025017, 2009.

[319] Marco A Gigosos, Manuel A Gonzalez, and Valentin Cardenoso, "Computer simulated Balmer-alpha, -beta and -gamma Stark line profiles for non-equilibrium plasmas diagnostics," *Spectrochimica Acta Part B: Atomic Spectroscopy*, vol. 58, pp. 1489-1504, 2003.

[320] M C Garcia, S N Gucker, and J E Foster, "Characterization of self-generated steam bubble discharge: plasma properties and decomposition efficiency," *Journal of Physics D: Applied Physics*, Submitted Nov 2014, under review.

[321] Scott Prahl. Oregon Medical Laser Center. [Online]. http://omlc.org/spectra/mb/

[322] Sheffield Hallam Univesity. Biosciences and Chemistry, Sheffield Hallam Univesity. [Online]. http://teaching.shu.ac.uk/hwb/chemistry/tutorials/chrom/gaschrm.htm

[323] J. Luque and D. R. Crosley, "LIFBASE: Database and spectral simulation (version 1.5)," SRI International Report MP 99-009, 1999.

[324] Zheng Wang, "Numerical Modeling of Chemistry, Turbulent Mixing and Aerosol Dynamics in Near-Field Aircraft Plumes," Mechanical Engineering, University of California at Berkeley, PhD Thesis 1998.

[325] The Engineering Toolbox. [Online]. http://www.engineeringtoolbox.com/gases-solubility-water-d_1148.html

[326] T. C. Manley, "The electric characteristics of the ozonator discharge," *J. Electrochem.*

Soc., vol. 84, no. 1, pp. 83-96, 1943.

[327] Helen J. Gallon, "Dry Reforming of Methane Using Non-Thermal Plasma-Catalysis," School of Chemistry, The University of Manchester, PhD Thesis 2010.

[328] J. F. Kolb, R. P. Joshi, S. Xiao, and K. H. Schoenbach, "Streamers in water and other dielectric liquids," *Journal of Physics D: Applied Physics*, vol. 41, no. 23, p. 234007, 2008.

[329] S. N. Gucker, B. S. Sommers, and J. E. Foster, "Plasma prodution in isolated bubbles," *IEEE Transactions on Plasma Science*, vol. 42, no. 10, p. 2636, 2014.

[330] J. Qian et al., *J. Applied Physics*, vol. 97, p. 113304, 2005.

[331] T. Takuma and B. Techaumnat, *Electric Fields in Composite Deielctrics and their Applications*. New York: Springer, 2010.

[332] N. Y. Babaeva and M. J. Kushner, "Structure of positive streamers inside gaseous bubbles immersed in liquids," *Journal of Physics D: Applied Physics*, vol. 42, no. 13, p. 132003, 2009.

[333] S. Gucker, B. Sommers, and J. Foster, "Breakdown Voltage Scaling in Gas Bubbles Immersed in Liquid Water," in *66th Annual Gaseous Electronics Conference*, vol. 58, Princeton, NJ, 2013.

[334] S. N. Gucker and J. E. Foster, "Breakdown voltage scaling relation of isolated gas bubbles in liquid water," in *2014 IEEE 41st International Conference on Plasma Sciences (ICOPS) held with 2014 IEEE International Conference on High-Power Particle Beams (BEAMS)*, Washington, DC, 2014, pp. DOI: 10.1109/PLASMA.2014.7012603.

[335] Hans-Jürgen Butt, Karlheinz Graf, and Michael Kappl, *Physics and Chemistry of Interfaces*. Weinheim, Germany: John Wiley & Sons, 2006.

[336] N. Škoro, D. Marić, G. Malović, W. G. Graham, and Z. Lj. Petrović, "Electrical Breakdown in Water Vapor," *Physical Review E*, vol. 84, no. 5, p. 055401, 2011.

[337] A. N. Prasad and J. D. Craggs, "Measurement of Ionization and Attachment Coefficients in Humid Air in Uniform Fields and the Mechanism of Breakdown," *Proceedings of the Physical Society*, vol. 76, no. 2, p. 223, 1960.

[338] Friedrich Paschen, "Ueber die zum Funkenübergang in Luft, Wasserstoff und Kohlensäure bei verschiedenen Drucken erforderliche Potentialdifferenz (On the potential difference required for spark initiation in air, hydrogen, and carbon dioxide at different pressures)," *Annalen der Physik*, vol. 273, p. 69, 1889.

[339] J. D. Cobine, *Gaseous Conductors*. New York: McGraw-Hill, 1941.

[340] E. M. Bazelyan and Y. P. Raizer, *Spark Discharge*. Boca Raton, FL: CRC Press, 1997.

[341] R. Stout and G. Dawson, "Primary ionization coefficients for dry and moist air; secondary ionization coefficients for a water surface," *Pure and Applied Geophysics*, vol. 116, no. 1, pp. 159-166, 1978.

[342] P. Debye and E. Hückel, "The theory of electrolytes. I. Lowering of freezing point and related phenomena.," *Physikalische Zeitschrift*, vol. 24, pp. 185-206, 1923.

[343] Malvern Instruments Ltd, "Zeta Potential: An Introduction in 30 Minutes," Technical Note MRK654-01,.

[344] nanoComposix. [Online]. http://nanocomposix.com/pages/characterization-techniques

[345] G. Quincke, *Ann. Phys. Chem.*, vol. 113, p. 513, 1861.

[346] B. W. Currie and T. Alty, "Adsorption at a Water Surface. Part 1," *Proceedings of the Royal Society of London A*, vol. 122, p. 622, 1929.

[347] A. Graciaa and et al., "The ζ-potential of gas bubbles," *Journal of Colloid and Interface Science*, vol. 172, pp. 131-136, 1995.

[348] Patrice Creux, Jean Lachaise, Alain Graciaa, James K. Beattie, and Alex M. Djerdjev, "Strong Specific Hydroxide Ion Binding at the Pristine Oil/Water and Air/Water Interfaces," *J. Phys. Chem. B*, vol. 113, p. 14146, 2009.

[349] M. Takahashi, "Zeta potential of microbubbles in aqueous solutions: Electrical properties of the gas-water interface," *Journal of Physical Chemistry B*, vol. 109, pp. 21858-21864, 2009.

[350] J. K. Beattie, A. M. Djerdjev, and G. G. Warr, "The surface of neat water is basic," *Faraday Discussions*, vol. 141, pp. 31-39, 2009.

[351] D. A. Wetz, J. J. Mankowski, J. C. Dickens, and M. Kristiansen, "The Impact of Field Enhancements and Charge Injection on the Pulsed Breakdown Strength of Water," *IEEE Transactions on Plasma Science*, vol. 34, no. 5, p. 1670, 2006.

[352] Markus Zahn, Steven Voldman, Tatsuo Takada, and David B. Fenneman, "Charge injection and transport in high voltage water/glycol capacitors," *Journal of Applied Physics*, vol. 54, no. 1, p. 315, 1983.

[353] M.M. Gongora-Nieto, P.D. Pedrow, B.G. Swanson, and G.V. Barbosa-Canovas, "Impact of air bubbles in a dielectric liquid when subjected to high field strengths ," *Innovative Food Science and Emerging Technologies*, vol. 4, pp. 57–67, 2003.

[354] Jeffrey D. Clogston and Anil K. Patri, "Zeta Potential Measurement," in *Characterization of Nanoparticles Intended for Drug Delivery* , Scott E McNeil, Ed.: Humana Press, 2011, vol. 697, pp. 63-70.

[355] Micahel B. Simth and Jerry March, *March's Advanced Organic Chemistry*. Hoboken, NJ: John Wiley & Sons, 2007.

[356] P. Bruggeman et al., "Characteristics of atmospheric pressure air discharges with a liquid cathode and a metal anode," *Plasma Sources Science and Technology*, vol. 17, p. 025012, 2008.

[357] Radu Burlica, Michael J. Kirkpatrick, and Bruce R. Locke, "Formation of reactive species in gliding arc discharges with liquid water," *Journal of Electrostatics*, vol. 64, pp. 35-43, 2006.

[358] John E. Foster, Bradley S. Sommers, Brandon Weatherford, Benjamin Yee, and Mahima Gupta, "Characterization of the evolution of underwater DBD plasma jet," *Plasma Sources Science and Technology*, vol. 20, no. 3, p. 034018, 2011.

[359] Satoshi Ikawa, Katsuhisa Kitano, and Satoshi Hamaguchi, "Effects of pH on Bacterial Inactivation in Aqueous Solutions due to Low-Temperature Atmospheric Pressure Plasma Application," *Plasma Processes and Polymers*, vol. 7, no. 1, pp. 33-42, 2010.

[360] Petr Lukeš, "Water Treatment by Pulsed Streamer Corona Discharge," Department of Water Technology and Environmental Engineering, Institute of Chemical Technology, Prague, PhD Thesis 2001.

[361] D. Moussa et al., "Acidity control of the gliding arc treatments of aqueous solutions: application to pollutant abatement and biodecontamination," *European Physical Journal: Applied Physics*, vol. 29, no. 2, p. 189, 2005.

[362] David B. Graves, "The emerging role of reactive oxygen and nitrogen species in redox biology and some implications for plasma applications to medicine and biology ," *J. Phys. D: Appl. Phys.*, vol. 45, p. 263001, 2012.

[363] R. Williams. pKa Data Compiled by R. Williams. [Online]. http://research.chem.psu.edu/brpgroup/pKa_compilation.pdf

[364] A S Hinman, "Expt. 5: Analysis of an Acid Mixture," in *University of Calgary, CHEM 311*

Lab.

[365] Rupali Shivapurkar and Damien Jeannerat, "Determination of the relative pKa's of mixtures of organic acids using NMR titration experiments based on aliased 1H–13C HSQC spectra ," *Analytical Methods*, vol. 3, p. 1316, 2011.

[366] Robert L. Petry, "Secondary Electron Emission from Tungsten, Copper and Gold," *Phys. Rev.*, vol. 28, p. 362, 1926.

[367] Ioana A. Biloiu and Earl E. Scime, "Ion acceleration in Ar-Xe and Ar-He plasmas. I. Electron energy distribution functions and ion composition," *Physics of Plasmas*, vol. 17, p. 113508, 2010.

[368] M. M. Mansour, N. M. El-Sayed, O. F. Farag, and M. H. Elghazaly, "Effect of He and Ar Addition on N2 Glow Discharge Characteristics and Plasma Diagnostics," *Arab Journal of Nuclear Science and Applications*, vol. 46, no. 1, pp. 116-125, 2013.

[369] M C Garcia, S N Gucker, and J E Foster, "Characterization of self-generated steam bubble discharge: plasma properties and decomposition efficiency," *Journal of Physics D: Applied Physics*, Under peer-review, Submitted Nov 2014.

[370] K. C. Chen, J. Y. Wu, W. B. Yang, and S. C. J. Hwang, "Evaluation of effective diffusion coefficient and intrinsic kinetic parameters on azo dye biodegradation using PVA-immobilized cell beads," *Biotechnol. Bioeng.*, vol. 83, pp. 821-832, 2003.

[371] Monica Magureanu, Daniela Piroi, Florin Gherendi, Nicolae Bogdan Mandache, and Vasile Parvulescu, "Decomposition of Methylene Blue in Water by Corona Discharges," *Plasma Chemistry and Plasma Processing*, vol. 28, no. 6, pp. 677-688, 2008.

[372] Tsunehiro Maehara et al., "Radio frequency plasma in water," *Japanese Journal of Applied Physics*, vol. 45, no. 11, pp. 8864-8868, 2006.

[373] T Ishijima, H Sugiura, R Saito, H Toyoda, and H Sugai, "Efficient production of microwave bubble plasma in water for plasma processing in liquid," *Plasma Sources Science and Technology*, vol. 19, p. 015010, 2010.

[374] Marie M. Mitani, Arturo A. Keller, Clifford A. Bunton, Robert G. Rinker, and Orville C. Sandall, "Kinetics and products of reactions of MTBE with ozone and ozone/hydrogen peroxide in water," *Journal of Hazardous Materials*, vol. B89, pp. 197-212, 2002.

[375] Sarah Nowak and John Foster, "Power studies of an underwater DBD plasma jet," in *2011 Abstracts IEEE International Conference on Plasma Science (ICOPS)*, Chicago, 2011.

[376] A. Chithambararaj, N. S. Sanjini, A. Chandra Bose, and S. Velmathi, "Flower-like hierarchical h-MoO3: new findings of efficient visible light driven nano photocatalyst for methylene blue degradation," *Catal. Sci. Technol.*, vol. 3, pp. 1405-1414, 2013.

[377] in *Twenty-First Symposium on Biotechnology for Fuels and Chemicals: Proceedings of the Symposium*, Fort Collins, CO, 1999.

[378] O I Aruoma, B Halliwell, B M Hoey, and J Butler, "The antioxidant action of N-acetylcysteine: its reaction with hydrogen peroxide, hydroxyl radical, superoxide and hypochlorous acid," *Free Radic Biol Med*, vol. 6, pp. 593-597, 1989.

[379] Bilal Bomani et al., "The Effect of Growth Environment and Salinity on Lipid Production and Composition of Salicornia virginica," NASA Glenn Research Center, NASA 2014-216645, 2014.

[380] Urs von Gunten, "Ozonation of Drinking Water: Part I. Oxidation kinetics and product formation," *Water Research*, vol. 37, pp. 1443-1467, 2003.

[381] Rogan Grant. (2014, Sept) MTT Assay. [Online]. http://commons.wikimedia.org/wiki/File:MTT_reaction.png

[382] P. Lukes, E. Dolezalova, and I., Clupek, M. Sisrova, "Aqueous-phase chemistry and bactericidal effects from an air discharge plasma in contact with water: evidence for the formation of peroxynitrite through a pseudo-second-order post-discharge reaction of H2O2 and HNO2," *Plasma Sources Science and Technology*, vol. 23, p. 015019, 2014.

[383] K. Oehmigen et al., "The Role of Acidification for Antimicrobial Activity of Atmospheric Pressure Plasma in Liquids," *Plasma Processes and Polymers*, vol. 7, pp. 250-257, 2010.

[384] Daniel Porter, Micah D. Poplin, Frank Holzer, Wright C. Finney, and Bruce R. Locke, "Formation of Hydrogen Peroxide, Hydrogen, and Oxygen in Gliding Arc Electrical Discharge Reactors With Water Spray," *IEEE Transactions on Industry Applications*, vol. 45, no. 2, pp. 623-629, March/April 2009.

[385] M C Garcia, S N Gucker, and J E Foster, "Characterization of self-generated steam bubble discharge: plasma properties and decomposition efficiency," *Journal of Physics D: Applied Physics*, Under peer-review, Submitted Nov 2014.

[386] A. I. Maximov, "Physics, Chemistry and Applications of the AC Diaphragm Discharge and Related Discharges in Electrolyte Solutions ," *Contrib. Plasma Phys.*, vol. 47, pp. 111-118, 2007.

[387] K. R. Stalder, J. Woloszko, I. G. Brown, and C. D. Smith, "Repetitive plasma discharges in

saline solutions," *Applied Physics Letters*, vol. 79, no. 27, p. 4503, 2001.

[388] Sarah Nowak and John Foster, "Power studies of an underwater DBD plasma jet," in *2011 Abstracts IEEE International Conference on Plasma Science (ICOPS)*, Chicago, 2011.

[389] E. Klimiuk, K. Kabardo, Z. Gusiatin, and U. Filipkowska, "The adsorption of reactive dyes from mixtures containing surfactants onto Chitin," *Polish J. Environ. Studies*, vol. 14, no. 6, pp. 771–780, 2005.

[390] M C Garcia, S N Gucker, and J E Foster, "Characterization of self-generated steam bubble discharge: plasma properties and decomposition efficiency," *Journal of Physics D: Applied Physics*.

[391] S.N. Gucker, B. Yee, and J.E. Foster, "Plasma treatment of contaminated liquid water: A comparison between steam bubble and gas bubble discharge," in *2013 Abstracts IEEE International Conference on Plasma Science (ICOPS)*, San Francisco, CA, 2013.

[392] Yifan Huang, Liancheng Zhang, Xuming Zhang, Zhen Liu, and Keping Yan, "The Plasma-Containing Bubble Behavior Under Pulsed Discharge of Different Polarities," *IEEE Transactions on Plasma Science*, vol. 43, no. 2, p. 567, 2015.

[393] Allen H. Olson and Stephen P. Sutton, "The physical mechanisms leading to electrical breakdown in underwater arc sound sources," *J. Acoust. Soc. Am.*, vol. 94, no. 4, p. 2226, 1993.

[394] T. Ishijima, H. Hotta, H. Sugai, and M. Sato, "Multibubble plasma production and solvent decomposition in water by slot-excited microwave discharge," *Applied Physics Letters*, vol. 91, p. 121501, 2007.

[395] S N Gucker and J E Foster, "Power studies of an underwater DBD plasma," in *38th IEEE International Conference on Plasma Science*, Chicago, IL, 2011.

[396] H. Wk. Lee et al., "Synergistic sterilization effect of microwave-excited nonthermal Ar plasma, H2O2, H2O and TiO2, and a global modeling of the interactions," *Plasma Sources Sci. Technol.*, vol. 22, p. 055008, 2013.

[397] M. Malik and A. Ghaffar, "Water purification by electrical discharges," *Plasma Sources Sci. Technol.*, vol. 10, pp. 82-91, 2001.

[398] Peter Bruggeman et al., "Electronic quenching of OH(A) by water in atmospheric pressure plasmas and its influence on the gas temperature determination by OH(A-X) emission," *Plasma Sources Science and Technology*, vol. 19, no. 1, p. 015016, 2010.

[399] G. Dilecce, P. F. Ambrico, M. Simek, and S. De Benedictis, "LIF diagnostics of hydroxyl radical in atmospheric pressure He-H2O dielectric barrier discharges," *Chemical Physics*, vol. 398, pp. 142-147, 2012.

[400] F. P. Sainct, D. A. Lacoste, M. J. Kirkpatrick, E. Odic, and C. O. Laux, "Temporal evolution of temperature and OH density produced by nanosecond repetitively pulsed discharges in water vapour at atmospheric pressure," *Journal of Physics D: Applied Physics*, vol. 47, no. 7, p. 075204, 2014.

[401] NIST Chemical Kinetics Database. NIST Standard Reference Database 17, Version 7.0 (Web Version), Release 1.6.8, Data version 2013.03. [Online]. http://kinetics.nist.gov/

[402] Peter Bruggeman and Daan C. Schram, "On OH production in water containing atmospheric pressure plasmas," *Plasma Sources Sci. Technol.*, vol. 19, p. 045025, 2010.

[403] Yukikazu Itikawa and Nigel Mason, "Cross Sections for Electron Collisions with Water Molecules ," *J. Phys. Chem. Ref. Data*, vol. 34, no. 1, p. 1, 2005.

[404] S. Nomura et al., "Characteristics of in-liquid plasma in water under higher pressure than atmospheric pressure," *Plasma Sources Science and Technology*, vol. 20, p. 034012, 2011.

[405] Baldur Eliasson and Ulrich Kogelschatz, "Modeling and Applications of Silent Discharge Plasmas," *IEEE Transactions on Plasma Science*, vol. 19, no. 2, p. 309, 1991.

[406] Ryo Ono and Tetsuji Oda, "Dynamics of ozone and OH radicals generated by pulsed corona discharge in humid-air flow reactor measured by laser spectroscopy," *J. Appl. Phys.*, vol. 93, p. 5876, 2003.

[407] J. H. Chen and P. X. Wang, "Effect of relative humidity on electron distribution and ozone production by DC coronas in air," *IEEE Transactions on Plasma Science*, vol. 33, no. 2, pp. 808-812, 2005.

[408] D. Moller, "Atmospheric hydrogen peroxide: evidence for aqueous-phase formation from a historic perspective and a one-year measurement campaign," *Atmos. Environ.*, vol. 43, no. 37, pp. 5923-5936, 2009.

[409] P. Lukes, A.T. Appleton, and B.R. Locke, "Hydrogen Peroxide and Ozone Formation in Hybrid Gas–Liquid Electrical Discharge Reactors," *IEEE Transactions on Industry Applications*, vol. 40, no. 1, pp. 60-67, 2004.

[410] Hideo Nojima et al., "Novel atmospheric pressure plasma device releasing atomic hydrogen: reduction of microbial-contaminants and OH radicals in the air," *Journal of*

Physics D: Applied Physics, vol. 40, pp. 501-509, 2007.

[411] N. A. Aristova and I. M. Piskarev, "Characteristic features of reactions initiated by a flash corona discharge," *Technol. Phys.*, vol. 47, p. 1246, 2002.

[412] S. Ognier, D. Iya-sou, C. Fourmound, and S. Cavadias, *Plasma Chem Plasma Proc.*, vol. 29, pp. 261-273, 2009.

[413] G. Mark et al., "OH-radical formation by ultrasound in aqueous solution – Part II: Terephthalate and Fricke dosimetry and the influence of various conditions on the sonolytic yield," *Ultrasonics Sonochemistry*, vol. 5, no. 2, pp. 41-52, 1998.

[414] S. M. Thagard, K. Takashima, and A. Mizuno, *Plasma Chem. Plasma Process.*, vol. 29, pp. 455-473, 2009.

[415] C. A. Wakeford, R. Blackburn, and P. D. Lickiss, *Ultrasonics Sonochemistry*, vol. 6, pp. 141-148, 1999.

[416] A. Y. Nikiforov and C. Leys, *Plasma Sources Sci. Technol.*, vol. 16, pp. 273-280, 2007.

[417] Z. Stara and F. Krcma, *Czech. J. Phys.*, vol. 54, pp. C1050-C5.

[418] P. Lukes, M. Clupek, P. Sunka, V. Babicky, and V. Janda, "Effect of ceramic composition on pulse discharge induced processes in water using ceramic-coated wire to cylinder electrode system," *Czech. J. Phys.*, vol. 52, p. D800, 2002.

[419] S. Potocky, N. Saito, and O. Takai, *Thin Solid Films*, vol. 518, pp. 918-923, 2009.

[420] H. Gao et al., "Analysis of Energetic Species Caused by Contact Glow Discharge Electrolysis in Aqueous Solution," *Plasma Sci. Technol.*, vol. 10, pp. 30-38, 2008.

[421] T. Sato and T. Furui, "Characteristics of a plasma flow generated in pure water vapor at atmospheric pressure and its sterilization efficacy," in *Int. Workshop on Plasmas with Liquids*, Matsuyama, Ehime, Japan, 2010.

[422] John Foster, Athena Sagadevan, Janis Lai, and Sarah Gucker, "Assessing the Plasma-Liquid Interface Using Single Bubble Studies," in *56th Annual Meeting of the APS Division of Plasma Physics*, vol. 59, New Orleans, LA, 15.

[423] Jim Clark. (2013, November) Chemguide. [Online]. chemguide.co.uk

[424] Katrin Oehmigen et al., "Volume Effects of Atmospheric-pressure Plasma in Liquids," *IEEE Transactions on Plasma Science*, vol. 39, no. 11, p. 2646, 2011.

[425] M. K. O. Bernardo and V. G. Organo, "Chlorophyll as a simple, inexpensive and environment-friendly colorimetric indicator for NO2 gas," *Orient J Chem*, vol. 30, no. 2, 2014.

[426] Tsunehiro Maehara et al., "Degradation of methylene blue by radio frequency plasmas in water under ultraviolet irradiation.," *Journal of Hazardous Materials*, vol. 174, pp. 473-476, 2010.

[427] Monica Magureanu, Nicolae Bogdan Mandache, and Vasile I. Parvulescu, "Degradation of organic dyes in water by electrical discharges," *Plasma Chemistry and Plasma Processing*, vol. 27, pp. 589-598, 2007.

[428] C. R. Cole, R. A., Champion Outlaw, D. H. Baker, and B. C. Holloway, "Contribution and origin of H3O+ in the mass spectral peak at 19 amu," *Journal of Vacuum Science & Technology A*, vol. 22, p. 2056, 2004.

[429] S N Gucker, M C Garcia, and J E Foster, "Optical Emission Spectroscopy of an Underwater DBD Plasma Jet," in *31st International Conference on Phenomena in Ionized Gases*, Granada, Spain, 2013, pp. ICPIG PS3-039.

[430] S N Gucker, M C Garcia, and J E Foster, "Time resolved spectroscopy of an underwater dielectric barrier discharge plasma jet," in *39th IEEE International Conference on Plasma Science*, Edinburgh, Scotland, 2012.

[431] Yoshiaki Hattori, Shinobu Mukasa, Shinfuku Nomura, and Hiromichi Toyota, "Optimization and analysis of shape of coaxial electrode for microwave plasma in water ," *Journal of Applied Physics*, vol. 107, p. 063305, 2010.

[432] Shinobu Mukasa, Shinfuku Nomura, Hiromichi Toyota, Tsunehiro Maehara, and Hiroshi Yamashita, "Internal conditions of a bubble containing radio-frequency plasma in water ," *Plasma Sources Science and Technology*, vol. 20, p. 034020, 2011.

[433] Shinobu Mukasa, Shinfuku Nomura, and Hiromichi Toyota, "Observation of Microwave In-Liquid Plasma using High-Speed Camera," *Japanese Journal of Applied Physics*, vol. 46, no. 9A, pp. 6015-6021, 2007.

[434] T Ishijima, H Sugiura, R Saito, H Toyoda, and H Sugai, "Efficient production of microwave bubble plasma in water for plasma processing in liquid," *Plasma Sources Science and Technology*, vol. 19, p. 015010, 2009.

[435] Yu. A. Lebedev, I. L. Epstein, V. A. Shakhatov, E. V. Yusupova, and V. S. Konstantinov, "Spectroscopy of Microwave Discharge in Liquid C7–C16 Hydrocarbons," *High*

Temperature, vol. 52, no. 3, pp. 319-327, 2014.

[436] Shinfuku Nomura and Hiromichi Toyota, "Sonoplasma generated by a combination of ultrasonic waves and microwave irradiation," *Applied Physics Letters*, vol. 83, p. 4503, 2003.

[437] Shinfuku Nomura, Hiromichi Toyota, Michinaga Tawara, Hiroshi Yamashita, and Kenya Matsumoto, "Fuel gas production by microwave plasma in liquid," *Applied Physics Letters*, vol. 88, p. 231502, 2006.

[438] Shinfuku Nomura et al., "Discharge Characteristics of Microwave and High-Frequency In-Liquid Plasma in Water," *Applied Physics Express*, vol. 1, p. 046002, 2008.

[439] José Ruiz-Herrera, *Fungal Cell Wall: Structure, Synthesis, and Assembly*. Boca Raton, FL: CRC Press, 1991.

[440] T. Leighton, *The Acoustic Bubble*. Waltham, MA: Academic Press, 2012.

[441] USP Technologies. H2O2.com. [Online]. http://www.h2o2.com/technical-library/physical-chemical-properties/physical-properties/default.aspx?pid=21&name=Coefficient-of-Diffusion